DISSERTATION

submitted to the

Combined Faculty for the Natural Sciences and for Mathematics

of the Ruperto-Carola University of Heidelberg, Germany

for the degree of

Doctor of Natural Sciences

presented by

Dipl.-Mol. Med. Christina Göngrich

born in Kaiserslautern, Germany

Oral examination:……..

METABOLIC ALTERATIONS IN CONNEXIN36 KNOCK-OUT MICE INDUCE GENDER-SPECIFIC CHANGES IN DENTATE GYRUS FUNCTION

Referees: Prof. Dr. Peter Horst Seeburg

Prof. Dr. Hannah Monyer

Hiermit erkläre ich, dass ich die vorliegende Dissertation selbst verfasst und mich dabei keiner anderen als der von mir ausdrücklich bezeichneten Quellen und Hilfen bedient habe. Des Weiteren erkläre ich, dass ich an keiner Stelle ein Prüfungsverfahren beantragt oder die Dissertation in dieser oder einer anderen Form bereits anderweitig als Prüfungsarbeit verwendet oder einer anderen Fakultät als Dissertation vorgelegt habe.

Heidelberg, 19. Juli 2008

Christina Göngrich

Für meine Eltern.

Acknowledgements

I would like to thank…

…Prof. Dr. Hannah Monyer for her support during my PhD thesis, for the possibility to work on this exciting and challenging subject and for the freedom to extend the research to areas that were novel to the group. I would also like to thank her for stimulating scientific discussions and for encouragement at times when experiments were progressing slowly.

…Prof. Dr. Peter Seeburg for scientific support, thesis supervision, evaluation and examination.

…Prof. Dr. Christoph Schuster and Prof. Dr. Stefan Frings for examination and for evaluating my thesis.

…Dr. Elke Fuchs for sharing the project, for contributing the behavioral experiments and the analysis of adult neurogenesis.

…Dr. Deborah Burks for collaboration, scientific discussions and analysis of metabolic and hormonal profiles of the $Cx36^{-/-}$ mice.

…Dr. Antonio Caputi for scientific discussions and help with the cloning strategy for the $5HT_{3A}$ - EGFP BAC construct that was my second project.

…Regina Hinz for genotyping of the Cx36 mice.

…Dr. Angelika Vogt and Dr. Julieta Alfonso for scientific (and also not so scientific) discussions, proof reading of my thesis, always having an open ear for problems and moral support in all situations.

…Dr. Kevin Allen for the introduction to statistics and statistical programs.

…Dr. Maria Kreuzberg, Verena Orth, Dr. Kevin Allen, Dr. Aleksandar Zivkovic, Dr. Olivia Dumitrescu, Dr. Nurith Jakob, Dr. Julieta Alfonso and Dr. Angelika Vogt for the short but perfect lunch and coffee breaks every day, for all the fun we had in the lab and for the things that would take up too much space to be mentioned here.

…all former and present lab members for the good working atmosphere, for scientific support, for teaching me new techniques, for help whenever I needed it and many more things.

I would like to thank my family and friends for continuous moral support, for advice in all situations and for encouragement throughout my PhD thesis.

Table of Contents

I. Introduction

I.1 Overview over Anatomy and Function of the Hippocampus

The hippocampal formation, a brain structure important for learning and memory, is part of the limbic system and consists of the hippocampus proper, dentate gyrus, subiculum, pre- and parasubiculum and entorhinal cortex.

The hippocampus proper is a cortical structure consisting of a rolled layer of excitatory glutamatergic pyramidal cells that is subdivided into the areas CA1, CA2 and CA3. Inhibitory GABAergic interneurons are mainly distributed basal and apical to the pyramidal cell layer in stratum oriens, stratum radiatum and stratum lacunosum-moleculare. The CA3 area of the hippocampus is capped by the dentate gyrus (DG) that consists of the densely packed glutamatergic granule cell layer (GCL), the hilus or polymorphic layer and the molecular layer. The somata of most DG GABAergic interneurons are located in the latter two regions and their processes ramify in very distinct patterns depending on the interneuron subtype (Ramón y Cajal S., 1893; Ramón y Cajal S., 1911; Lorente de Nó R., 1934; Freund and Buzsaki, 1996) (**Fig. 1A**).

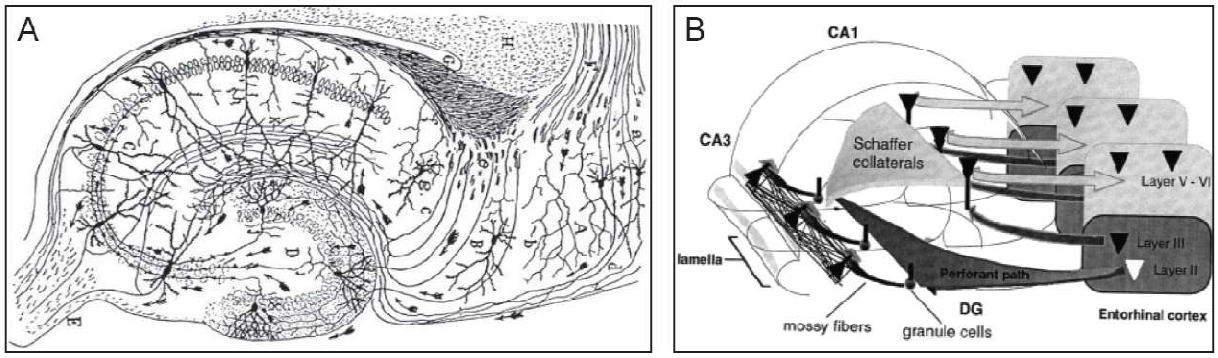

Figure 1: Basic anatomy of the hippocampus.
A: Drawing of the basic neuronal circuit of the rodent hippocampus as it was initially described by Ramón y Cajal (Ramón y Cajal S., 1911).
B: Schematic representation of the rodent hippocampus with emphasis on the major connections within the hippocampus (Freund and Buzsaki, 1996). CA1: cornu ammonis 1, CA3: cornu ammonis 3, DG: dentate gyrus.

The principal cells of the hippocampus and the DG are linked via the so-called trisynaptic loop: Granule cells of the DG, which are the primary target for afferent input from the entorhinal cortex, synapse via their axons, the mossy fibers, onto the somata of CA3 pyramidal cells (Lomo, 1971). The axons of CA3 pyramidal cells form the Schaffer collateral pathway to the CA1 area, where they contact the proximal dendrites of pyramidal cells via excitatory synapses (Schaffer, 1892). CA1 pyramidal cell axons, in turn, project to the entorhinal cortex and thus convey the processed information back into the cortex (Andersen et al., 1969). The function of this principal cell network is modified by interneurons that shape the activity of pyramidal and granule cells by complex feedback and feedforward inhibitory mechanisms (Andersen et al., 1963; Buzsaki and Eidelberg, 1981) (**Fig 1B**).

Neurons, however, are not only connected via chemical, but also via electrical synapses (Brightman and Reese, 1969; Kosaka, 1983a; Kosaka, 1983b) that play an important role in synchronizing network activity (Draguhn et al., 1998; Hormuzdi et al., 2001; Buhl et al., 2003).

These chemical and electrical interactions between excitatory and inhibitory neurons, generate synchronous oscillations of the membrane potentials of larger cell assemblies within the hippocampus (Mann and Paulsen, 2007). Hippocampal oscillations occurring in distinct frequency bands are the subject of extensive research and have been correlated with different cognitive states and behaviors, such as wakefulness, different sleep phases or exploratory activity (Vanderwolf, 1969; Buzsaki et al., 1983; Buzsaki et al., 1992).

The central role of the hippocampus in forming new memories became apparent in the 1950s in patient HM, who underwent bilateral medial temporal lobe resection to treat a severe form of epilepsy. Following surgery, patient HM suffered from anterograde amnesia and a temporally graded retrograde amnesia (Scoville and Milner, 1957; Corkin, 2002). The importance of the hippocampus in exploration and spatial navigation was initially demonstrated in rats by O'Keefe and colleagues, who showed by *in vivo* recordings in behaving rats the existence of place cells. Place cells were shown to be preferentially active when the animal moves through a specific location in the environment (O'Keefe and Dostrovsky, 1971; O'Keefe, 1976). Regarding the formation of spatial representations in the hippocampus, the DG-CA3 network needs to be mentioned: Due to the low probability of two CA3 pyramidal cells receiving input from identical subsets of DG granule cells, the DG can function as a pattern separator for

incoming spatial information and thus facilitate the resolution of spatially related cues (Rolls, 1989; Gilbert et al., 2001).

Furthermore, the hippocampus is unique among cortical structures because it contains one of the rare neurogenic niches in the adult rodent brain. Throughout life, new neurons are generated in the subgranular zone of the DG (Altman and Das, 1965). Mechanisms and implications of adult neurogenesis will be discussed in the following sections.

I.2 Adult Neurogenesis

Traditionally it was assumed that all neurons are generated during embryogenesis. This dogma was shaken already in the 1960s by the studies of Smart (Smart, 1961) and Altman and Das (Altman and Das, 1965; Altman and Das, 1966) who could show the incorporation of the DNA synthesis marker ^{3}H-thymidine into neurons of the subventricular zone (SVZ) of the lateral ventricle and the subgranular zone (SGZ) of the DG in young postnatal and adult rodent brains (**Fig. 2A**). The SVZ gives rise to neuroblasts that migrate via the rostral migratory stream into the olfactory bulb, where they differentiate into GABAergic granule and periglomerular cells (Altman, 1969) (**Fig. 2C**). In contrast to the SVZ, the SGZ gives rise to glutamatergic granule cells, the principal cells of the dentate gyrus (Altman and Das, 1965) (**Fig. 2B**). In both cases, the newborn neurons integrate into preexisting neuronal networks after reaching their final destination (van Praag et al., 2002; Belluzzi et al., 2003). Although the existence of adult neurogenesis was under debate for several years, by now the SVZ and the SGZ are widely accepted to be neurogenic niches in the postnatal brain (Kaplan and Hinds, 1977; Rakic, 1985; Kaplan, 2001; Rakic, 2002; Zhao et al., 2008) (**Fig. 2**).

The function of adult neurogenesis in the DG as well as in the olfactory bulb is not yet fully understood. Employing different techniques to ablate adult neurogenesis, it has been shown that postnatal hippocampal neurogenesis affects hippocampus-dependent learning and memory in some paradigms but not in others (Shors et al., 2001; Shors et al., 2002; Leuner et al., 2006; Saxe et al., 2007; Zhang et al., 2008). The same holds true for SVZ neurogenesis that has been both positively and negatively correlated with olfactory memory and olfactory discrimination (Rochefort et al., 2002; Mechawar et al., 2004; Magavi et al., 2005). Despite conflicting evidence on the exact role of adult neurogenesis on hippocampal and olfactory memory, this process is an important mechanism that adds an additional degree of plasticity to the adult brain.

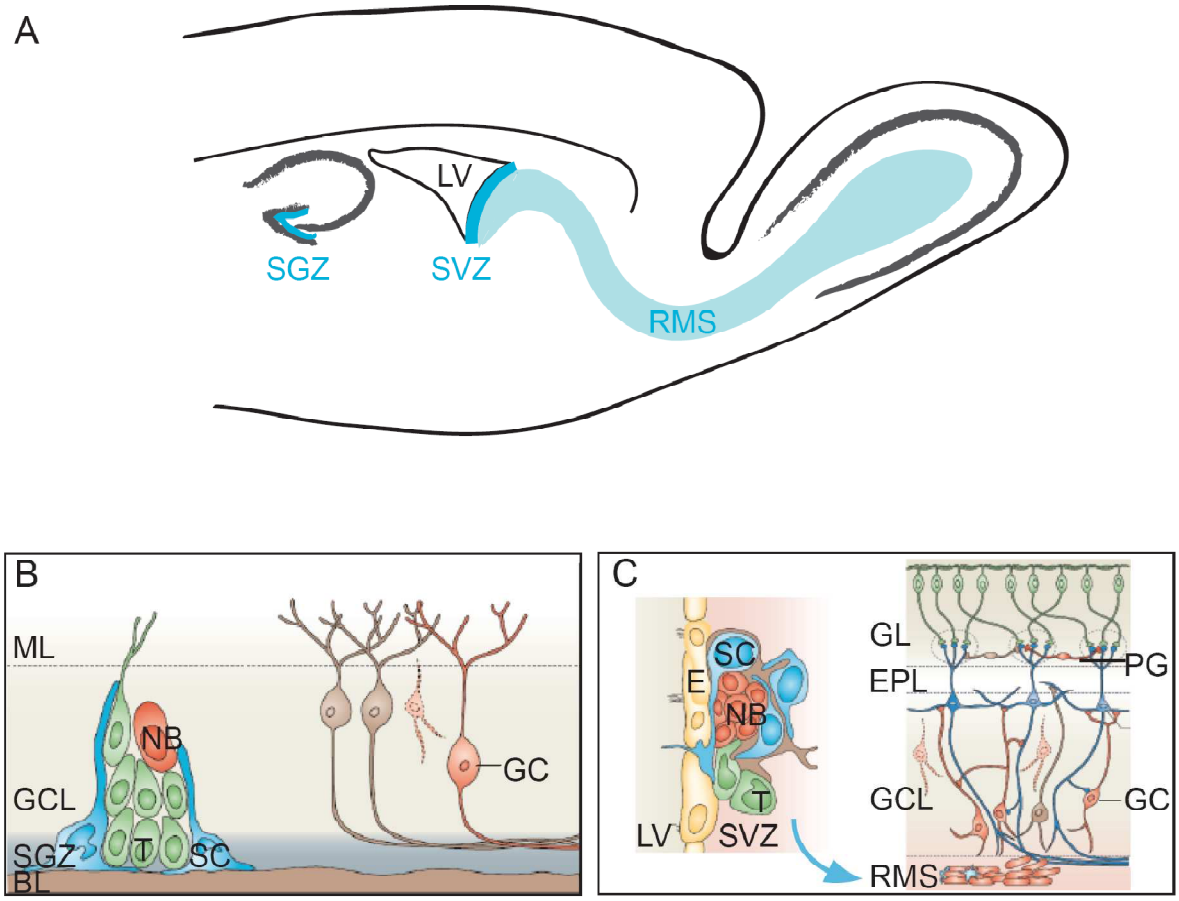

Figure 2: Neurogenic niches in the adult rodent brain.
A: Schematic representation of the two confirmed neurogenic niches in the adult rodent brain. The subgranular zone (SGZ) is located in a narrow zone between the hilus and the granule cell layer of the DG. The second neurogenic niche is the subventricular zone (SVZ) of the lateral ventricle (LV) that generates neurons destined for the olfactory bulb.
B: The cell types involved in neurogenesis in the SGZ are astroglial-like stem cells, transit amplifying cells and neuroblasts. Stem cells generate, via the stage of transit amplifying cells, neuroblasts that differentiate into glutamatergic granule cells and integrate into the existing neuronal network of the granule cell layer. BL: basal lamina, GC: granule cell, GCL: granule cell layer, ML: molecular layer, NB: neuroblasts, SC: stem cell, SGZ: subgranular zone, T: transit amplifying cells (modified from Lledo et al., 2006).
C: The cell types involved in SVZ neurogenesis are the same as described in (B). Newly generated neuroblasts leave the SVZ and migrate via the RMS into the olfactory bulb where they mature into GABAergic granule cells and periglomerular cells. E: epithelium, EPL: external plexiform layer, GC: granule cell, GCL: granule cell layer, GL: glomerular layer, LV: lateral ventricle, NB: neuroblasts, PG: periglomerular cells, RMS: rostral migratory stream, SC: stem cell, SVZ: subventricular zone, T: transit amplifying cell (modified from Lledo et al., 2006).

I.2.1 Developmental Steps in Adult SGZ Neurogenesis

The current model for hippocampal neurogenesis in the SGZ consists of six developmental steps, starting from a putative stem cell, resulting in a mature, postmitotic neuron (**Fig. 3**). The involved cell types have been classified according to their morphology and the expression of marker proteins (Kempermann et al., 2004; Zhao et al., 2008).

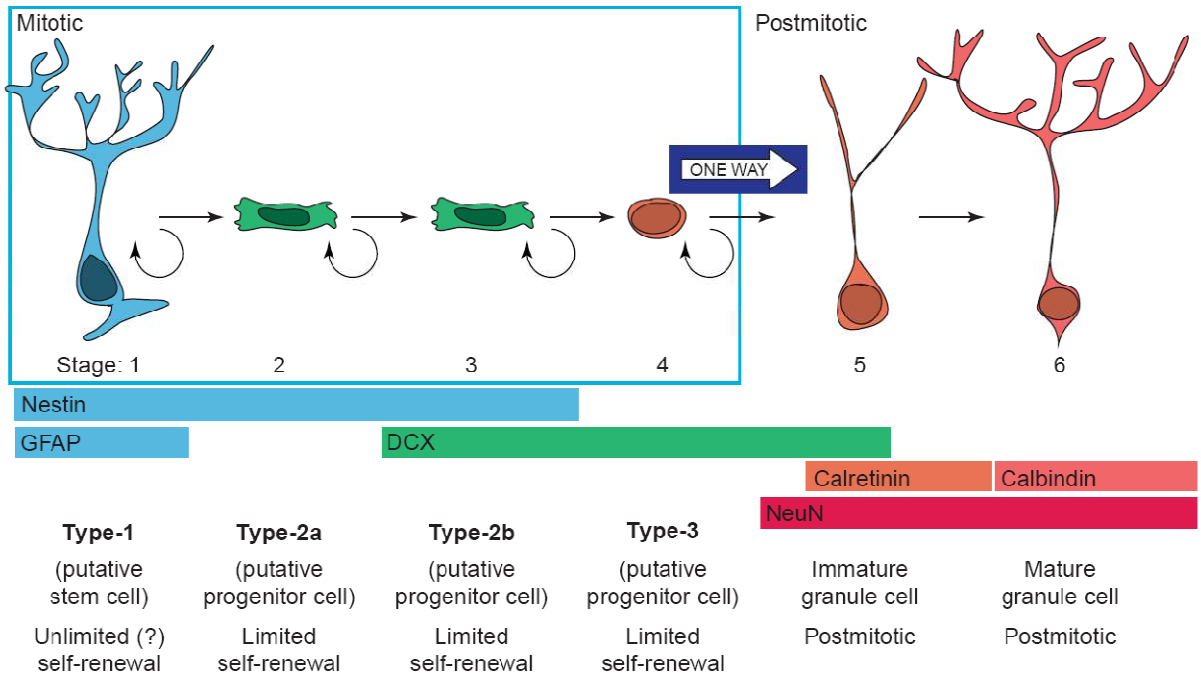

Figure 3: Current model of adult neurogenesis in the SGZ.
According to this model, adult neurogenesis can be divided into six developmental steps starting from a glial-like stem cell resulting in a mature granule cell. The different stages are characterized by typical morphological traits of the respective cell type and the expression of distinct sets of marker proteins (modified from Kempermann et al., 2004).

The type-1 cell is the multipotent stem cell of the adult SGZ with possibly unlimited self-renewal capacity due to asymmetric cell divisions. It expresses glial fibrillary acidic protein (GFAP) and nestin as molecular markers, shows an astrocyte-like morphology and passive membrane properties (Seri et al., 2001; Filippov et al., 2003; Fukuda et al., 2003; Babu et al., 2007). The daughter cells (type-2 cells) lose GFAP expression and have tangentially oriented short processes (Filippov et al., 2003). These highly proliferative cells are probably already

lineage committed and can be further subdivided into type-2a and 2b cells, the latter acquiring expression of polysialated neuronal cell adhesion molecule (PSA-NCAM) and doublecortin (DCX), a marker for migrating neuroblasts (Seki and Arai, 1993; Gleeson et al., 1998; des Portes et al., 1998; Kronenberg et al., 2003). Furthermore, type-2 cells already show voltage-gated Na^+ currents. Type-2b progenitors subsequently develop into type-3 neuroblasts that are still proliferative but are in a transitional state to become postmitotic. In addition to DCX and PSA-NCAM, they express NeuroD and Prox1, transcription factors characteristic for neurons and specifically DG granule cells, thus showing further neuronal lineage commitment (Lee et al., 1995; Liu et al., 2000). The fifth stage according to this model is reached about three days after the initial division and is characterized by migration into the granule cell layer, cell cycle exit and the start of transient calretinin (CR) expression. CR-positive cells express in addition DCX and NeuN, a marker for postmitotic neurons (Mullen et al., 1992; Brandt et al., 2003). In the following two weeks axons are extended to CA3, initial dendritic spines are developed and the newly generated cells are selected for survival or eliminated via apoptosis (Hastings and Gould, 1999; Biebl et al., 2000; Kuhn et al., 2005; Zhao et al., 2006). The switch from CR to calbindin (CB) expression about two weeks after the last cell division marks the onset of the final developmental stage. During this maturational phase, the threshold for long-term potentiation (LTP) induction in young granule cells is significantly reduced and thus, network properties should differ substantially depending on the number of immature granule cells present in the DG at a given time point (Wang et al., 2000; Schmidt-Hieber et al., 2004). Additional evidence for a continuing functional maturation comes from a study analyzing the activity-dependent expression of immediate early genes, i.e. cFos, that was not detected until six weeks after the birth of the neuron (Kee et al., 2007). Only after a time span of several months the newly generated cells are morphologically as well as electrophysiologically indistinguishable from fully mature granule cells (van Praag et al., 2002; Zhao et al., 2006).

I.2.2 Factors Influencing Adult Neurogenesis

The process of adult neurogenesis can be subdivided into proliferation of precursor cells, maturation of the newly generated neuroblasts and their survival, which is critically linked to

network integration. Regulation occurs at any of these stages by a plethora of factors, including environment, hormones, hippocampal activity, exercise and age. The influence of these factors on adult neurogenesis and their intracellular signaling cascades have been investigated by several studies (Kuhn et al., 1996; Kempermann et al., 1997; Tanapat et al., 1999; van Praag et al., 1999a; Tozuka et al., 2005).

The focus of the following sections will be the effect of hormones, especially of estradiol, and of hippocampal activity on adult neurogenesis in the SGZ.

I.2.2.1 Hormones and Neurogenesis

Hormones, by definition factors secreted into the blood stream (Starling, 1905), are systemically acting compounds that have a tremendous effect on brain function and interact with each other in a tightly regulated network. An important group of hormones influencing SGZ neurogenesis are the gonadal hormones but also corticosteroids and thyroid hormone are modulators of adult neurogenesis (Desouza et al., 2005; Mirescu and Gould, 2006; Galea, 2008).

I.2.2.1.1 Regulation of Circulating Estradiol Levels

The serum concentration of estrogens is regulated by positive and negative feedback mechanisms within the hypothalamic-pituitary-gonadal (HPG) axis in the female (**Fig. 4A**). Gonadotropin releasing hormone (GnRH) is produced and secreted by hypothalamic GnRH neurons that are a small group of neurons scattered over a comparatively wide area of the hypothalamus (Wray and Hoffman, 1986). GnRH is secreted in a pulsatile manner into the hypothalamo-hypophyseal portal circulation and regulates the secretion of luteinizing hormone (LH) and follicle-stimulating hormone (FSH) from the anterior pituitary gland (Belchetz et al., 1978; Levine and Ramirez, 1982). LH and FSH stimulate the maturation of ovarian follicles and subsequent steroid production (Gougeon, 1996). Antral follicles, which are characterized by development of a fluid filled cavity under the control of FSH and LH, are the major source of estradiol (Boland et al., 1993). During most of the approximately 5 day estrous cycle in mouse and rat, estradiol exerts a negative feedback on the secretion of LH, FSH and GnRH, and thus, on its own production. On the day of proestrus, however, estradiol concentration peaks and

increases the secretion of GnRH via a positive feedback loop to trigger ovulation (reviewed in Levine, 1997; and in Herbison, 1998) (**Fig. 4A + B**).

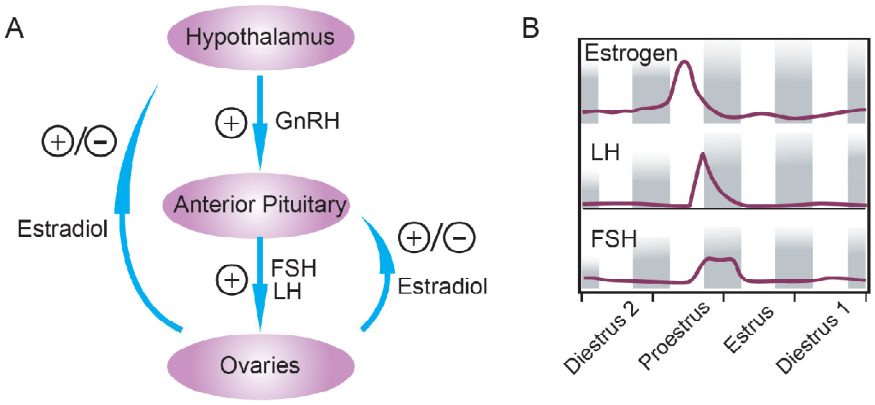

Figure 4: Simplified schematic of the hormonal fluctuations during the estrous cycle and key regulatory mechanisms.
Pulsatile release of GnRH from hypothalamic neurons positively regulates the secretion of LH and FSH from cells of the anterior pituitary gland. These two hormones initiate and maintain the growth of ovarian follicles that are the main source of estradiol. During most of the estrous cycle estradiol exerts a negative feedback on the secretion of GnRH, LH and FSH until estradiol concentration peaks in the afternoon of proestrus and triggers increased release of the three factors. B: modified from Staley and Scharfmann (2005).

The HPG axis, and consequently estradiol concentration, is also regulated by insulin: Binding of insulin to neuronal insulin receptors on GnRH neurons in the hypothalamus stimulates the secretion of GnRH (Burcelin et al., 2003). Additional evidence on the importance of this pathway comes from the analysis of neuron-specific insulin receptor knockout mice. In females of this mouse line, LH secretion from the anterior pituitary is reduced to 10 %, while the effect is less pronounced in males (Bruning et al., 2000; Burcelin et al., 2003).

The activity of GnRH neurons is further regulated by input from the suprachiasmatic nucleus (SCN) of the hypothalamus (Gray et al., 1978; van der Beek et al., 1993). The monosynaptic input from vasocative intestinal polypeptide (VIP) positive fibers is counterbalanced by a feedback loop from GnRH neurons onto these cells (van der Beek et al., 1993; van der Beek et al., 1997).

I.2.2.1.1 Influence of Estradiol on SGZ Neurogenesis

Initial evidence on the influence of gonadal hormones on adult neurogenesis in the rodent SGZ came from a study demonstrating that approximately 45 % more granule cells are produced in the DG of female rats compared to the DG of male rats. The rate of granule cell precursor proliferation varies across the estrous cycle and is positively correlated with estradiol concentration. Net granule cell production, however, does not differ between male and female rats due to a potentially higher survival rate of newborn granule cells in males (Tanapat et al., 1999). Along these lines two studies, one performed in female, ovariectomized rats, the other in female meadow voles, demonstrated that 4 h after exposure to estradiol proliferation of precursor cells is increased, while 48 h after exposure to a high doses of estradiol their proliferation is decreased (Ormerod and Galea, 2001; Ormerod et al., 2003). Since proestrus (high estradiol) proceeds estrus (low estradiol) by approximately 48 h, these studies corroborate the findings of Tanapat et al. (Tanapat et al., 1999). In contrast to rats, there is no difference in the proliferation of granule cell precursors in the SGZ of C57BL/6 male and female mice. This study also showed an unaltered proliferation rate across the menstrual cycle (Lagace et al., 2007).

Survival of newly generated granule cells has been linked to low estradiol levels in female meadow voles: in non-reproductive females serum estradiol is low and survival of granule cells is increased during the investigated time period of five weeks (Ormerod and Galea, 2001). In addition, the influence of estradiol on neurogenesis does not only depend on the duration of the treatment, but also on the time point of administration during the neuroblasts' lifespan. In castrated male meadow voles estradiol enhances cell survival if administered 6-10 days after the last cell division, but has no effect on survival beyond this time span (Ormerod et al., 2004).

Estradiol acts via two different estrogen receptors. Estrogen receptor α (ERα) (Green et al., 1986) as well as ERβ (Kuiper et al., 1996) have been shown to be expressed by progenitor cells isolated from the SGZ and by DCX-positive neuroblasts (Brannvall et al., 2002; Isgor and Watson, 2005). Both receptors have additionally been found on the somata of pyramidal cells, mature DG granule cells and interneurons in the hippocampus and other brain areas. Interneuronal expression of ERβ is mainly restricted to parvalbumin (PV) positive interneurons

(Weiland et al., 1997; Milner et al., 2001; Blurton-Jones and Tuszynski, 2002; Milner et al., 2005). Classical estrogen receptors are nuclear receptors that dimerize upon hormone binding and function subsequently as transcription factors. However, it seems that ERβ can function as a non-nuclear receptor in DCX-positive neuroblasts and likewise ERα in interneurons and principal cells in the hippocampus, as shown by the extranuclear localization of the receptors (Jensen and Jacobson, 1962; Milner et al., 2001; Herrick et al., 2006).

Besides the direct effects of estrogen on proliferating cells, it can also indirectly influence neurogenesis via changes in neuronal network activity by regulating NMDA receptor expression and increasing spine density in the hippocampus (Woolley and McEwen, 1992; Weiland, 1992).

I.2.2.2 Hippocampal Activity and Neurogenesis

Young DG granule cells have fundamentally different electrophysiological properties than fully mature granule cells. As mentioned before, the inhibitory neurotransmitter GABA hyperpolarizes mature neurons, while in immature neurons binding of GABA to its ionotropic receptors leads to depolarization of the cell (Mueller et al., 1983). Already before receiving any synaptic input, adult generated granule cells respond with depolarization to ambient GABA. This tonic activation is necessary for the proper development of the dendritic arbor of granule cells and for the establishment of GABAergic and glutamatergic synapses (Ge et al., 2006). Moreover, it has been shown that at a later developmental stage, depolarizing synaptic GABAergic input increases intracellular Ca^{2+} concentration and promotes neuronal differentiation (Tozuka et al., 2005). Furthermore, the threshold for induction of LTP is drastically reduced in comparison to fully mature neurons and can be induced in young granule cells without blocking GABA receptors (Wang et al., 2000; Schmidt-Hieber et al., 2004). In addition, young neurons were shown to generate Ca^{2+} spikes mediated by T-type Ca^{2+} channels thus decreasing action potential threshold (Schmidt-Hieber et al., 2004). Hence, shifting the composition of the DG neuronal network towards a higher proportion of young neurons by increasing neurogenesis, increases excitability.

Hippocampal seizures, which are the most extreme form of increased network activity, can be induced by several experimental paradigms. When induced by a single kainic acid

injection, they lead to an increase in type-3 neuroblasts (**Fig. 3**) (Steiner et al., 2008). The same was observed for kindling induced seizures that also increase immature granule neurons as assessed by BrdU birthdating experiments (Smith et al., 2005). On the other hand, seizures are not only promoting neurogenesis, but seizure induction can be facilitated by higher proportions of immature neurons within the network. In a model of pilocarpine induced seizures, blockade of adult neurogenesis attenuates the occurrence of spontaneous recurrent seizures (Jung et al., 2004), thus demonstrating the tight bidirectional connection between neurogenesis and hippocampal activity.

I.3 Gap Junctions

Gap junctions are made up of plaques of intercellular channels that connect the cytoplasm of two adjacent cells via hydrophilic pores and were initially identified in electron microscopy studies (Robertson, 1963; Revel and Karnovsky, 1967; Brightman and Reese, 1969; Goodenough, 1976) (**Fig. 5A**). By allowing the passive diffusion of ions, second messengers and small metabolites between connected cells, gap junctions functionally and metabolically couple these cells, and thus fulfill important functions in processes like insulin secretion, cardiac and smooth muscle contraction, pattern formation during embryogenesis and neuronal network synchronization (Bruzzone et al., 1996).

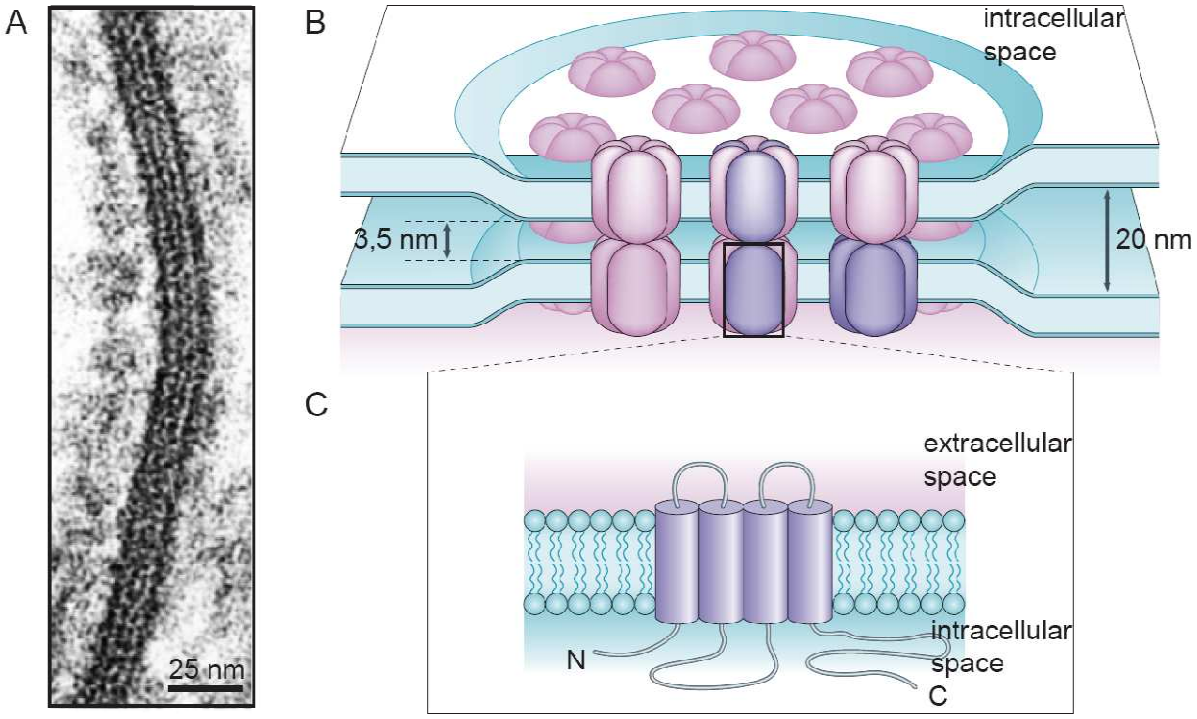

Figure 5: Electronmicroscopic view and schematic representation of a gap junction.
A: Electronmicroscopic view of a gap junction plaque sectioned perpendicular to the membrane plane shows the seven-layered structure that gap junctions form (modified from Bennett et al., 1991).
B: Schematic overview of a gap junctional plaque comprising an array of junctional channels. The channels are formed by head-to-head assembly of two connexons, or hemichannels, which themselves consist of six Cx subunits. (modified from Sohl et al., 2005)
C: Domain structure of a Cx subunit. N- and C-terminus of Cxs as well as a loop connecting transmembrane domains 2 and 3 reside in the intracellular space. The docking to other Cx subunits in a channel is mediated by two extracellular loops (modified from Sohl et al., 2005).

In vertebrates, the channel-forming proteins are the connexins (Cxs) and in invertebrates the structurally related innexins (Bruzzone et al., 1996; Phelan, 2005). After the cloning of the first Cx cDNA from rat liver in 1986 (Paul, 1986), the field has progressed rapidly and by now, 20 different Cx genes have been identified and characterized in the mouse. With the exception of erythrocytes, thrombocytes, spermatocytes and adult skeletal muscle, Cxs show a widespread tissue distribution throughout development and adulthood (Sohl et al., 2004).

The protein structure of Cxs is highly conserved (**Fig. 5C**): they contain four transmembrane domains that are linked by two extracellular and one intracellular loop, with N- and C-termini of the proteins located intracellularly (Milks et al., 1988). Monomers assemble into a hexameric complex to form a hemichannel, the so-called connexon, which docks in a head-to-head fashion to a second connexon in the adjacent cell (**Fig. 5B**). This non-covalent interaction leads to the formation of a gap junction channel (Makowski et al., 1977; Unwin and Zampighi, 1980).

The functional properties of gap junction channels are highly dependent on the involved Cx subunits. Most cannot only assemble with Cxs of the same kind (homomeric channels), but also with other Cxs (heteromeric channels), so that many functionally different types of gap junctions are possible. This versatility is increased by the fact that connected cells can express different sets of Cx subunits, so that not only connexons of equal subunit composition can form channels (homotypic channels), but also connexons composed of different subunit (heterotypic channels) (Koval, 2006). So far, only Cx31 and Cx36 have been shown to form exclusively homotypic channels (Elfgang et al., 1995; Teubner et al., 2000). Conductance, ion selectivity, molecular permeability and gating vary greatly between channel types. Conductance of homomeric channels has been measured in heterologous expression systems and varies by a factor of 30 from 10 pS (Cx30.2) to 310 pS (Cx37) (Veenstra et al., 1994; Kreuzberg et al., 2005). The bandwidth of ion selectivities ranges from slight anion-selectivity to cation-selectivity but is not connected to the permeability for larger charged molecules (Harris, 2007). Gating, the opening and closing of intercellular channels, is regulated by transjunctional voltage, intracellular pH, intracellular Ca^{2+} and phosphorylation of the protein subunits (Bruzzone et al., 1996; Moreno and Lau, 2007).

Besides connexins, pannexins have been discussed as an additional gap junction forming protein family in mammals (Bruzzone et al., 2003). However, although sharing structural and *in vitro* electrophysiological features, there is increasing evidence that pannexins do not form functional gap junctions but hemichannels *in vivo* (Bruzzone et al., 2003; Pelegrin and Surprenant, 2006; Thompson et al., 2006).

I.3.1 Cx36: Expression Pattern and Channel Properties

In the central nervous system, gap junctions are the morphological correlate of electrical synapses, which play an important role in shaping hippocampal oscillatory activity. The major gap junction forming protein in neurons is Cx36 (Rash et al., 2001) which was identified in 1998 by degenerate RT-PCR from rat inferior olive RNA and is, in the brain, exclusively expressed by neurons. The Cx36 coding region spans roughly 4 kb on mouse chromosome 2 and is interrupted by a single intron 71 bp after the translation initiation site. It encodes a 321 amino acid protein with a calculated molecular weight of 36 kDa (Condorelli et al., 1998).

Expression of Cx36 starts at E7.5 in extra-embryonic tissue and localizes to the developing forebrain by E9.5, a time point when neurogenesis is starting (Gulisano et al., 2000). By E14 to E18 Cx36 has been shown to be expressed in the cerebral cortex, with higher expression in the cortical plate and the ventricular zone than in the intermediate zone (Cina et al., 2007).

The postnatal expression of Cx36 in the brain has been systematically analyzed at the anatomical as well as at the functional level by several studies in rat and mouse. At early postnatal stages mRNA expression of Cx36 is widespread and peaks around P7 to P16 (**Fig. 6A**) depending on the brain region and the species (Sohl et al., 1998; Belluardo et al., 2000). At this time in development, GABAergic interneurons as well as GABAergic and glutamatergic neurons are coupled by Cx36 (Venance et al., 2000).

In the adult rat brain, highest levels of Cx36 mRNA expression are detected in the olfactory bulb, CA3, inferior olive and pineal gland (Condorelli et al., 1998). Additionally, Cx36 mRNA has been detected in a subpopulation of cells in the molecular layer and the granular

layer of the cerebellum, in a cell population in the anterior pituitary gland and in the ganglion cell layer and inner nuclear layer of the retina (Belluardo et al., 2000; Hansen et al., 2005).

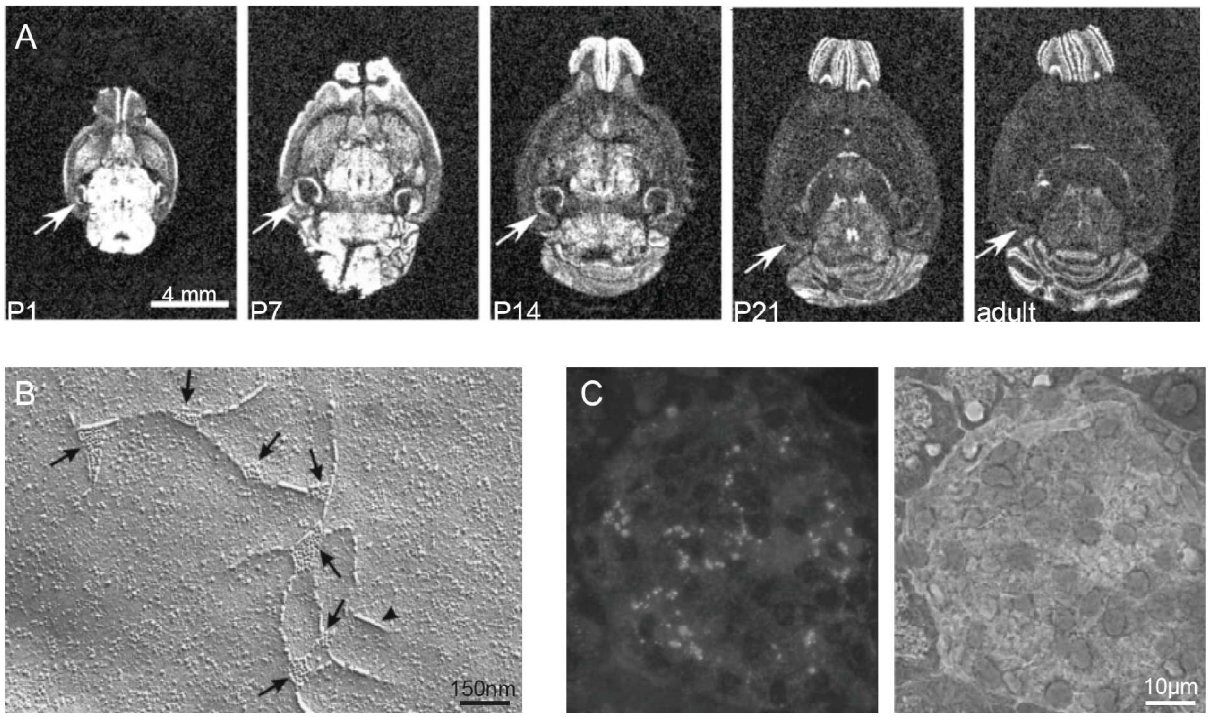

Figure 6: Cx36 expression in brain and pancreas.
A: Developmental expression pattern of Cx36 mRNA in wt mouse brains. Cx36 is highly expressed in young postnatal brains and downregulated with increasing age. In the adult, expression is easily detectable only in the olfactory bulb and the cerebellum (modified from Hormuzdi et al., 2001).
B: Freeze-fracture electron microscopy of rat pancreatic β-cells reveals gap junction plaques (arrows) in association with tight junction fibrils (arrowheads) (modified from Nlend et al., 2006).
C: Immunohistochemical labeling shows the expression of Cx36 in gap junction plaques between rat pancreatic β-cells (left picture). The picture on the right is the phase contrast view of the same islet (modified from Nlend et al., 2006).

A more quantitative analysis has been performed in the hippocampal formation and the cerebral cortex. In the cortex, sparse immunohistochemical labeling for Cx36 is distributed throughout layers II to VI. mRNA levels are highest in layers IV and V of rat cerebral cortex, where approximately 10 % of all neurons and 55 % of all PV-positive GABAergic interneurons contain Cx36 transcripts. In the rat hippocampus, protein expression has been shown to be rather modest in all subregions, while mRNA is expressed in and close to the DG GCL in 24 % and

in the hilus in 70 % of all neurons. In strata oriens, radiatum and lacunosum-moleculare of CA1 and CA3, where mostly interneuron somata are located, 30 – 80 % of all neurons and the same percentage of PV-positive GABAergic interneurons express this Cx subunit (Belluardo et al., 2000). In contrast to the rat hippocampus, Cx36 has been shown to be absent in mouse CA3 pyramidal cells by P30, and to be restricted to GABAergic interneurons (Hormuzdi et al., 2001). In fact, it has been demonstrated that Cx36 is the only gap junction-forming protein in GABAergic interneurons (Hormuzdi et al., 2001; Fukuda et al., 2006).

Apart from neurons, Cx36 is expressed by β-cells of the pancreas and by chromaffin cells of the adrenal medulla (Serre-Beinier et al., 2000; Martin et al., 2001; Degen et al., 2004). β-cells in the islets of Langerhans sense blood glucose concentration and secrete insulin in a pulsatile manner in response to elevated blood glucose. Fluorescence immunohistochemical and electron microscopical analyses have shown that Cx36 localizes exclusively to appositions of β-cell membranes (Serre-Beinier et al., 2000; Nlend et al., 2006) (**Fig. 6B + C**). Chromaffin cells are organized in cell clusters within the adrenal medulla (Hillarp, 1949) and release catecholamines in response to nicotinic stimulation (Iijima et al., 1992). Cx36 mRNA and protein have been identified in chromaffin cells by single-cell RT-PCR analysis and immunohistochemical stainings, respectively (Martin et al., 2001; Li et al., 2004).

The biophysical properties of channels formed by Cx36 are quite distinct from most other Cxs. Cx36 forms exclusively homotypic channels that show a very low single channel conductance of approximately 15 pS, a weak transjunctional voltage dependence and a relative insensitivity to absolute membrane potential in heterologous expression systems. Especially the low voltage dependence is important with regard to the neuronal expression: it allows the channels to remain open during the wide range of fluctuating membrane potentials occurring during neuronal activity (Srinivas et al., 1999; Teubner et al., 2000; Al-Ubaidi et al., 2000).

I.3.2 Phenotype of Cx36$^{-/-}$ Mice

The functional role of Cx36 containing gap junction channels became apparent after the generation of the first Cx36$^{-/-}$ mice in 2001 (Hormuzdi et al., 2001; Deans et al., 2001). The neuronal phenotype of these mice has since been analyzed electrophysiologically *in vitro* and *in*

vivo and also behaviorally. In addition, the analysis of these mice has demonstrated the role of Cx36 in pancreatic insulin secretion.

I.3.2.1 Electrophysiological Characterization of Cx36$^{-/-}$ Mice

In the brain, GABAergic interneurons are the main site of Cx36 expression. Ablation of Cx36 uncouples interneurons in the cortex, hippocampus, reticular thalamus and inferior olive. Basic electrophysiological properties of interneurons are left intact, except for an increased input resistance (Hormuzdi et al., 2001; Deans et al., 2001; Long et al., 2002; Landisman et al., 2002) (**Fig. 7A**). Intracellular recordings of hippocampal pyramidal cells and interneurons in Cx36$^{-/-}$ mice demonstrated that rhythmic membrane hyperpolarizations occurring at depolarized

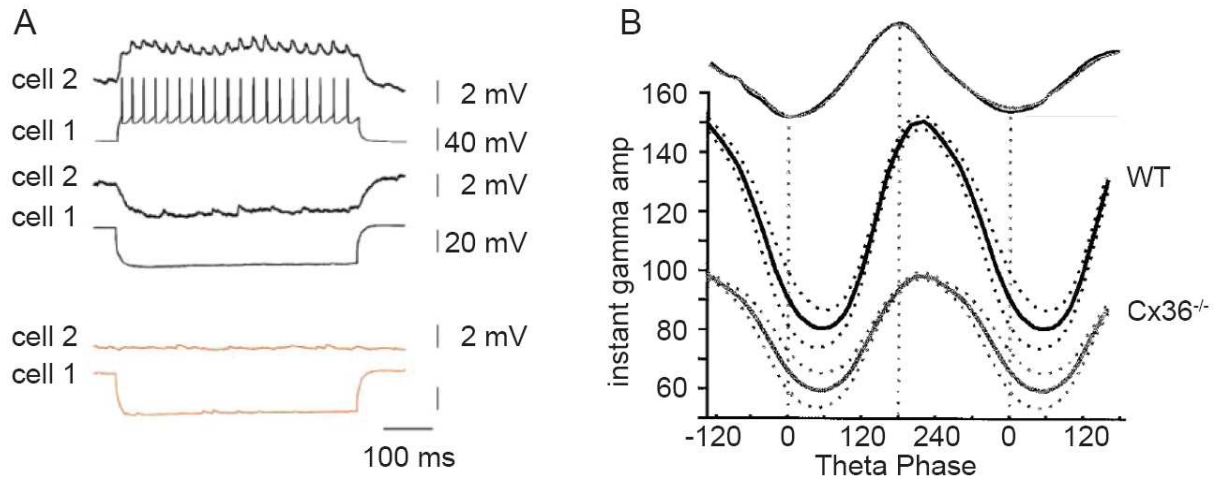

Figure 7: ***In vitro*** **and** ***in vivo*** **electrophysiological recordings in Cx36$^{-/-}$ mice.**
A: In wt mice (black traces) injection of a depolarizing or hyperpolarizing current in DG fast-spiking interneurons (cell 1) leads to a reflection of the voltage response in a second DG fast-spiking interneuron (cell 2), while current injection in interneurons from Cx36$^{-/-}$ mice shows that fast-spiking cells of the DG are uncoupled (from Hormuzdi et al., 2001).
B: *In vivo* electrophysiological recordings during wheel running from wt and Cx36$^{-/-}$ mice show the amplitude of gamma-frequency oscillations as a function of theta phase. In Cx36$^{-/-}$ mice the mean power of gamma oscillations is reduced compared to wt (from Buhl et al., 2003).

membrane potentials are impaired in rhythmicity and amplitude in comparison to wild-type (wt). This cellular impairment is also obvious at the network level *in vitro*, where ripple activity persists but the power of gamma-oscillations is reduced (Hormuzdi et al., 2001; Deans et al., 2001). More thorough analysis of ultra-fast rhythms showed that the frequency of sharp-wave and ripple occurrence is attenuated. Furthermore, the lack of Cx36 leads to reduction of epileptiform discharges in slices (Maier et al., 2002).

In vivo electrophysiological analysis of theta, gamma and ripple activity in the hippocampus by and large confirmed the *in vitro* findings. Ablation of Cx36 reduces the amplitude of gamma-oscillations during voluntary wheel running without altering the power of theta oscillations or the power and peak frequency of ripples (Buhl et al., 2003) (**Fig. 7B**).

I.3.2.2 Behavioral Analysis

Data from the behavioral analysis of $Cx36^{-/-}$ is limited to two studies that have been carried out in male mice. These studies show that $Cx36^{-/-}$ mice are not ataxic, display a regular walking pattern and reach equal performance levels on the rotarod (Kistler et al., 2002; Frisch et al., 2005). Also, anxiety-related behavior in the elevated plus-maze and open field arena as well as exploratory behavior in the open field are unaltered in $Cx36^{-/-}$ mice. In the Y-maze, a more complex environment, $Cx36^{-/-}$ mice habituate significantly less than wt mice during a spatial exploration task one day and four days after the first trial. This impairment is discussed to be due to memory defects. In an object recognition test, $Cx36^{-/-}$ mice are also impaired after delays of 45 min and 90 min, but not after shorter delay times, suggesting a defect in recognition memory (Kistler et al., 2002; Frisch et al., 2005).

I.3.2.3 Analysis of the Metabolic Phenotype

Besides the brain, Cx36 is also expressed in insulin secreting β-cells of pancreatic islets of Langerhans that do not express any other Cx genes (Serre-Beinier et al., 2000; Theis et al., 2004). In the $Cx36^{-/-}$ mouse, β-cells are uncoupled (**Fig. 8A**). This leads to elevated intracellular Ca^{2+} concentrations and a loss of synchronous Ca^{2+} oscillations in β-cells during glucose

stimulation. Additionally, Cx36$^{-/-}$ islets do not show a pulsatile insulin secretion in response to glucose stimulation but reach overall normal insulin secretion rates. The decline of insulin secretion from the pancreas at the end of glucose stimulation, however, has significantly slower shut-off kinetics in Cx36$^{-/-}$ mice compared to wt mice. At basal glucose levels, isolated islets as well as the perfused pancreas, show an increased insulin secretion rate (Ravier et al., 2005; Speier et al., 2007) (**Fig. 8B**). The influence of these changes on *in vivo* physiology has not been investigated yet.

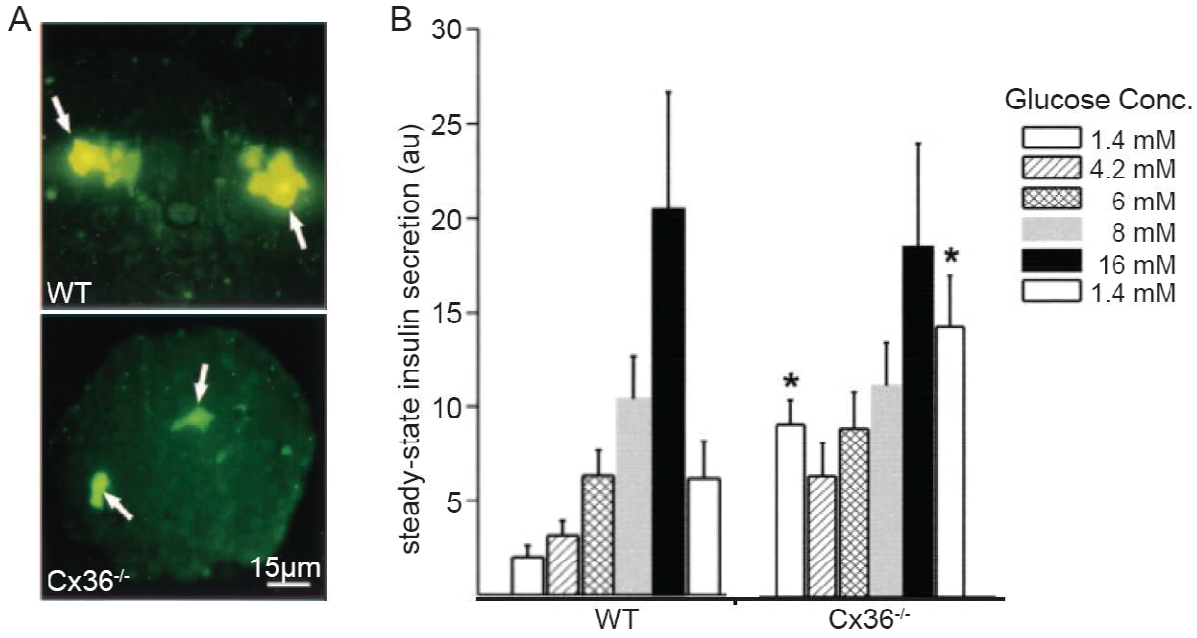

Figure 8: Effect of Cx36 ablation on pancreatic β-cells.
A: In Cx36$^{-/-}$ mice β-cells are uncoupled as shown by lack of Lucifer yellow diffusion between β-cells in Cx36$^{-/-}$ but not in wt mice.
B: The insulin secretion response to basal glucose concentration is increased in perfused pancreata from Cx36$^{-/-}$ mice compared to wt (modified from Ravier et al., 2005).

I.4 Aim of the Study

In vertebrates, connexins are the only protein family that couples cells electrically and metabolically and thus permits the concerted action of cell assemblies. Among the 20 different Cx proteins of the mouse, Cx36 shows very specific channel properties and a very restricted expression pattern. In the adult brain, for example, Cx36 is expressed only by GABAergic interneurons. $Cx36^{-/-}$ mice have been generated by several groups and male $Cx36^{-/-}$ mice have been already characterized at the anatomical, electrophysiological and behavioral level.

To understand the function of the protein better, we extended the analysis of male and female $Cx36^{-/-}$ mice and unexpectedly found a gender-specific phenotype. Thus, we identified a link between Cx36 and adult neurogenesis in the SGZ and showed an increase in immature neurons in the female DG. Interestingly, the observed effect was not directly caused by interneuronal uncoupling, and thus altered network activity in the hippocampus, but most likely by the metabolic and hormonal alterations in $Cx36^{-/-}$ females.

II. Materials and Methods

II.1 Materials

II.1.1 Mice

Cx36 knock-out mice ($Cx36^{-/-}$) generated in our group by Dr. Sheriar Hormuzdi were used for all experiments. Genotyping was performed by Regina Hinz (Hormuzdi et al., 2001).

For behavioral and immunohistochemical analysis as well as for determination of hormone levels, 5 to 6 months old $Cx36^{-/-}$ mice and their wt littermates were used. Analysis of the estrous cycle was started when wt and $Cx36^{-/-}$ females were 4 months of age.

For *in situ* hybridization experiments wt mice of different ages (P12, P21 and adult) were used. Gender specific expression analysis of Cx36 by real-time PCR was carried out in 2 months old wt animals.

II.1.2 Oligonucleotides

Oligonucleotides were custom-synthesized by Invitrogen GmbH, Karlsruhe.

Table 1: Oligonucleotides for real-time PCR.

β-actin sense	5'-caacttgatgtatgaaggctttggt-3'
β -actin antisense	5'-acttttattggtctcaagtcagtgtacag-3'
glucose-6-phosphate-dehydorgenase sense	5'-tgaccaattccatactccatggt-3'
glucose-6-phosphate-dehydorgenase antisense	5'-attctagctgctgtgcttgcct-3'
cyclophilin sense	5'-caaatgctggaccaaacacaa-3'
cyclophilin antisense	5'-gccatccagccactcagtct-3'
Cx36 sense	5'-tggcttcagtgttccaggcttgta-3'
Cx36 antisense	5'-cgctcacagcaaacatgaacacca-3'

Table 2: Oligonucleotides for *in situ* hybridization.

Cx36 is1	5'-ggtggtctctgtgttctgcagcaccccattgaccatggc-3'
Cx36 is2	5'-ctgggctccccggacagccagtttgatcttccgccat-3'

II.1.3 Antibodies

Antibodies were stored at - 20 °C or at + 4 °C according to the manufacturer's protocol.

Table 3: Primary antibodies.

Antibody	Concentration	Species	Supplier
anti - 5-Bromo-2-deoxyuridine(BrdU)	1:500	Rat	Accurate
anti - active caspase 3	1:10000	Rabbit	R&D Systems
anti - calbindin	1:5000	Mouse	Swant
anti - calretinin	1:5000	Rabbit	Swant
anti - cFos	1:10000	Rabbit	Calbiochem
anti - doublecortin	1:1000	Goat	Santa Cruz
anti - NeuN	1:1000	Mouse	Chemicon
anti - parvalbumin	1:3000	Mouse	Sigma

Table 4: Secondary antibodies.

Antibody	Concentration	Species	Supplier
anti - rabbit Alexa 488	1:1000	Goat	Invitrogen
anti - rabbit Alexa 488	1:1000	Donkey	Invitrogen
anti - mouse Alexa 488	1:1000	Goat	Invitrogen
anti - rabbit Cy3	1:2000	Goat	Dianova
anti - mouse Cy3	1:2000	Goat	Dianova
anti - goat Cy3	1:2000	Donkey	Dianova
anti - rat Cy3	1:1000	Goat	Dianova
anti - rabbit biotinylated	1:500	Goat	Vector Laboratories
anti - mouse biotinylated	1:500	Goat	Vector Laboratories

II.1.4 Special Chemicals and Kits

0.9 % NaCl	B. Braun Melsungen AG, Melsungen
3,3'-diaminobenzidine (DAB)	Sigma-Aldrich, München
BioSpin® 6 chromatography columns	BioRad, München
Bovine serum albumin	Sigma-Aldrich, München
BrdU	Sigma-Aldrich, München
Chrom(III) potassium sulfate dodecahydrate	Merck, Darmstadt
Diethylpyrocarbonat	Carl Roth, Karlsruhe
Elite ABC Kit	Vector Laboratories Burlingame,CA, USA
Eukitt	O. Kindler GmbH, Freiburg
Glucometer	Bayer, Leverkusen
Hematoxylin according to Harris	Carl Roth, Karlsruhe
High Capacity cDNA Reverse Transcription Kit	Applied Biosystems, Darmstadt
Insulin ELISA kit	Mercodia, Uppsala, Sweden
Isoflurane	Baxter, Unterschleißheim
Ketanest®	Pfizer, Karlsruhe
Kodak® BioMax MR film	Sigma-Aldrich, München
Papanicolaou's orange solution 2a	Carl Roth, Karlsruhe
Papanicolaou's polychromatic solution 3b	Carl Roth, Karlsruhe

Paraformaldehyde	Carl Roth GmbH, Karlsruhe
Polyvinyl alcohol 40-88	Fluka, Buchs, Switzerland
RNase free DNase	Qiagen, Hilden
RNeasy® MinElute™ Kit	Qiagen, Hilden
Rompun®	Bayer, Leverkusen
(α)-^{35}S- dATP	PerkinElmer, Rodgau- Jügesheim
SYBR® green PCR Master Mix	Applied Biosystems, Darmstadt
Terminal deoxynucleotide transferase	Roche, Mannheim
TRIzol	Invitrogen, Karlsruhe

II.1.5 Buffers and Solutions

All aequous buffers and solutions were prepared using desalted water from a MilliQ water purification system (Millipore).

Acid alcohol	1 % HCl in 70 % ethanol
Ammonia water	0.2 % concentrated NH_4OH in H_2O
10 x Phosphate-buffered saline	1.37 M NaCl 2.7 mM KCl 80 mM Na_2HPO_4 27.5 mM KH_2PO_4 adjust pH to 7.4
10 x SSC	1.5 M NaCl 0.15 M sodium citrate
Gelatine	5 g gelatine 2 mM Chrom(III) potassium sulfate dodecahydrate H_2O ad 1l
Maximalist buffer	50 % formamide 0.6 M NaCl 0.06 M sodium citrate 10 % dextrane

Mowiol	6 g glycerol 2.4 g polyvinyl alcohol 40-88 in 18 ml 0.13 M Tris-HCl pH 8.0
Nissl staining solution	1 % Lauth's violet acetate salt 0.1 M acetic acid 0.1 M sodium acetate In H_20
Tissue-wet buffer	50 % formamide 4 x SSC

II.1.6 Equipment

AbiPrism 7000 Sequence Detection System	Applied Biosystems, Darmstadt
Accelerating Rotarod model V4.0	TSE Systems, Bad Homburg
Camera System	INTAS
Confocal Laser Scanning Microscope Zeiss Axiovert 200 M	Carl Zeiss AG, Jena
Cryostat HM 500	Microm International GmbH, Walldorf
Fluorescence Microscope Olympus BX51	Olympus Deutschland GmbH, Hamburg
Leica Vibratome VT1000S	Leica, Wetzlar
Scintillation Counter Beckman LS6000SC	Beckman-Coulter, Krefeld

II. 2 Methods

II.2.1 Behavioral Experiments

Behavioral studies were performed by Dr. Elke Fuchs (Department of Clinical Neurobiology, University of Heidelberg, Germany). Male and female Cx36$^{-/-}$ mice and their wt littermates were maintained at the animal facilities of the University of Heidelberg in polypropylene macrocolon cages with food and water *ad libitum*. Lights were on from 7 a.m. to 7 p.m. and the temperature and humidity were kept at 20 $\pm$ 1 °C and 50 $\pm$ 10 %, respectively. All animal tests were approved by the Regierungspräsidium Karlsruhe (Germany). The testing person was not aware of the genotype of the animals.

II.2.1.1 Rotarod Test

Motor activity was tested using an accelerating rotarod with a corrugated black rubber surface (3.5 cm axis diameter). The mouse was placed on the rotarod while the drum was rotating at 4 rpm. In the course of one trial speed increased to 40 rpm over a period of 5 min and latency to fall was recorded as a measure for motor performance. Each mouse was tested in two blocks per day for three days with one block consisting of three 5 min trials.

II.2.1.2 Open Field Test

Locomotor activity was assessed by recording horizontal and vertical activity in an open field arena. The open field arena was a gray wooden box (50 x 30x 18 cm) that was divided into 15 10 x 10 cm squares. The test was carried out under normal room illumination conditions. Individual mice were placed into a corner of the test arena facing the sidewall. During the 5 min testing session the number of squares that were crossed (horizontal activity) and the number of rears (vertical activity) were recorded. The second session was performed the next day under the same conditions.

II.2.1.3 Exposure to a Novel Environment to Assess DG Activation

The test paradigm to assess dentate gyrus activation entailed an open field test with three objects placed into the test arena previously described. Experimentally naïve mice were accustomed to handling for 4 days and exposed to the novel environment twice for 10 min with a 15 min inter-trial-interval in their home cage. In the second session the position of one object was changed. Horizontal and vertical activity of the mice and their interactions with the objects were quantified from movies recorded with a camcorder. Object interaction was any kind of object exploration except for sitting on the object or moving the object. 2 h after the exploratory test, the mice were sacrificed and the brains were processed for immunohistochemical detection of cFos.

II.2.2 Histology

All experimenters were blinded to the genotype of the mice at the time of experiment.

II.2.2.1 Tissue Preparation

Wt and $Cx36^{-/-}$ mice were deeply anaesthetized by intraperitoneal injection of ketamine hydrochloride and xylazine hydrochloride, and transcardially perfused with 4 % parafomaldehyde (PFA) in PBS pH 7.4. Subsequently, brains were removed from the skull, postfixed for 2 h in 4 % PFA and stored in PBS at 4 °C. For BrdU immunohistochemical experiments brains were cut in 40 µm serial sections on a Leica VT1000S vibratome. 50 µm serial sections were cut for all other immunohistochemical experiments. For long-term storage of the sections PBS was supplemented with 0.05 % sodium azide.

Ovaries were dissected from wt and $Cx36^{-/-}$ females in the afternoon of the first day of estrus and fixed in 4 % PFA. They were shipped on wet ice and further processed by Dr. Deborah Burks (Centro de Investigación Príncipe Felipe, Valencia, Spain). After embedding in paraffin, serial 5 µm sections were prepared.

II.2.2.2 Staining Procedures and Image Acquisition

For imaging of brain sections an Olympus BX51 connected to an INTAS camera system was used. The applied software was MagnaFire 2.1C. Confocal imaging was done with a Zeiss Axiovert 200 M LSM 5 confocal laser scanning microscope using the Pascal 4.0 SP1 software.

II.2.2.2.1 Haematoxylin-eosin Staining of Ovaries

Briefly, sections were deparaffinized in xylol, rehydrated in descending ethanol concentrations and rinsed in water. Staining in Harris haematoxylin solution was followed by a wash in running tap water, differentiation in acid alcohol and bluing in ammonia water. After extensive washing and 10 rinses in 95 % ethanol, sections were counterstained with eosin solution, dehydrated and embedded in xylol-based mounting medium. Area and diameter measurements were made with the Image J program (NIH). This experiment was performed by Dr. Deborah Burks.

II.2.2.2.2 Nissl Stainings of Brain Sections

50 µm vibratome sections were mounted on gelatine-coated object slides and air dried. 30 sec to 1 min incubation in 0.1% Nissl staining solution was followed by destaining for 2 min under running tap water. After dehydration in ascending ethanol concentrations and clearing in xylol the sections were coverslipped with Eukitt.

II.2.2.2.3 Fluorescence Immunohistochemistry

All washing steps and incubations were carried out on a horizontal shaker and PBS was used as wash solution and diluent unless otherwise stated.

Free-floating sections were washed twice for 10 min at room temperature. Prior to antibody incubation, sections were permeabilized and blocked in 5 % bovine serum albumin (BSA) containing 0.02 % TritonX-100 for 45 min to 2 h at room temperature (RT). Primary antibodies were diluted according to **Tab. 3** and incubation was carried out for 18 to 48 h at 4 °C in a total volume of 500 µl. After removal of unbound primary antibody by three washing steps,

incubation with the fluorescent secondary antibody (**Tab. 4**) was carried out in the dark at RT for 2 h. Subsequently, the sections were washed three times in PBS and mounted onto gelatine-coated object slides. The air-dried slides were coverslipped in Mowiol.

For BrdU detection, the DNA was denatured prior to the above described immunohistochemical staining protocol. Briefly, this was achieved by incubation of the sections in 1 M HCl for 45 min at 45 °C followed by 15 min incubation in 10 mM Tris-HCl pH 8.5 at RT. After extensive washing with PBS, the staining protocol proceeded as decribed above.

II.2.2.2.4 DAB Immunohistochemistry

For DAB immunohistochemical analysis free-floating sections were washed twice and cryoprotected in 30 % sucrose in PBS for 3 h at 4 °C before permeabilization by five freeze - thaw cycles. Treatment with 1 % H_2O_2 for 10 min and blocking in 5 % BSA for 45 min to 2 h was followed by incubation with primary antibody dilution for 18 to 48 h at 4 °C. After several washing steps and incubation with biotinylated secondary antibody for 2 h, the sections were incubated in solutions A+B from the Elite ABC kit for 1.5 h at room temperature to enhance the signal. Subsequently, the buffer was changed to 20 mM Tris-HCl pH 7.4 and 5 mg/ml diamino-benzidine (in 20 mM Tris-HCl) were added to the sections as substrate for the color reaction. The reaction was started by addition of H_2O_2 to a final concentration of 0.02 %. For metal-enhanced DAB-immunohistochemistry, 1 mM nickelammoniumsulfate was added in parallel with H_2O_2. After antibody-specific development times the reaction was stopped by transferring the sections to 20 mM Tris-HCl. Sections were mounted on gelatine-coated slides, dehydrated and coverslipped in Eukitt after clearing in 100 % Xylol.

II.2.2.2.5 Quantification of Immunohistochemical Experiments

cFos positive nuclei were counted from at least 3 non-consecutive coronal sections per mouse between Bregma – 1.3 mm and -1.8 mm and cFos immunoreactive cells per section were calculated. For the remaining quantifications, cells were counted on every sixth section throughout the rostro-caudal extent of the hippocampus and the result was multiplied by six to

obtain total cell numbers for one hippocampus per animal. The data was statistically analyzed by ANOVA. Quantification of CR expression and of BrdU incorporation was performed by Dr. Elke Fuchs.

II.2.3 Analysis of Adult Neurogenesis

During the course of the experiment mice were kept in standard housing cages on a 12 h light-dark cycle with *ad libitum* access to food and water. Cages were changed once a week and except for the injections and cage changes mice were left undisturbed. These analyses were carried out by Dr. Elke Fuchs.

To analyze proliferation of adult stem cells, wt and $Cx36^{-/-}$ female mice were intraperitoneally injected with 50 mg/kg BrdU in 0.9 % NaCl twice a day, 6 h apart, on three consecutive days. Mice were perfused 24 h after the last BrdU pulse. To analyze maturation of newborn neurons wt and $Cx36^{-/-}$ mice were injected for a period of six days with the same protocol and sacrificed 28 d after the last injection. Brains were removed from the skull and the tissue was processed for immunohistochemical detection of BrdU or BrdU and NeuN. Quantification was performed as decribed for all immunohistochemical experiments.

II.2.4 Cx36 Expression Analysis

Expression analysis for Cx36 was carried out by radioactive *in situ* hybridization experiments and by quantitative real-time PCR analysis.

II.2.4.1 Radioactive *In Situ* Hybridization

II.2.4.1.1 Labeling of the Oligonucleotide Probes

Radiocative *in situ* hybridization was carried out using specific oligonucleotide probes 3'endlabeled with α-S^{35}-dATP. The labeling of the oligonucleotides (**Tab. 2**) was performed as previously described (Wisden and Morris, 2002) using terminal deoxynucleotide transferase according to the following protocol: All components except for the enzyme were combined and

well mixed by vortexing. The reaction was started by addition of 1 µl terminal transferase and the reaction mix was incubated at 37 °C for 5-7 min. After purification of the labeled oligonucleotide using a BioRad chromatography column, the labeling was assessed by measuring specific counts in a scintillation counter. Good labeling resulted in 50,000 to 300,000 cpm. Labeled oligonucleotides were stabilized by addition of 20 mM dithiothreitol (DTT) and stored at -20 °C until usage (a few days). Both oligonucleotide probes gave qualitatively similar results.

Reaction Mix:

oligonucleotide (5 ng/µl)	1 µl
5 x reaction buffer	1.5 µl
$CoCl_2$ (25 mM)	0.9 µl
α-S^{35}-dATP (12.5 µCi/µl)	1.5 µl
H_2O	9.1µl
terminal transferase (400 u/µl)	1 µl

II.2.4.1.2 Tissue Preparation and Hybridization

Mice were anaesthetized in isoflurane, decapitated and the brains were removed from the skull and immediately frozen on a metal plate placed on dry ice. Using a microtome-cryostat the brains were cut into 16 µm sagittal sections and mounted on superfrost object slides. The air-dried sections were then fixed for 5 min in ice-cold 4 % PFA in PBS, rinsed in PBS and subsequently dehydrated in ascending ethanol concentrations. Sections were again air-dried and hybridized overnight at 42 °C in 100 µl maximalist buffer containing 1 pg/µl labeled oligonucleotide and 2 µl 1M DTT in a wet chamber containing tissue-wet buffer. After 12-16 h of hybridization, sections were rinsed at RT in 1 x SSC and subsequently washed in 1 x SSC at 55 °C for 30 min. This was followed by a cooling step in RT 1 x SSC, subsequent washing in RT 0.1 x SSC and dehydration in ethanol. The dry sections were exposed to Kodak® BioMax MR film for four weeks.

II.2.4.2 Real-time PCR

II.2.4.2.1 RNA Preparation for cDNA Synthesis

Total RNA from hippocampus and hypothalamus was prepared using the TRIzol reagent. Brain tissue was dissected on ice, immediately submerged in 750 µl TRIzol and homogenized using a 21 G cannula attached to a 2 ml syringe. The succeeding steps of crude RNA preparation were carried out according to the TRIzol protocol. Following RNA precipitation, the air-dried RNA pellets were resuspended in 50µl total volume DNaseI digestion mix containing 3 µl DNaseI and 5 µl 10 x reaction buffer. Samples were incubated for 10 min at 37 °C to remove any genomic DNA present in the RNA preparation. Samples were further purified using the RNeasy® MinElute™ RNA clean-up kit. The purified RNA was eluted from the columns in two steps using 25 µl RNase-free H_2O in each step. Concentration of the RNA was determined by measuring OD_{260nm}.

II.2.4.2.2 First Strand cDNA Synthesis

First strand cDNA synthesis was performed according to the High Capacity cDNA Reverse Transcription Kit protocol. 0.5 µg total RNA (0.05 µg/µl) were used in the reverse transcription reaction in a total reaction volume of 20 µl:

RNA	10 µl
10 x buffer	2 µl
dNTPs	0.8 µl
Random hexamer oligonucleotides	2 µl
RNase inhibitor	1 µl
Reverse transcriptase (5 u/µl)	1 µl
H_2O	3.2 µl

All components were mixed and RNA was added. The reaction was carried out at 37 °C for 2 h followed by heat-inactivation of the enzyme for 5 min at 85 °C.

II.2.4.2.3 Real-time PCR

Expression of different genes of interest was quantitated by real-time PCR using the SYBR® green PCR Master Mix in a total reaction volume of 25 µl. Each sample was run in duplicate to correct for pipetting inaccuracy. Gene-specific oligonucleotides (**Tab. 1**) with a T_m of 60 °C were used in the amplification reaction. For each primer combination a standard curve was derived using genomic DNA in three different concentrations. This standard curve was used to calculate relative amounts of cDNAs from C_T values. Expression levels were calculated by normalizing values obtained for Cx36 to values obtained for different housekeeping genes.

Reaction Mix:

cDNA (1/40 dilution)	4 µl
SYBR® green PCR Master Mix	12.5 µl
Sense oligonucleotide	0.75 µl
Antisense oligonucleotide	0.75 µl
H_2O	7 µl

II.2.5 Hormone and Glucose Measurements

All hormone and metabolite measurements were carried out by Dr. Deborah Burks. Serum was prepared from trunk blood of wt and $Cx36^{-/-}$ and shipped on dry ice.

Insulin concentration was determined in serum prepared from the blood of fasted or fed mice with the use of a commercial insulin ELISA kit. Glucose was measured from the same serum samples by Glucometer.

Estradiol concentration was measured in serum from wt and $Cx36^{-/-}$ female mice that were sacrificed in the afternoon of the first day of estrus.

II.2.6 Analysis of the Estrous Cycle

Prior to measuring hormone levels and prior to RNA preparation, the cycle stage of females was determinded by analysis of cytological changes in the vaginal epithelium. To this end mice were handled for two weeks to accustom them to the treatment and then vaginal

smears were taken daily at 10 a.m. ± 1 h. The cells obtained by the lavage were smeared onto object slides and stained according to Papanicolaou's protocol (Papanicolaou, 1942). Briefly, this entailed fixation of the cells in 100 % ethanol for 30 min, followed by rehydration in descending ethanol concentrations and nuclear staining in Harris' haematoxylin solution. After dehydration in ascending ethanol concentrations the cytoplasm was stained using Papanicolaou's orange solution 2a and Papanicolaou's polychromatic solution 3b. The stained vaginal smears were again dehydrated, cleared in xylol and embedded in Eukitt. The different cell poplulations were counted using a light microsope. From the ratios of the different cell types the cycle stage was determined daily. These data were used to calculate the total cycle length and the average time spent in each cycle stage. A majority of nucleated epithelial cells in combination with a thin smear of leukocytes indicated proestrus. In estrus the smears contained almost exclusively cornified epithelial cells, while in diestrus the smears consisted mainly of leukocytes. Metestrus is an intermediate state in which the vaginal smears consist of approximately 50 % cornified epithelial cells and 50 % leukocytes (Cohen et al., 2002)

II.2.7 Statistical Analysis

Statistical analysis of the behavioral experiments and of the estrous cycle analysis was performed by ANOVA and the appropriate post hoc test (SigmaStat). cFos counts were analyzed by ANOVA using the SSPS 16.0 software, while the remaining immunohistochemical data sets were analyzed using SigmaStat. Student's t-test was used for data analysis of Cx36 expression levels (SSPS 16.0), from hormone and glucose measurements as well as from morphological analyses of the ovaries (SigmaPlot).

All data represent mean ± standard error of the mean (SEM) or mean ± standard deviation (STD).

III. Results

III.1 Behavioral Analysis of Cx36$^{-/-}$ Males and Females

The phenotype of Cx36$^{-/-}$ mice that were generated by our group and others (Hormuzdi et al., 2001; Deans et al., 2001) has been characterized at the electrophysiological (Hormuzdi et al., 2001; Deans et al., 2001; Buhl et al., 2003) as well as at the behavioral level (Kistler et al., 2002; Frisch et al., 2005). All analyses, however, were restricted to male Cx36$^{-/-}$ mice.

To increase our understanding of the function of Cx36, we started a pilot behavioral study of female Cx36$^{-/-}$ mice in comparison to male Cx36$^{-/-}$ mice entailing analysis of motor performance on the rotarod and analysis of exploratory activity in an open field arena.

III.1.1 Lack of Cx36 does not Alter Motor Coordination

Cx36 mRNA is expressed in the molecular and the granular layers of the cerebellar cortex and in the inferior olive, which are brain regions important for motor coordination (Llinas and Welsh, 1993; Belluardo et al., 2000). Thus, ablation of Cx36 might influence motor behavior. A previous study investigating motor performance has shown that male Cx36$^{-/-}$ mice show a regular walking pattern and are normal on the accelerating rotarod (Kistler et al., 2002).

To analyze motor learning, male and female mice were trained on the accelerating rotarod in two blocks per day on three consecutive days. One block consisted of three 5 min trials with gradually increasing speed from 4 rpm to 40 rpm. In each trial the latency to fall was recorded as a measure of motor performance. In females an effect of block was apparent but neither an effect of genotype nor a genotype by block interaction could be observed (two-way ANOVA: effect of genotype: $F_{(1,96)} = 1.075$, $P = 0.302$; effect of block: $F_{(5,96)} = 13.809$, $P < 0.001$; genotype by block interaction: $F_{(5,96)} = 2.272$, $P = 0.053$) (**Fig. 9B**). Also in males there was an effect of block but neither an effect of genotype nor a genotype by block interaction could be detected (two-way ANOVA: effect of genotype: $F_{(1,102)} = 2.164$, $P = 0.144$; effect of block: $F_{(5,102)} = 9.607$, $P < 0.001$; genotype by block interaction $F_{(5,102)} = 0.275$, $P = 0.926$) (**Fig. 9A**).

Thus, both male and female Cx36$^{-/-}$ mice did not differ from their wt littermates in motor coordination and improved their performance across trials.

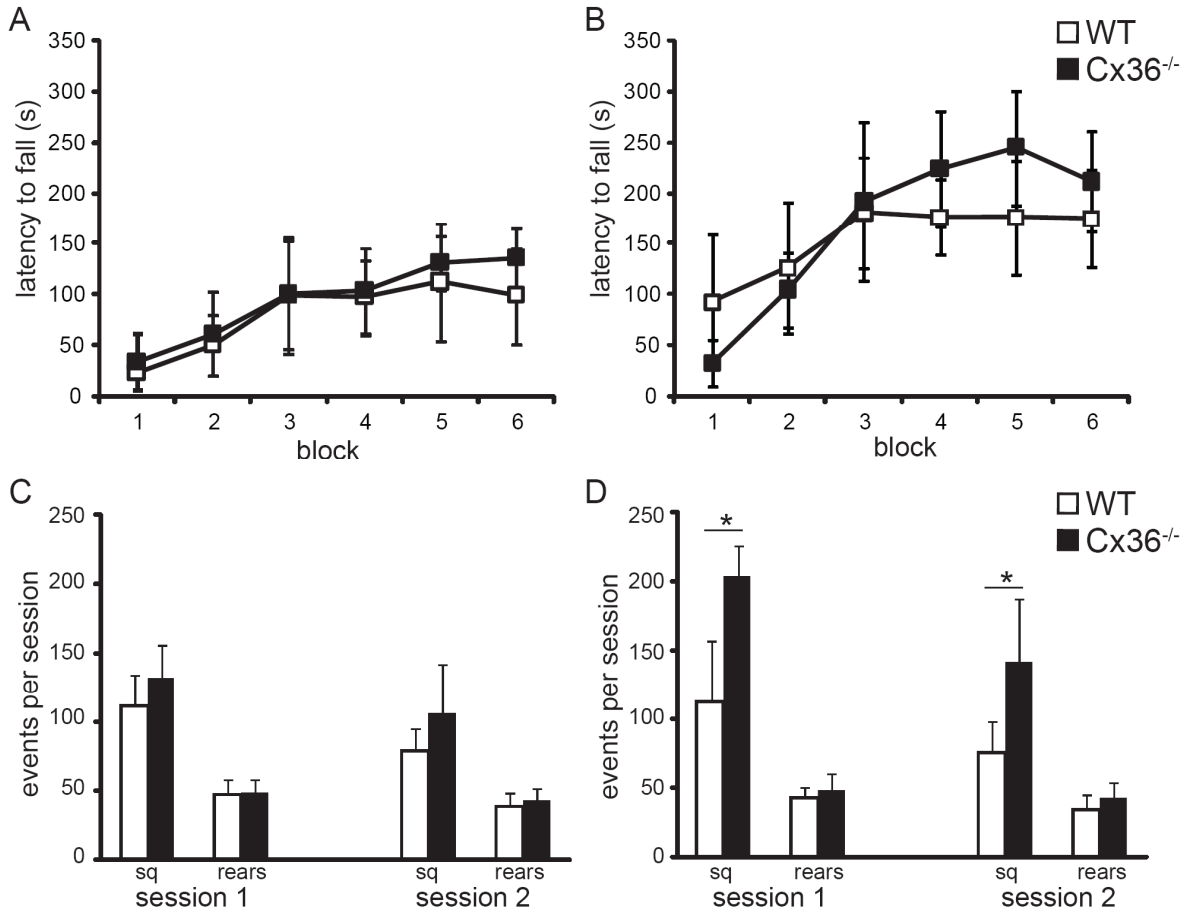

Figure 9: Behavioral analysis of Cx36$^{-/-}$ males and females revealed normal motor performance but novelty-induced hyperactivity in Cx36$^{-/-}$ females.

A + B: Analysis of wt and Cx36$^{-/-}$ males (A) and females (B) on the accelerating rotarod. Each block consisted of three 5 min trials and in each trial the rotarod accelerated from 4 rpm to 40 rpm. Latency to fall was recorded as a measure of motor performance. Blockwise comparison of mean latency to fall showed that there was no difference in the motor performance at the beginning or the end of training between genotypes. All four groups of mice improved with training and were thus able to learn the task. Data represent mean ± SEM. Males: $n_{(wt)} = 9$, $n_{(Cx36-/-)} = 10$; females: $n_{(wt)} = 9$, $n_{(Cx36-/-)} = 9$.

C + D: Analysis of spontaneous exploratory activity in the open field arena on two consecutive days in wt and Cx36$^{-/-}$ males (C) and females (D). On both days of testing, wt and Cx36$^{-/-}$ males (C) did not differ in horizontal (number of squares) or vertical activity (number of rears). Cx36$^{-/-}$ females (D) showed doubled horizontal activity compared to wt females in both sessions, while they did not differ in the number of rears. Data represent mean ± SEM. Males: $n_{(wt)} = 14$, $n_{(Cx36-/-)} = 11$; females: $n_{(wt)} = 16$, $n_{(Cx36-/-)} = 13$. (*, $P \leq 0.05$). These experiments were carried out by Dr. Elke Fuchs.

III.1.2 Lack of Cx36 Increases Exploratory Activity in Females

In Cx36$^{-/-}$ mice hippocampal GABAergic interneurons are electrically uncoupled and thus the synchronization of the neuronal network is perturbed (Venance et al., 2000; Hormuzdi et al., 2001; Buhl et al., 2003). Since the hippocampus has been reported to be highly involved in exploration (O'Keefe and Dostrovsky, 1971; O'Keefe, 1976), we analyzed exploratory behavior of Cx36$^{-/-}$ mice.

Spontaneous exploratory behavior of male and female Cx36$^{-/-}$ mice and their respective wt littermates was tested in an open field arena (50 x 30 x 18 cm) on two succeeding days. As a measure of exploratory activity the number of squares the mice crossed (horizontal activity) and the number of rears (vertical activity) per 5 min session was recorded. Male Cx36$^{-/-}$ mice did not differ from their wt littermates in either horizontal or vertical activity ($P \geq 0.05$) (**Fig. 9C**). Female Cx36$^{-/-}$ mice, however, crossed approximately twice as many squares as their wt littermates in both trials, while the number of rears did not differ (number of squares session 1: wt: 113.5 ± 43.9, Cx36$^{-/-}$: 204.5 ± 21,4; $F_{(1,27)}$= 100.018, $P < 0.001$; number of squares trial 2: wt: 75.6 ±22.8, Cx36$^{-/-}$: 142.4 ± 45; H = 11.556, $P < 0.001$) (**Fig. 9D**). Summarizing, female Cx36$^{-/-}$ mice showed increased spontaneous activity in the open field arena compared to their wt littermates, while male Cx36$^{-/-}$ did not differ from their respective littermates.

III.2 DG Activation is Altered in Cx36$^{-/-}$ Females

Among the three main subregions of the hippocampus the DG is thought to function as a “filter” for most incoming information from neocortical regions into the hippocampus by potentially working as a pattern separator (Marr, 1971; Rolls, 1989). During exploration of novel environments a rapid pattern separation is presumably involved in the fast formation of an intrahippocampal representation of the environment (Lee et al., 2005). Additionally, place fields have been demonstrated for DG granule cells (Jung and McNaughton, 1993) indicating that during exploration of an environment specific subsets of cells may be repeatedly activated.

To assess activation of the DG during exploration, a test paradigm was employed that entailed exploration of a novel environment followed by immunohistochemical detection of the

immediate-early gene cFos, which is a general marker for neuronal activation (Morgan et al., 1987; Sagar et al., 1988).

Experimentally naïve mice explored an open field arena containing three objects twice for 10 min with a 15 min intertrial interval (ITI). During exploration of the novel environment, horizontal and vertical activity and the time spent with objects was recorded. Following the test, the mice were kept in their homecage for 2 h to allow for the expression of the marker gene cFos. Analysis of exploratory behavior in the novel environment confirmed the results obtained in the open field test: Male $Cx36^{-/-}$ mice did not differ from their wt littermates in either the number of squares they crossed (session 1: wt: 139.3 ± 33.5, $Cx36^{-/-}$: 170.7 ± 48.6; $F_{(1,11)}$= 1.180, P = 0.301; session 2: wt : 100 ± 29.4, $Cx36^{-/-}$: 148.3 ± 29.1; $F_{(1,11)}$ = 3.898, P = 0.074) or the number of rears (session 1:wt: 70.9 ± 18.4, $Cx36^{-/-}$: 70 ± 19; $F_{(1,11)}$ = 0.00409, P = 0.950; session 2: wt: 55.4 ± 17.3, $Cx36^{-/-}$: 61.2 ± 16.8; $F_{(1,11)}$ = 0.269, P = 0.614 (**Fig. 10A**). Mice of both genotypes showed a trend towards lower exploratory acitivity in the second trial. Male wt and $Cx36^{-/-}$ mice also did not differ in the time they spent exploring the presented objects (session 1: wt: 62 ± 9.1 s, $Cx36^{-/-}$: 77.7 ± 18.6 s; $F_{(1,11)}$ = 2.362, P = 0.153; session 2: wt: 45.6 ± 7.5 s, $Cx36^{-/-}$: 52.2 ± 11.3 s; $F_{(1,11)}$ = 0.918, P = 0.359) (**Fig. 10C**).

Female $Cx36^{-/-}$ mice, in contrast, showed an increase in horizontal activity of approximately 80 % in the first session and of about 130 % in the second session compared to wt littermate controls (number of squares session 1: wt = 159.1 ± 31, $Cx36^{-/-}$ = 289.1 ± 60.6; $F_{(1,14)}$ = 13.324, P = 0.003; session 2: wt = 112.4 ± 26.9, $Cx36^{-/-}$: 255.9 ± 78.8; H = 9.114, P = 0.003). In contrast to this, wt females showed a trend towards decreased horizontal activity in the second session. Vertical activity was increased in the second but not in the first session (number of rears session 1: wt: 53.1 ± 18.4, $Cx36^{-/-}$: 72.9 ± 19.5; H = 2.696, P = 0.101; session 2: wt: 40 ± 13.7, $Cx36^{-/-}$: 73.7 ± 18.3; $F_{(1,14)}$ = 8.547, P = 0.011) (**Fig. 10B**). Additionally, $Cx36^{-/-}$ females spent approximately twice as much time with object exploration than their wt littermates (session 1: H = 6.745, P = 0.009; session 2: $F_{(1,14)}$ = 17,383, P ≤ 0.001) (**Fig. 10D**). Thus, female $Cx36^{-/-}$ mice showed hyperactivity at initial exposure to a novel environment and, in contrast to wt females and males of both genotypes, failed to habituate during a second trial of exploration.

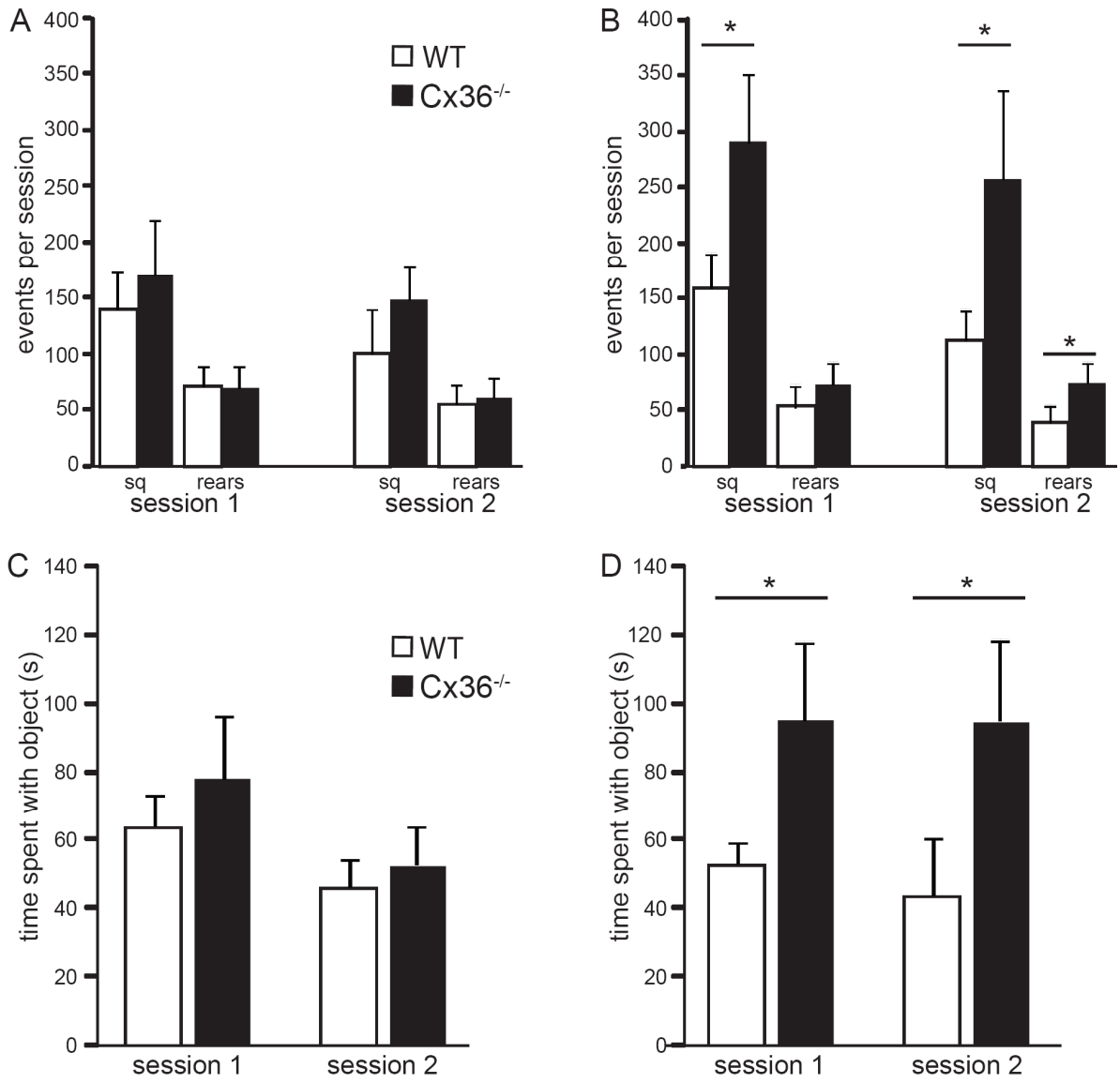

Figure 10: Exploratory test in a novel environment to analyze DG activation.
To analyze activation of the DG by an exploratory task, wt and Cx36$^{-/-}$ mice of both genders were allowed to explore a novel environment twice for 10 min with a 15 min ITI during which one of the three objects was exchanged.
A + C: As in the open field test male Cx36$^{-/-}$ mice did not differ from wt littermates in either horizontal or vertical activity (A). Also the time they spent exploring the presented objects was not significantly different between genotypes (C). Data represent mean ± SEM. $n_{(wt)} = 7$, $n_{(Cx36-/-)} = 6$.
B + D: Confirming the data obtained in the open field test, Cx36$^{-/-}$ females crossed significantly more squares in both sessions. The increase in the number of rears reached significance only in session 2 (B). In both sessions, Cx36$^{-/-}$ mice spent approximately twice more time exploring the objects than wt females (D). Data represent mean ± SEM. $n_{(wt)} = 7$, $n_{(Cx36-/-)} = 9$. (*, $P \leq 0.05$). This experiment was carried out by Dr. Elke Fuchs.

Cage control mice were treated like the mice that underwent the test. On the day of perfusion, the animals were handled, placed back into their homecage for 2h and subsequently sacrificed.

To analyze activation of the DG, the brains were processed for cFos immunohistochemistry. cFos positive nuclei in the DG were counted in at least 3 non-consecutive sections of the hippocampus between Bregma – 1.3 mm and – 1.8 mm and the average number of activated cells per section was calculated.

In all analyzed animals, cFos immunoreactivity in the DG localized mostly to nuclei of granule cells and less frequently to hilar neurons (**Fig. 11A + 12A**). Cage control males, wt as well as $Cx36^{-/-}$, displayed only few cFos immunoreactive nuclei and therefore activated cells in the suprapyramidal blade of the DG GCL (cells/section wt: 2.05 ± 2.66; $Cx36^{-/-}$: 5.97 ± 4.13; $F_{(1,9)}$ = 2.448, P = 0.152). Following exploration, the mean number of activated granule cells per section in the suprapyramidal blade of the GCL increased to 18.58 ± 3.76 in wt males ($F_{(1,10)}$ = 43.275, P ≤ 0.001) and to 20.18 ± 7.04 in $Cx36^{-/-}$ males ($F_{(1,10)}$ = 7.889, P = 0.019). This increase was not significantly different between genotypes ($F_{(1,11)}$ = 0.113, P = 0.743) (**Fig. 11B**). Furthermore, the number of activated cells in the infrapyramidal blade or the hilus under control and test conditions did not differ between wt and $Cx36^{-/-}$ males. In addition to the suprapyramidal blade, exploratory activity substantially augmented the number of cFos immunoreactive cells also in the infrapyramidal blade of wt mice (cage control: 0.95 ± 0.97 cells/section, test: 6.4 ± 2.5 cells/section; $F_{(1,10)}$ = 13,588, P = 0.004) (**Fig. 11B**).

As in males, very few neurons were activated in the DG of cage control wt females (suprapyramidal blade: 6.09 ± 1.91 cells/section; infrapyramidal blade: 1.39 ± 0.5 cells/section). In mice that performed the exploratory test, four times more cells in the suprapyramidal and in the infrapyramidal blade of the DG expressed cFos (suprapyramidal blade: 24.65 ± 5.86 cells/section; $F_{(1,10)}$ = 26.939, P ≤ 0.001; infrapyramidal blade: 6.55 ± 2.1 cells/section; $F_{(1,10)}$ = 15.139, P = 0.003) (**Fig. 12**).

In $Cx36^{-/-}$ females, in contrast, many neurons in the suprapyramidal and infrapyramidal blade were activated under cage control conditions and expressed cFos (suprapyramidal blade: 12.44 ± 2.89 cells/section; infrapyramidal blade: 3.7 ± 1.3 cells/section). In comparison to wt cage control females, the number of activated cells was significantly increased (suprapyramidal

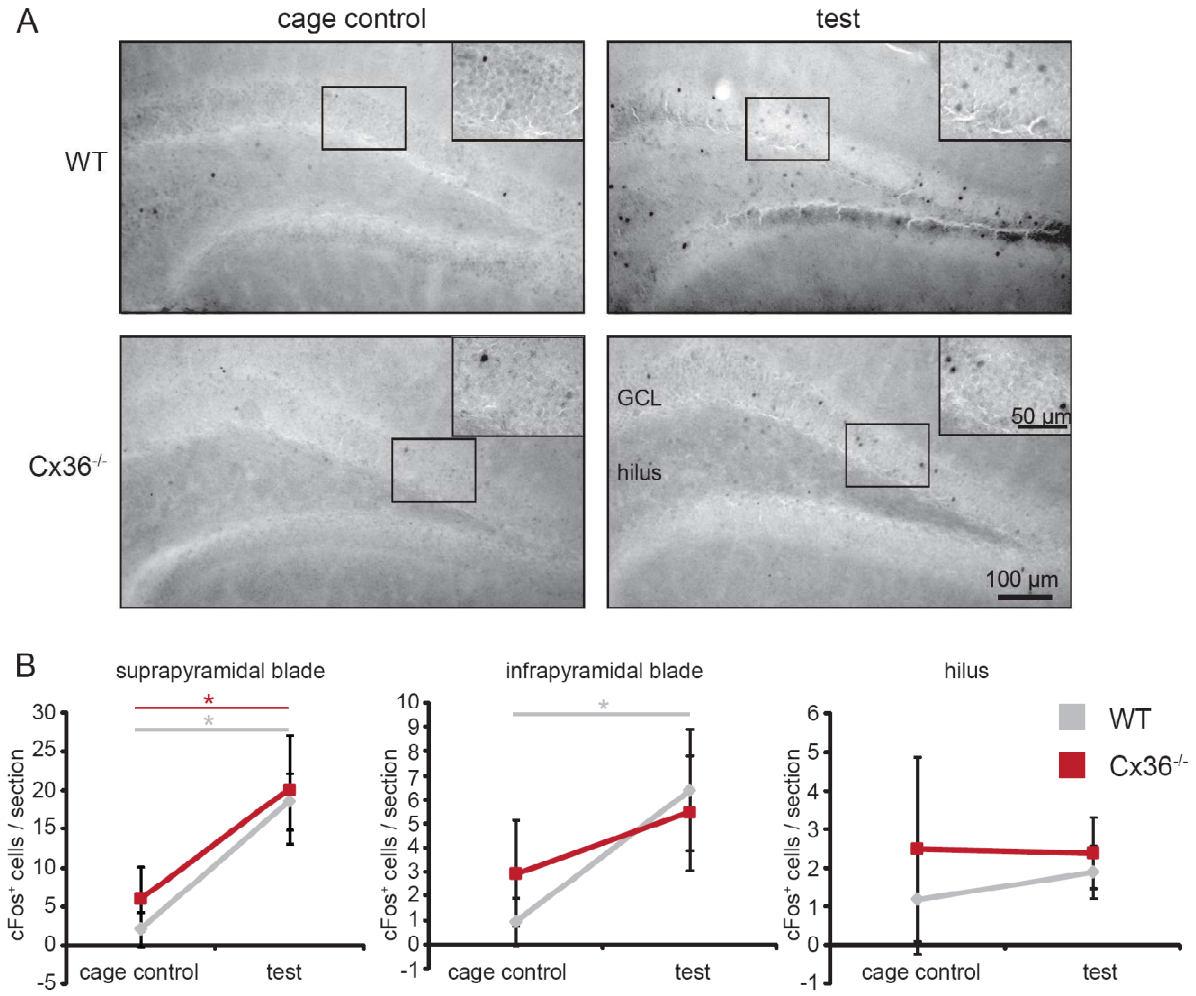

Figure 11: Exploratory activity increases cFos positive granule cells in wt and Cx36$^{-/-}$ males.
A: Nickel-enhanced DAB-immunohistochemical experiments showed nuclear localization of cFos protein (insets), mostly in the GCL of the DG and less frequently in the hilus. The DG of cage control mice (left panels) displayed very low numbers of activated cells, while the exploratory test stongly increased the number of cFos expressing cells (right panels).
B: At least three non-consecutive coronal sections were analyzed for cFos expression and cell counts normalized to the number of analyzed sections. Quantification of cFos expression in the suprapyramidal blade, infrapyramidal blade and hilus of the DG revealed that wt and Cx36$^{-/-}$ were never significantly different from each others, while induction of cFos expression by the test was significant in the suprapyramidal blade in both genotypes and in the infrapyramidal blade in wt. Data represent mean ± SEM. Test: $n_{(wt)} = 7$, $n_{(Cx36-/-)} = 6$; cage control: $n_{(wt)} = 5$, $n_{(Cx36-/-)} = 6$. (*, $P \leq 0.05$ in wt (control vs. test); *, $P \leq 0.05$ in Cx36$^{-/-}$ (control vs. test).

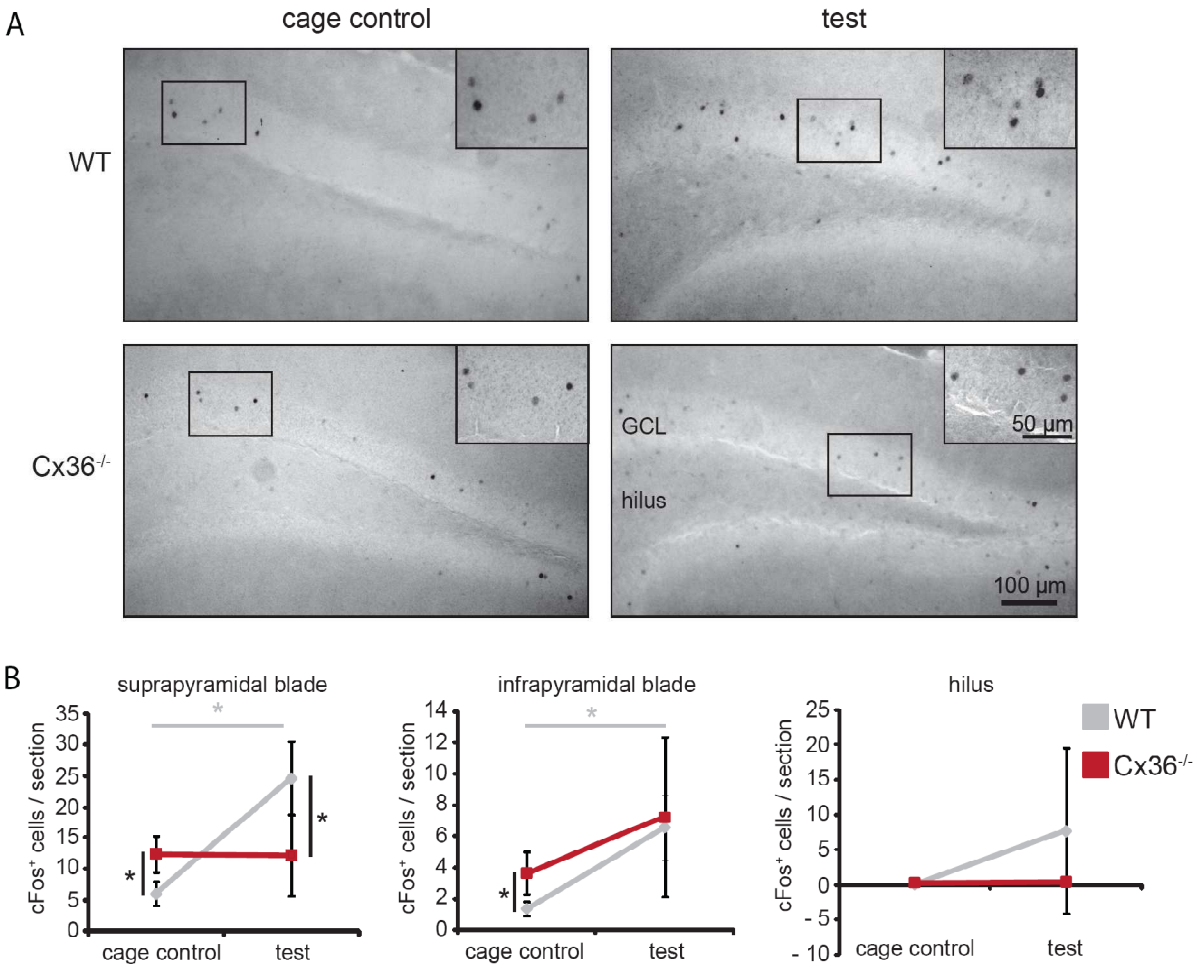

Figure 12: Lack of Cx36 causes an increase in activated cells in the female DG following exploration of a novel environment.

A: Immunohistochemical expression analysis of the immediate-early gene cFos in the DG of $Cx36^{-/-}$ and wt females following exploratory activity (right panels) and control experiment (left panels). As in males, cFos expression was analyzed by nickel-enhanced DAB-immunohistochemistry and the signal localized mostly to nuclei of granule cells in both genotypes and conditions (insets) and less frequently to the nuclei of hilar neurons.

B: Quantification of cFos positive cells in the DG of wt and $Cx36^{-/-}$ females demonstrated increased activity of DG granule cells in $Cx36^{-/-}$ females under control conditions in the suprapyramidal and infrapyramidal blade. In these mice the test failed to increase the activation level in both areas, while in wt exploration led to significant higher numbers of cFos expressing cells. cFos expression in the hilus was neither affected by genotype nor by treatment. Data represent mean ± SEM. Test: $n_{(wt)} = 7$, $n_{(Cx36-/-)} = 9$; cage control: $n_{(wt)} = 5$, $n_{(Cx36-/-)} = 8$; (*, $P \leq 0.05$ in wt (control vs. test); *, $P \leq 0.05$ in $Cx36^{-/-}$ (control vs. test); *, $P \leq 0.05$ (wt vs. $Cx36^{-/-}$).

blade: $F_{(1,11)}$ = 7.703, P = 0.018; infrapyramidal blade: $F_{(1,11)}$ = 6.106, P = 0.031). Remarkably, exploration failed to further activate the DG of Cx36$^{-/-}$ females (suprapyramidal blade: 12.28 ± 6.59 cells/section, $F_{(1,15)}$ = 0.002, P = 0.965 (cage control vs. test); infrapyramidal blade: 7.26 ± 5.1 cells/section; $F_{(1,15)}$ = 1.772, P = 0.203 (cage control vs. test)). As in males, the number of cFos positive cells in the hilus did not differ between groups (**Fig. 12**).

In summary, the employed test paradigm revealed a gender specific difference in the behavioral reaction of Cx36$^{-/-}$ mice to a novel environment. This was accompanied by a change in the activation level of the DG. Unlike males of both genotypes and female wt mice, Cx36$^{-/-}$ females displayed a high baseline activation of the DG under cage control conditions. In males and wt females exploration significantly activated the DG, whereas in Cx36$^{-/-}$ female mice no increase in activity of DG granule cells was observed.

III.3 Anatomical Analysis of the DG

To investigate if anatomical alterations were underlying the observed phenotype, we performed immunohistochemical experiments and analyzed the expression of different neurochemical markers of the DG.

To rule out gross morphological alterations in the hippocampus as a reason for the observed phenotype, Nissl stainings were performed. In Fig. 13 low magnification views of Nissl stained hippocampi from males and females of both genotypes and higher magnification views of the DG are shown. These stainings did not reveal differences in the gross anatomy of the hippocampus. Closer inspection of the DG also failed to show any disruption of the GCL or other morphological changes (**Fig. 13**).

Since Cx36 is expressed in about 50 % of all PV-positive interneurons (Belluardo et al., 2000) and since this class of interneurons plays an important role in hippocampal function (Vreugdenhil et al., 2003; Fuchs et al., 2007), the number of PV-positive cells in GCL and hilus was analyzed by fluorescence immunohistochemistry. Cells were counted on serial sections throughout the rostro-caudal extent of the hippocampus. Comparison of cell counts in the GCL and hilus showed that wt and Cx36$^{-/-}$ males as well as wt and Cx36$^{-/-}$ females did not differ in the number of PV cells (**Tab. 5**).

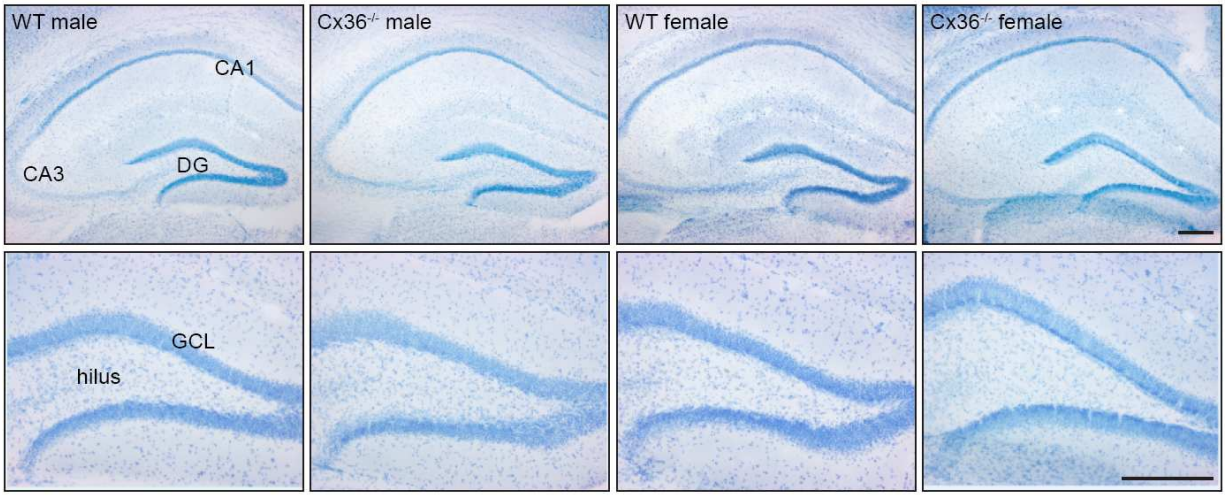

Figure 13: Nissl stainings did not reveal any gross morphological defects in Cx36$^{-/-}$ hippocampi.
Low magnification view of Nissl stained sections from male and female wt and Cx36$^{-/-}$ brains did not reveal any obvious morphological differences (upper panels). Higher magnification view of the DG of the same sections confirmed that the layering of the DG was undisrupted (lower panels). Scale bars: 250 µm.

Table 5: Quantification of PV expressing cells in the DG.

	GCL (cells/DG)		hilus (cells/DG)	
	wt	**Cx36$^{-/-}$**	**wt**	**Cx36$^{-/-}$**
male	288.9 ± 164.7	265 ± 147.4	39.4 ± 18.6	54 ± 17.1
female	266 ± 42.9	334.8 ± 81.4	74 ± 62.5	51 ± 41

males: $n_{(wt)} = 7$, $n_{(Cx36-/-)} = 6$; females: $n_{(wt)} = 6$, $n_{(Cx36-/-)} = 10$.
Data represent mean ± SEM.

The expression of calbindin (CB), another marker for a specific subset of GABAergic interneurons and for mature granule cells, was analyzed next (Freund and Buzsaki, 1996; Kempermann et al., 2004). Antibody stainings of coronal sections suggested reduced CB expression in patches of the GCL of female Cx36$^{-/-}$ mice (**Fig. 14**), but, in conjunction with the Nissl stainings, not a reduction of the number granule cells (**Fig. 13**). This staining pattern was not observed in male Cx36$^{-/-}$ or wt mice (**Fig. 14**).

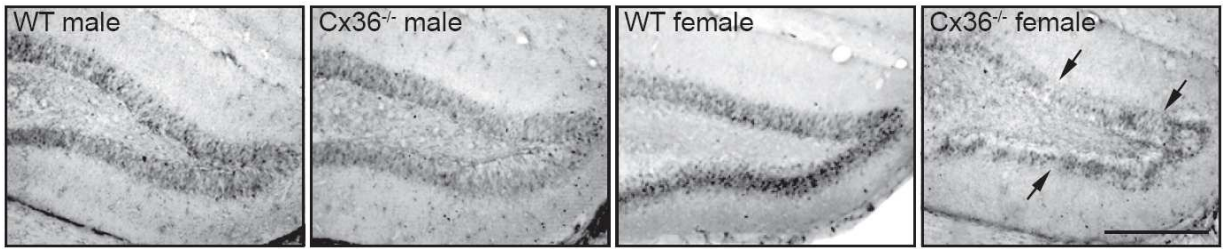

Figure 14: Patches in the GCL of female Cx36$^{-/-}$ DG are devoid of CB expression.
DAB-immunohistochemical stainings for the calcium binding protein CB showed that patches of granule cells (arrows) in the DG of Cx36$^{-/-}$ females were devoid of CB immunoreactivity. This was not caused by loss of granule cells, since the Nissl stainings (Fig. 13) did not display a disruption of the GCL. Scale bar: 250 µm.

Calretinin (CR) is a marker for yet another subpopulation of GABAergic interneurons and also for immature granule cells in the DG. Immature granule cells can be distinguished from interneurons by their location and the size of their soma: the latter have a bigger soma and are mainly located outside the GCL and the SGZ of the DG (Freund and Buzsaki, 1996; Kempermann et al., 2004). Initial analysis of sections from wt and Cx36$^{-/-}$ mice revealed an obvious increase in small CR expressing cells in the GCL of Cx36$^{-/-}$ female mice. To quantify this, CR immunoreactive cells were counted on serial coronal sections throughout the hippocampus (**Fig. 15**). The SGZ of female wt mice contained on average half as many CR-positive cells, than the SGZ of Cx36$^{-/-}$ females ($n_{(wt)}$ = 6, $n_{(Cx36-/-)}$ = 6, P ≤ 0.01). The increase of CR expressing cells was even more pronounced in the GCL. The wt GCL contained on average 110 ± 80 CR-positive cells, while the mean number of CR-positive cells in the GCL of Cx36$^{-/-}$ females was 1946.7 ± 382.8 (P ≤ 0.001) (**Tab. 6**). In males the number of CR cells did not differ between genotypes in any of the two investigated regions of the DG (**Fig. 15, Tab.6**).

Table 6: CR expressing cells in the DG.

	GCL (cells/DG)		SGZ (cells/DG)	
	Wt	**Cx36$^{-/-}$**	**wt**	**Cx36$^{-/-}$**
male	123 ± 86	73 ±19	669 ± 238	589 ± 183.3
female	110 ± 80	1946.7 ± 382.8*	989.2 ± 413.8	2059 ± 331*

males: $n_{(wt)}$ = 6, $n_{(Cx36-/-)}$ = 6; females: $n_{(wt)}$ = 6, $n_{(Cx36-/-)}$ = 6.; *, P ≤ 0.05.
Data represent mean ± SEM.

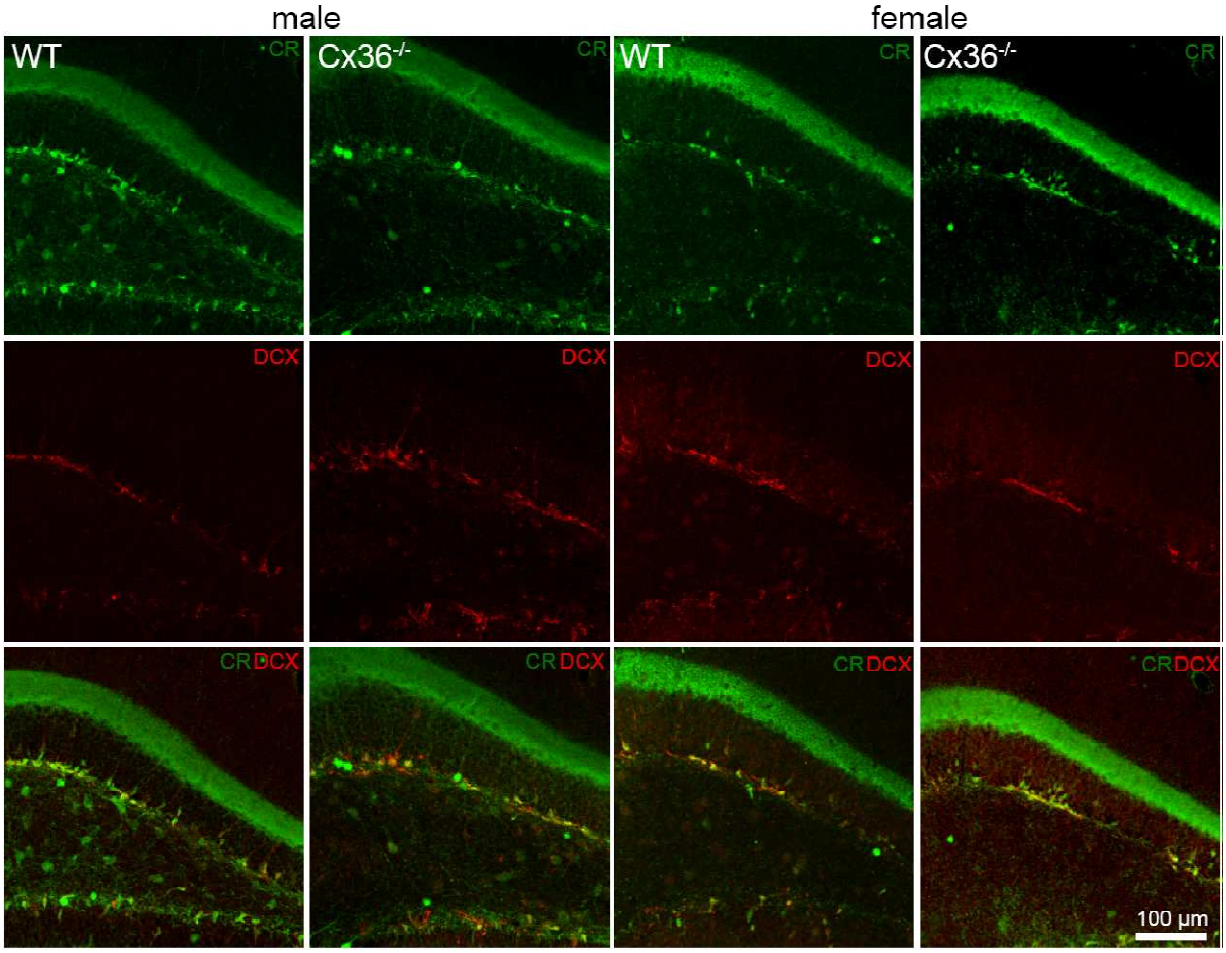

Figure 15: Co-labeling for CR and DCX revealed an increase in CR positive cells in the DG of Cx36$^{-/-}$ females.
Confocal images of CR / DCX double-labeled sections show that in comparison to wt females, there was an increase of CR expressing cells in the GCL of Cx36$^{-/-}$ females. Moreover, they were often found deeper in the GCL than in wt females. Male Cx36$^{-/-}$ mice did not show this phenotype. Double-labeling for the neuroblast marker DCX confirmed the immature phenotype of the CR-positive cells.

To investigate if the excess CR-positive cells in the GCL were indeed immature neuroblasts, double labeling experiments for CR and DCX, a marker for migrating neuroblasts (Gleeson et al., 1998; des Portes et al., 1998), were performed. These experiments showed that most of the presumptive young granule cells were double positive for CR and DCX, proving their immature developmental stage (**Fig. 15**). Additionally, CR-positive cells were frequently found deeper in the GCL of Cx36$^{-/-}$ females than in any other investigated group. Together with the finding that CB immunoreactivity was reduced in patches within the GCL of Cx36$^{-/-}$ females, this

led us to the assumption that the maturation of newly born granule cells was retarded and that this retardation was reflected in a delayed switch from CR to CB expression.

Taken together, these results showed that lack of Cx36 did not cause gross morphological alterations or changes in the different populations of GABAergic interneurons in the hippocampus of male or female mice. However, analysis of the different neurochemical markers strongly suggested alterations in adult neurogenesis of the SGZ in female $Cx36^{-/-}$ mice.

III.4 Analysis of Adult Neurogenesis

Neurogenesis can be subdivided into proliferation of precursor cells, maturation of newborn neurons and survival of these neurons. The sum of the three processes determines the net rate of neurogenesis.

III.4.1 Proliferation and Maturation

To analyze adult neurogenesis, birthdating studies using the nucleotide analog BrdU were performed. Intraperitoneal injection of BrdU is a widely used method to specifically label mitotic cells during S-phase of the cell cycle. BrdU is integrated into genomic DNA instead of dTTP and can be detected by immunohistochemical stainings (Gratzner, 1982). These labeling experiments were carried out in female mice because the earlier described immunohistochemical analysis of cell type specific markers did not suggest any alterations in adult neurogenesis in males (**Fig. 16**).

In these experiments we analyzed both proliferation of precursor cells and maturation of newborn granule cells using two different BrdU administration protocols. To investigate the proliferation of granule cell precursors, BrdU was injected twice a day for three days. The mice were sacrificed 24 h after the last injection, brains were processed for BrdU immunohistochemical analysis and BrdU-positive cells were quantified on serial coronal sections in GCL and SGZ. 24 h after the last BrdU injection the cell population containing BrdU in their genome was heterogeneous due to our labeling protocol. It comprised cells born 1 – 4 d before analysis and thus it was a mix of proliferating and postmitotic cells. Yet, immunoreactive cells mostly localized to the SGZ both in $Cx36^{-/-}$ and wt females (**Fig. 16A**). Quantification showed that both groups of mice contained roughly the same number of BrdU-positive cells in the SGZ and GCL ($P_{(SGZ)} \geq 0.05$, $P_{(GCL)} \geq 0.05$) (**Fig. 16C**) so that we concluded that proliferation of precursors and initial steps of maturation were unaltered.

For maturation analysis of newborn granule cells, BrdU was injected twice a day for six days and the mice were sacrificed 28 d after the last injection. Immunohistochemical analysis of BrdU incorporation was carried out as before and revealed an obvious difference in the number of BrdU-positive cells between wt and $Cx36^{-/-}$ (**Fig. 16B**). Quantification confirmed this impression: the SGZ of $Cx36^{-/-}$ females contained approximately 5 times and the GCL 9 times

more BrdU-positive cells than the wt SGZ and GCL respectively ($P_{(SGZ)} \leq 0.05$, $P_{(GCL)} \leq 0.05$) (**Fig. 16D**).

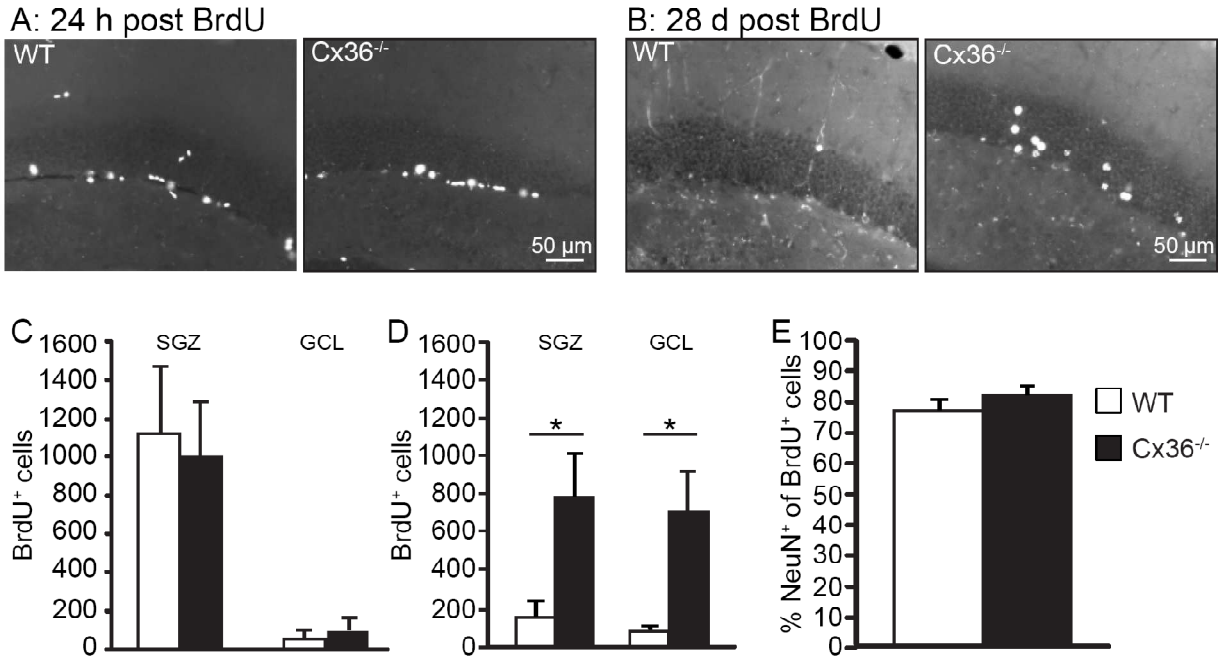

Figure 16: Lack of Cx36 causes enhanced survival of adult generated granule cells in female mice.
A + C: Immunohistochemical analysis of BrdU incorporation in female mice sacrificed 24 h after the last BrdU pulse detected proliferating cells and young neuroblasts (A). Quantifications showed that at that time the vast majority of BrdU-positive cells resided in the SGZ (C). Data represent mean ± SEM. $n_{(wt)} = 5$, $n_{(Cx36-/-)} = 6$.
B + D: Immunohistochemical stainings for BrdU incorporation in female mice sacrificed 28 d after the last BrdU pulse labeled the population of newly generated cells that have matured into granule cells. In wt females only few BrdU-positive cells were still present, while they were abundant in the SGZ and the GCL in $Cx36^{-/-}$ females (B). Quantification revealed five- and nine-fold increased numbers of BrdU positive cells in $Cx36^{-/-}$ compared to wt in the SGZ and GCL respectively (D). Data represent mean ± SEM. $n_{(wt)} = 6$, $n_{(Cx36-/-)} = 5$. (*, $P \leq 0.05$).
E: Co-labeling for NeuN and BrdU showed that in both genotypes about 80 % of all BrdU-positive cells also expressed NeuN, and thus that the same percentage of cells generated at the time of BrdU injection matured into neurons. $n_{(wt)} = 4$, 96 cells, 76.8 ± 2.9 % , $n_{(Cx36-/-)} = 3$, 355 cells, 81.8 ± 2.4 %.
These experiments were carried out by Dr. Elke Fuchs.

To evaluate if the newborn cells matured into neurons or if there was a shift towards a glial cell fate in $Cx36^{-/-}$ mice, sections were double labeled for BrdU and NeuN, a nuclear protein expressed by mature neurons. In both genotypes approximately 80 % of all BrdU-positive cells expressed NeuN, and thus cell fate was not altered by the lack of Cx36 expression (**Fig. 16E**).

Taken together, significantly more new neurons survived for one month in the DG of $Cx36^{-/-}$ females than in the DG of wt females, while the rate of proliferation did not differ between the genotypes.

III.4.2 Analysis of Apoptosis

One mechanism to control the absolute cell number is the removal of excess cells by apoptosis (Biebl et al., 2000). During apoptosis, activation of caspase-3 is an essential step (Porter and Janicke, 1999), and it is therefore a good immunohistochemical marker for apoptotic cells. The data presented above suggest that fewer cells undergo programmed cell death in $Cx36^{-/-}$ females. Therefore, immunohistochemical stainings for this marker were carried out on serial coronal sections and cells were quantified as described before. In general only one to two active-caspase-3 expressing cells could be found in the GCL per section. The morphology of these cells was similar to the morphology of the cell shown in **Fig. 17A**. Labeling for active-caspase-3 was intense in the cytoplasm, while the nucleus was devoid of labeling. On average the GCL of one $Cx36^{-/-}$ DG contained 30 ± 10.3 cells, while in wt females the mean was 16.8 ± 8.2 cells. Although there seemed to be a trend towards more apoptotic cells in $Cx36^{-/-}$ females, the difference was not significant due to the high variation ($n_{(wt)}$ = 5, $n_{(Cx36-/-)}$ = 7; P = 0.140). Also between wt and $Cx36^{-/-}$ males there was no difference in apoptosis (wt: 21 ± 7 cells/GCL, n = 6; $Cx36^{-/-}$: 19.2 ± 5.8 cells/GCL, n = 5) (**Fig. 17B**).

Thus, since there was no difference in the absolute number of apoptotic cells between wt and $Cx36^{-/-}$ mice in both genders, we had to rule out a decrease in apoptosis as a cause of the increased survival of young granule neurons in $Cx36^{-/-}$ females. Combination of this data set with the data obtained from the CR and CB expression study, suggested delayed maturation of newly generated granule cells in female $Cx36^{-/-}$ mice with a developmental arrest at the stage of transient CR expression.

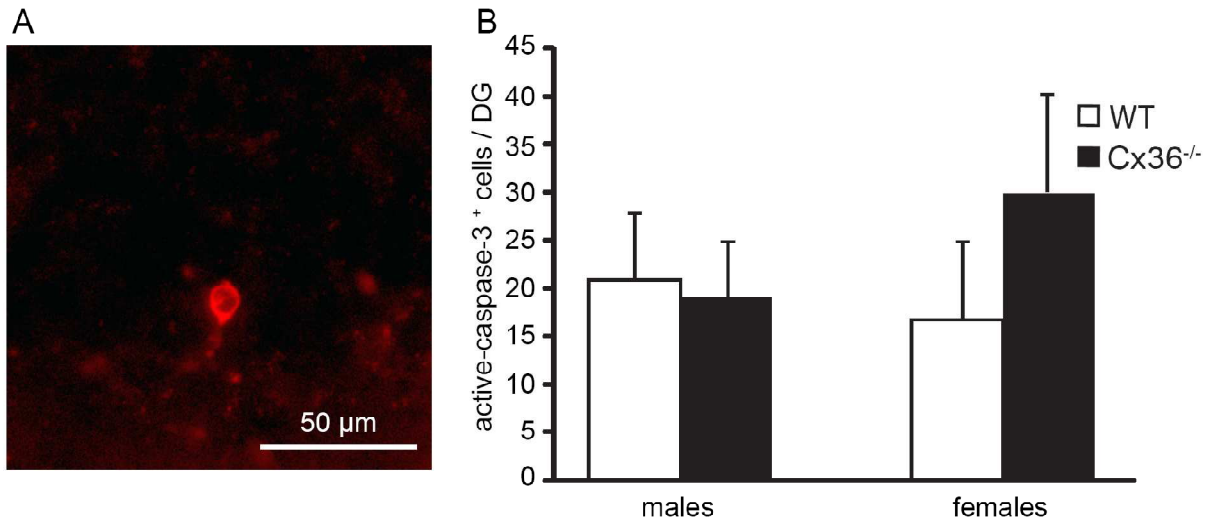

Figure 17: The number of apoptotic cells in the GCL is not significantly different between wt and Cx36$^{-/-}$ females or males.

A: Typical appearance of a cell positive for activated-caspase-3 in the GCL of the DG at the fluorescence microscopic level. Antibody labeling was intense in the cytoplasm, while the nucleus was devoid of signal.

B: Quantification of activated-caspase-3 in wt and Cx36$^{-/-}$ females revealed a trend to more apoptosis in Cx36$^{-/-}$ mice, but the difference did not reach significance due to the high variation. In wt and Cx36$^{-/-}$ male mice there was no difference detectable. Data represent mean ± SEM. Males: $n_{(wt)} = 6$, $n_{(Cx36-/-)} = 5$; females: $n_{(wt)} = 5$, $n_{(Cx36-/-)} = 7$.

III.5 Analysis of the Gender Difference

Surprisingly, lack of Cx36 leads to gender specific effects in behavior, DG activation and adult neurogenesis. Therefore, we analyzed if there were any gender specific differences in the expression of Cx36 in the brain, and also if the ablation of Cx36 in extraneuronal tissues lead to a gender specific phenotype.

III.5.1 Cx36 is not Differentially Expressed in Males and Females

Since differential expression of Cx36 in male and female mice could be a possible explanation for the observed gender difference, we reanalyzed the expression pattern of Cx36 at the mRNA level by radioactive *in situ* hybridization experiments and by real-time PCR analysis.

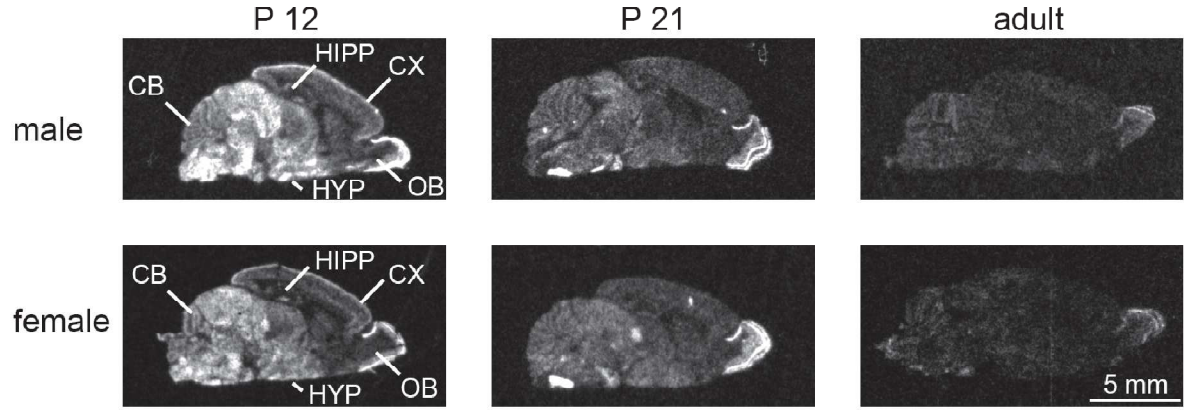

Figure 18: Cx36 mRNA expression pattern does not differ between male and female mice.
Postnatal Cx36 expression was analyzed by radioactive *in situ* hybridization experiments in P12, P21 and adult males and females. The experiments revealed an overall decrease of Cx36 expression with age but no obvious difference between genders. At P12 expression was strongest in glomerular and mitral cell layers of the OB, in layer I of the cortex in several hypothalamic nuclei, midbrain and medulla oblongata. In P21 and adult animals, Cx36 was only detectable in the OB and in P21 mice in addition in the spinal cord. CB: cerebellum, CX: cortex, HIPP: hippocampus, HYP: hypothalamus, OB: olfactory bulb.

Radioactive *in situ* hybridization experiments were performed at three different postnatal stages (P12, P21, adult) on sagittal brain sections of male and female wt mice using an antisense oligonucleotide probe for Cx36 (Hormuzdi et al., 2001). This expression study showed decreasing expression of Cx36 in both male and female brains with age, in accordance with

previously published data (Hormuzdi et al., 2001). At P12, expression was highest in the glomerular and the mitral cell layer of the olfactory bulb, in neocortical layer I, in several hypothalamic nuclei, in the midbrain and in the medulla oblongata. Expression in the hippocampus and the thalamus as well as in cortical layers II to VI and the cerebellum was rather weak (**Fig. 18, left panels**). By P21 expression had declined drastically and was only easily detectable in the previously mentioned layers of the olfactory bulb (**Fig. 18, middle panels**). This expression pattern remained stable well into adulthood (**Fig. 18, right panels**).

Comparing the expression between males and females, the overall Cx36 mRNA expression seemed to be higher in males than in females at P12. This difference had disappeared by P21. In none of the analyzed sections an obvious spatial expression difference could be detected between the genders (**Fig. 18**).

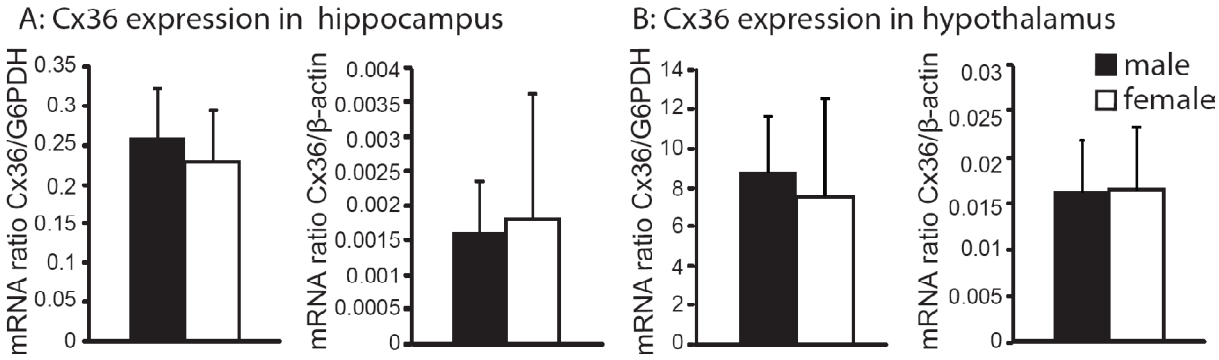

Figure 19: Quantitative analysis of Cx36 mRNA showed that there is no expression difference between genders in the hypothalamus or the hippocampus.
Hippocampal Cx36 expression was normalized to expression of the housekeeping genes G6PDH (A and B, left charts) and β-actin (A and B, right charts). Comparison of the normalized Cx36 expression levels proved that there was no expression difference in the hippocampus (A) or the hypothalamus (B) between adult wt male and female mice. Data represent mean ± STD. $n_{(male)} = 8$, $n_{(female)} = 6$.

Expression of Cx36 in the adult hippocampus and hypothalamus was below the detection threshold of the *in situ* hybridization method we used. To quantify a possible expression difference between males and females in those brain regions, we performed real-time PCR analysis on cDNA prepared from adult wt hippocampal and hypothalamic RNA. Cx36 expression was normalized to expression of the housekeeping-genes β-actin and glucose-6-phosphate-dehydrogenase (G6PDH). This analysis showed that there was no quantitative difference in the

expression of Cx36 in males (n = 8) compared to females (n = 6) in either the hippocampus (**Fig. 19A**) or the hypothalamus (**Fig. 19B**).

Thus, we were able to rule out a difference in the native Cx36 expression pattern between males and females as a cause for the observed gender difference in behavior, DG activation and adult SGZ neurogenesis of $Cx36^{-/-}$ mice.

III.5.2 Uncoupling of Pancreatic β-Cells Leads to Increased Serum Insulin Levels in Female $Cx36^{-/-}$ Mice

In addition to the brain, Cx36 is also expressed in the islets of Langerhans of the pancreas (Serre-Beinier et al., 2000). Since Cx36 ablation is not neuron-specific in the mouse line we used for this study, the effect of peripheral Cx36 ablation and its influence on brain function might offer an explanation for the described phenotype in female $Cx36^{-/-}$ mice. Previously, it has been reported that Langerhans islets derived from $Cx36^{-/-}$ mice have a higher basal insulin secretion rate *in vitro* than wt islets (Ravier et al., 2005). To our knowledge there are no reports about the effect of Cx36 ablation on insulin concentration *in vivo*.

Besides the homeostatic effect on glucose concentration, insulin has been shown to influence the secretion of GnRH from hypothalamic neurons. Consequently the release of LH from the anterior pituitary will be affected, which in turn is important for regulation of estrogen secretion from the ovaries (Bruning et al., 2000; Burcelin et al., 2003).

Thus, we hypothesized that alteration of *in vivo* insulin concentration might lead via alterations in the hypothalamic-pituitary-gonadal axis to altered estrogen levels. Since estrogen itself is a potent regulator of adult SGZ neurogenesis (Galea, 2008), this mechanism could serve to explain our observations.

To test this hypothesis, we analyzed basal and feeding serum insulin concentrations in $Cx36^{-/-}$ males and females in comparison to the appropriate littermates. To measure feeding insulin levels, mice were sacrificed at 5 pm ± 1 h, to measure basal insulin levels mice were food deprived for 12 - 14 h and subsequently sacrificed at 9 am. Serum was prepared from trunk blood and analyzed by commercial ELISA assays for murine insulin and by use of a Glucometer for glucose.

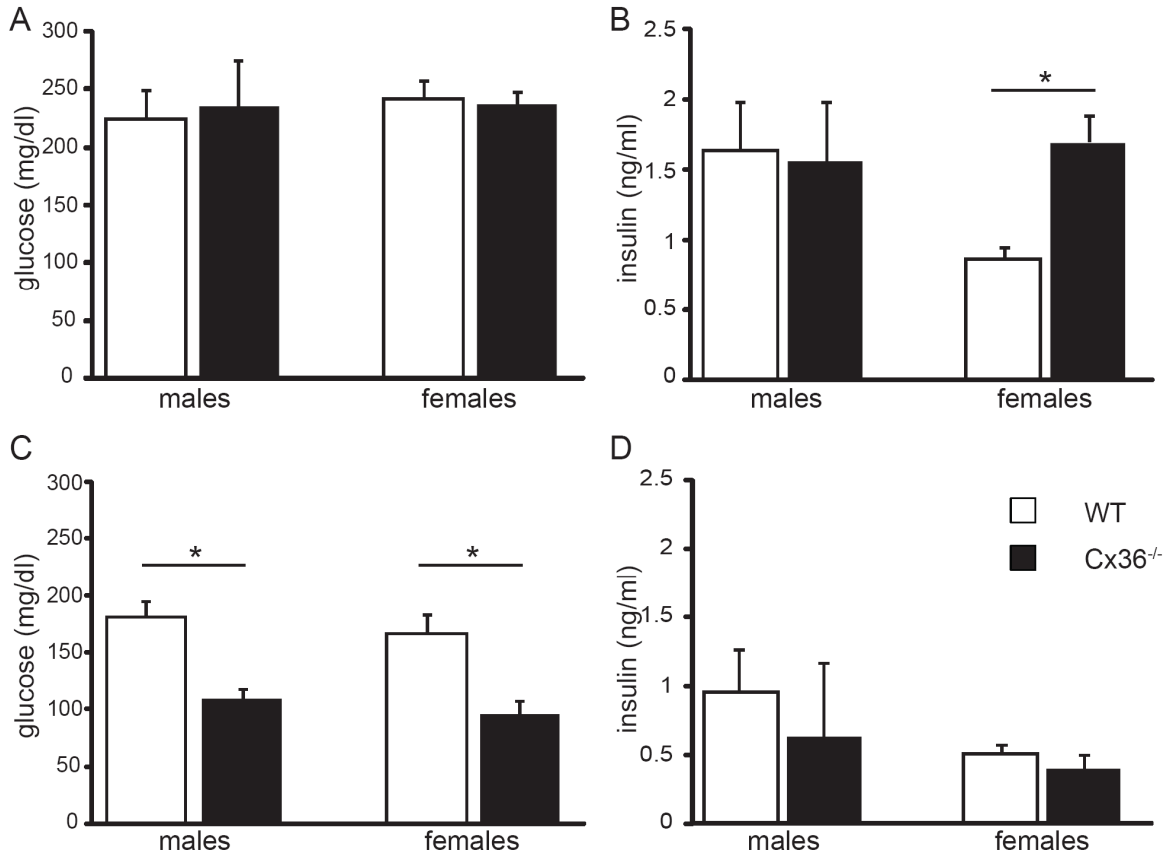

Figure 20: Glucose homeostasis is impaired in food deprived Cx36$^{-/-}$ mice of both genders, while insulin concentration is increased only in fed Cx36$^{-/-}$ females without alteration of blood glucose concentration.

A + B: Wt and Cx36$^{-/-}$ male and female mice with ad libitum access to food and water were sacrificed and serum was prepared. Glucose was measured from serum by Glucometer (Bayer), insulin concentration was determined by ELISA. While blood glucose concentration did not differ between wt and Cx36$^{-/-}$ males and females (A), insulin concentration was approximately doubled in Cx36$^{-/-}$ females compared to wt females (B). Data represent mean ± SEM. Males: $n_{(wt)}$ = 5, $n_{(Cx36-/-)}$ = 7, exception: for glucose determination $n_{(Cx36-/-)}$ = 4 ; females: $n_{(wt)}$ = 12, $n_{(Cx36-/-)}$ = 11. (*, P = 0.00042).

C + D: Wt and Cx36$^{-/-}$ males and females were fasted overnight with ad libitum access to water and sacrificed in the morning. Glucose concentration was significantly lower in Cx36$^{-/-}$ males and females compared to wt controls (C). Serum insulin concentration, however, did not differ between genotypes (D). Data represent mean ± SEM. Males: $n_{(wt)}$ = 5, $n_{(Cx36-/-)}$ = 7; females: $n_{(wt)}$ = 7, $n_{(Cx36-/-)}$ = 5. (*, $P_{(males)}$ = 0.0009, $P_{(females)}$= 0.002).

Data was contributed by Dr. Deborah Burks.

Feeding insulin concentration, determined in blood of mice that had free access to food and water, was unaltered in male Cx36$^{-/-}$ mice compared to littermates but was approximately doubled in serum from Cx36$^{-/-}$ females in comparison to wt females (males: wt: 1.64 ± 0.35 ng/ml, Cx36$^{-/-}$: 1.56 ± 0.42 ng/ml, P ≥ 0.05; females: wt: 0.86 ± 0.09 ng/ml, Cx36$^{-/-}$: 1.70 ± 0.19

ng/ml, P = 0.0042) (**Fig. 20B**). The respective glucose concentrations were in the range of 230 mg/dl and varied only slightly between genotypes (P ≥ 0.05 for males and females) (**Fig. 20A**).

Basal insulin concentrations were measured in serum from overnight food deprived mice. In contrast to the findings from an *in vitro* study (Ravier et al., 2005), concentrations did not differ between genotypes in either males or females (males: wt: 0.85 ± 0.29 ng/ml, $Cx36^{-/-}$: 0.56 ± 0.49 ng/ml, P ≥ 0.05; females: wt: 0.45 ± 0.07 ng/ml, $Cx36^{-/-}$: 0.36 ± 0.09 ng/ml, P ≥ 0.05) (**Fig. 20D**). Glucose concentration was measured in the same samples and was significantly decreased in $Cx36^{-/-}$ males and females as compared to the respective littermates (males: wt: 180.45 ± 14.81 mg/dl, $Cx36^{-/-}$: 108.24 ± 9.1 mg/dl, P = 0.0009; females: wt: 166 ± 16.45 mg/dl, $Cx36^{-/-}$: 95.56 ± 12.35 mg/dl, P = 0.002) (**Fig. 20C)**.

The reason why lack of Cx36 expression has a greater impact on the female pancreas regarding insulin secretion than on the male pancreas is unclear but the result shows that the brains of female $Cx36^{-/-}$ mice are exposed to much higher insulin concentrations under standard housing conditions than the brains of wt females.

III.5.3 Increased Insulin is Associated with Decreased Estradiol in Estrus

The result obtained from the insulin measurements prompted us to pursue our hypothesis that altered insulin levels, via alterations in gonadal hormones, might be the primary cause for the differences observed in adult neurogenesis and in the activation of the female DG. To get a preliminary impression about gonadal hormone function in $Cx36^{-/-}$ females, the duration of the different estrous cycle stages was analyzed. Since the composition of the vaginal epithelium changes in response to hormone fluctuations during the estrous cycle, analysis of the epithelium is a good indirect means to determine cycle stages. For this analysis, mice were housed in pairs of wt and $Cx36^{-/-}$ in standard cages on a 12 h light-dark cycle. The vaginal smears were taken 4 h ± 1 h after lights on and the cells were stained according to Papanicolaou's method (Papanicolaou, 1942) (**Fig. 21A**). For each mouse at least three consecutive cycles were evaluated. The absolute duration of the cycle in $Cx36^{-/-}$ was 5.26 ± 0.5 days and did not differ from wt where one estrous cycle lasted for 5.49 ± 1.3 days. However, the duration of estrus, normalized to total cycle length, was significantly prolonged in wt in comparison to $Cx36^{-/-}$ mice

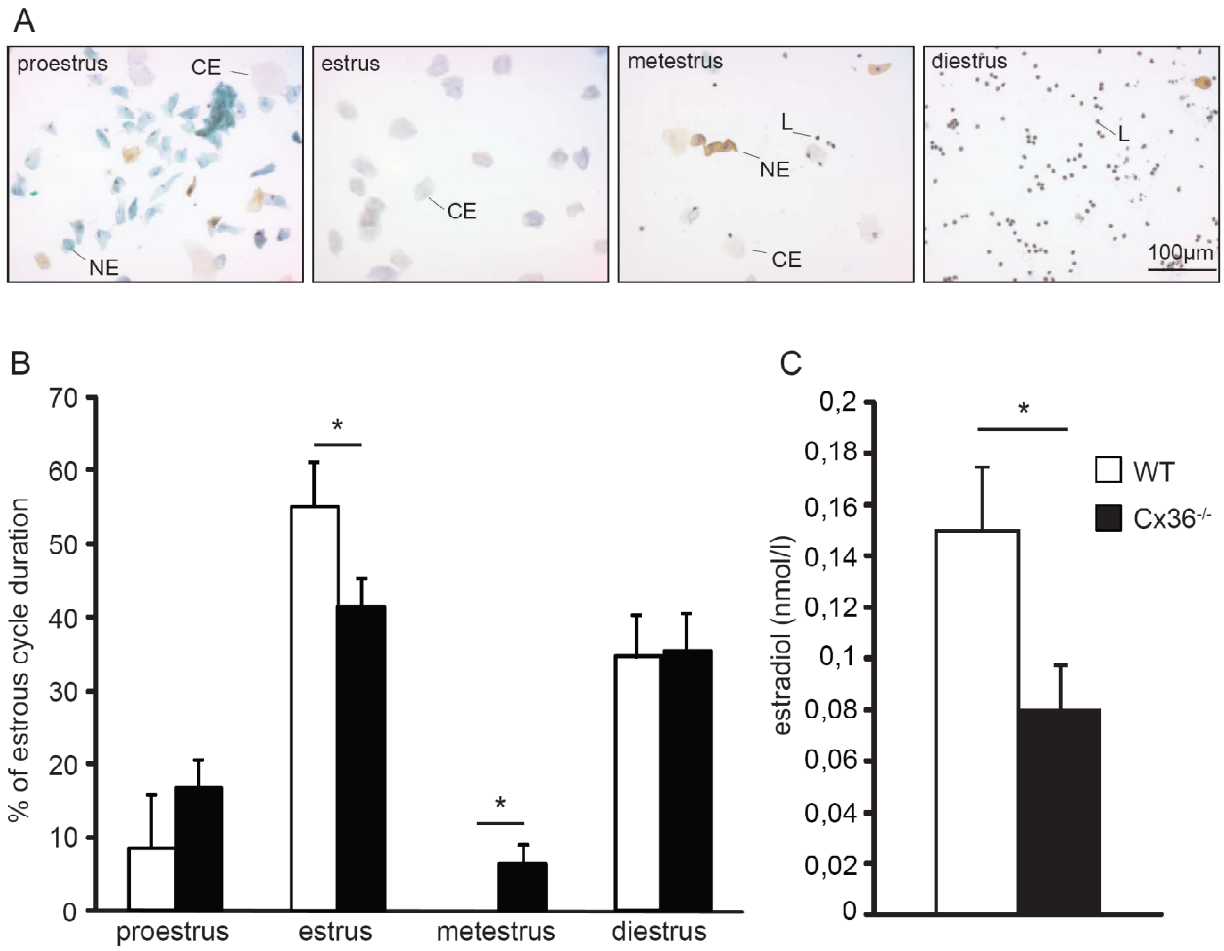

Figure 21: Lack of Cx36 leads to a reduction of estradiol concentration during estrus.
A: Vaginal smears were stained according to the Papanicolaou method to determine the different stages of the estrous cycle. In proestrus the smear consisted mainly of nucleated epithelial cells, in estrus of cornified epithelial cells, while in diestrus leukocytes were the predominant cell type. Metestrus was characterized by approximately 50 % cornified epithelial cells and 50 % leukocytes.
B: $Cx36^{-/-}$ females stayed for a significantly reduced proportion of the estrous cycle in estrus, while they were significantly longer in metestrus, a phase in which wt mice were never found to be. Data represent mean ± SEM. $n_{(wt)} = 5$, $n_{(Cx36-/-)} = 5$, ≥ three consecutive cycles/mouse. (*, $P \leq 0.05$).
C: For estradiol measurements mice were sacrificed in the morning of the first day of estrus. The hormone concentration was determined by HPLC analysis of the serum and estradiol concentration was reduced by approximately 50 %. Data represent mean ± SEM. $n_{(wt)} = 6$, $n_{(Cx36-/-)} = 7$. (*, $P \leq 0.05$). Estradiol concentration was measured by Dr. Deborah Burks.

(wt: 55 ± 5.7 % of total cycle length; $Cx36^{-/-}$: 41.4 ± 4.1 % of total cycle length; P = 0.013). Additionally, wt mice were never found to be in metestrus (**Fig. 21B**). In support of our hypothesis, these findings pointed towards alterations in gonadal hormone concentrations.

Quantification of estradiol concentration was achieved by HPLC analysis of serum from mice sacrificed on the evening of the first day of estrus. Estradiol concentration was 0.15 ± 0.02 nmol/l in wt as opposed to 0.081 ± 0.017 nmol/l in Cx36$^{-/-}$ females (**Fig. 21C**). This decrease by approximately 50 % was statistically significant (P = 0.025).

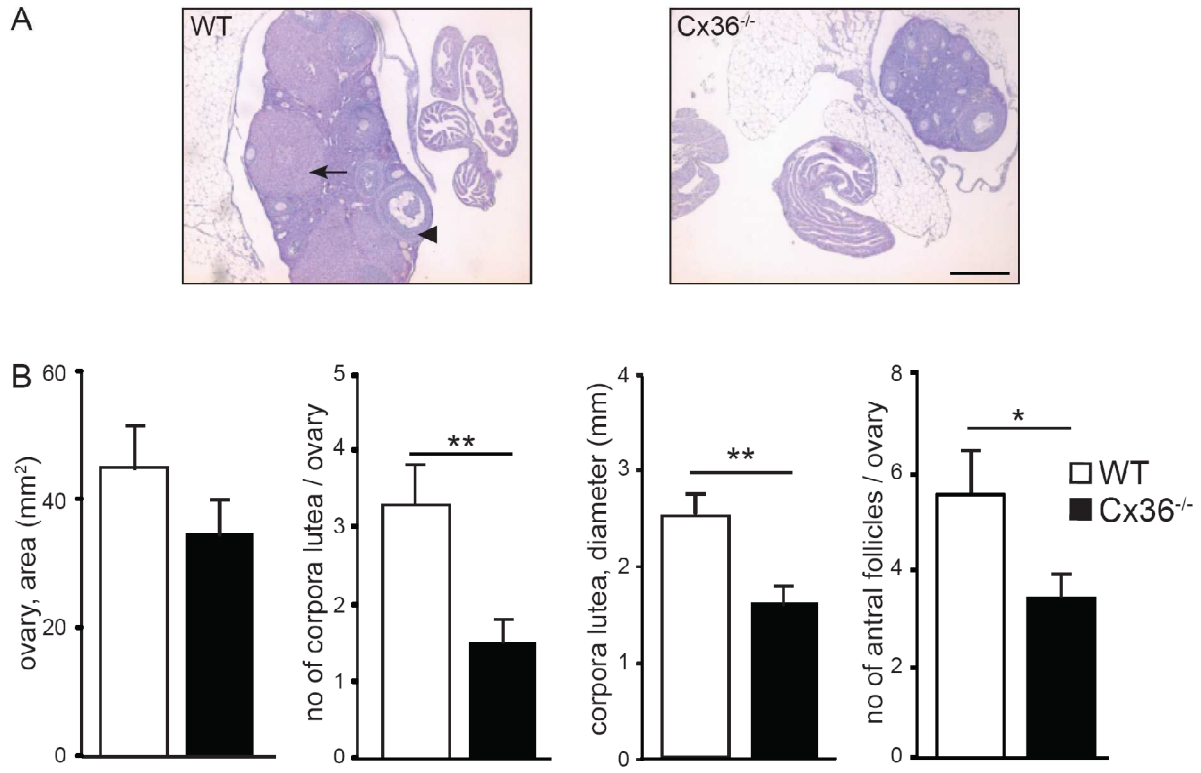

Figure 22: Ovaries of Cx36$^{-/-}$ females contain fewer and smaller corpora lutea and fewer antral follicles.
A: Haematoxylin-eosin stained stained paraffin sections of wt and Cx36 ovaries. The arrow points to a typical copus luteum, the arrowhead to an antral follicle. Scale bar: 500 µm.
B: Quantifications revealed a reduction in the number and size of corpora lutea and a reduction in the number of antral follicles in Cx36$^{-/-}$ mice, while the total ovarian area was unaltered. The analysis was performed by Dr. Deborah Burks.
Data represent mean ± SEM. $n_{(wt)}$ = 10 ovaries from 5 mice, $n_{(Cx36-/-)}$ = 12 ovaries from 6 mice; corpus luteum diameter: $n_{(wt)}$ = 22 from 10 ovaries, $n_{(Cx36-/-)}$ = 15 from 12 ovaries. (*, P ≤ 0.05; **; P ≤ 0.01).

Ovaries are the major source of estrogens. Because estradiol concentration was about 50 % lower in $Cx36^{-/-}$ females than in wt, we examined if ovarian morphology was normal in these mice. The morphological analyses were carried out on ovaries from animals sacrificed for the estradiol measurements. Haematoxylin-eosin stainings of paraffin sections (**Fig. 22A**) revealed a decrease in the number of antral follicles, the major estradiol producing subcompartment of the ovary (Boland et al., 1993) (wt: 3.29 ± 0.52, $Cx36^{-/-}$: 1.54 ± 0.31, P = 0.008). In addition, the number of corpora lutea as well as their diameter was reduced (wt: 5.57 ± 0.84, $Cx36^{-/-}$: 3.36 ± 0.53, P = 0.032; diameter wt: 5.5 ± 0.19 mm, $Cx36^{-/-}$: 1.63 ± 0.2 mm, P = 0.004). All these reductions were statistically significant while the total ovarian area did not differ between genotypes (**Fig. 22B**). Hence, we concluded that the ovaries of $Cx36^{-/-}$ females were highly dysfunctional which would explain the reduction of serum estradiol.

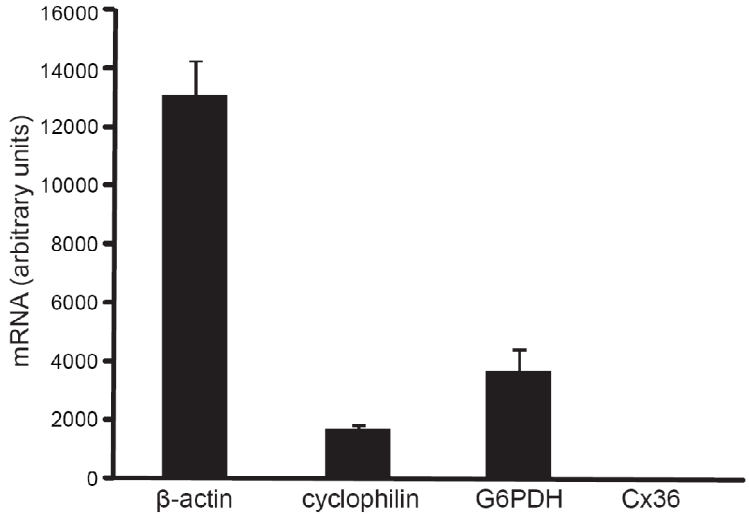

Figure 23: Cx36 is not expressed in ovaries.
Total RNA was extracted from three ovaries for reverse transcription. Cx36 was not expressed in this pooled sample as assessed by real-time PCR analysis so that lack of Cx36 in the ovaries could be excluded as primary cause for the observed follicular abnormalities. Data represent the mean of duplicates ± STD. n = 3 ovaries.

However, the ovarian phenotype could be a direct consequence of a potential loss of Cx36 expression in the ovary itself, instead of being a consequence of changes in the HPG axis. Despite the thorough expression analyses that have been carried out in the past by several

groups (Sohl et al., 1998; Belluardo et al., 2000; Serre-Beinier et al., 2000), we could not find any reports on Cx36 expression in ovaries. Therefore, we analyzed ovarian RNA prepared from three wt mice by real-time PCR. We could not detect any Cx36 transcripts in the samples while we could amplify the transcripts of three different housekeeping genes from this cDNA in the same experiment. As further controls, we amplified all four genes, including Cx36, from genomic DNA in this experiment (**Fig. 23**). Thus, loss of Cx36 in the ovaries themselves could be ruled out as a cause for any of our observations. In accordance with previous literature we also found Cx36 mRNA to be expressed in the pituitary (Belluardo et al., 2000).

Summarizing, the results presented above are supporting our hypothesis, that the increase in insulin could be the primary cause for the decrease in estradiol concentration in $Cx36^{-/-}$ females. However, it is conceivable that Cx36 is expressed in neurons of the hypothalamus and pituitary cells that are more important in the female reproductive axis than in that of the male, a distinction we could not make with the methods used in this study.

IV. Discussion

Cx36 is expressed in GABAergic interneurons, in pancreatic beta cells of the islands of Langerhans and in adrenal medullary cells. In the hippocampus, electrical uncoupling of GABAergic interneurons due to lack of Cx36 leads to reduction of *in vitro* and *in vivo* gamma oscillations (Hormuzdi et al., 2001; Buhl et al., 2003). Also pancreatic β-cells are uncoupled due to the lack of Cx36. β-cells derived from $Cx36^{-/-}$ mice show a higher basal insulin secretion rate *in vitro* as well as slower insulin secretion shut-off kinetics (Ravier et al., 2005; Speier et al., 2007). The functional effect of Cx36 ablation on adrenal medullary cells has not yet been examined. Behaviorally, $Cx36^{-/-}$ males do not show any obvious deficits in motor performance or in anxiety related behaviors but are impaired in recognition memory. To improve our understanding of the functional role of cell coupling by Cx36, we analyzed male and female $Cx36^{-/-}$ mice in more detail.

This study demonstrates the first link between Cx36 and adult SGZ neurogenesis, a connection that is not direct but mediated by hormonal changes in $Cx36^{-/-}$ females. The increase in immature granule neurons is caused by delayed maturation of newly generated cells and most likely causes functional alterations in the activation of the DG granule cell network during exploration of a novel environment and under resting conditions. These conclusions are based on the following observations: We found that $Cx36^{-/-}$ females were hyperactive in a novel environment and this hyperactivity went along with increased numbers of activated DG granule cells under cage control conditions that could not be further augmented by exploratory behavior. Additionally, $Cx36^{-/-}$ females displayed an increase in young granule cells at the stage of CR expression in conjunction with unaltered proliferation and apoptosis but extended survival of adult generated granule neurons. These neurological phenotypes were accompanied by a gender specific increase in serum insulin in $Cx36^{-/-}$ females as well as a decrease in serum estradiol during estrus. Correlative evidence suggests a causal link between the increase in serum insulin, the decrease in estradiol at the stage of estrus and the extended survival of immature granule cells that we observed.

IV.1 Exploratory Behavior and DG activation

In accordance to literature, motor performance on the rotarod (**Fig. 9A**) was not altered in male Cx36$^{-/-}$ mice (Kistler et al., 2002). Also females did not show any behavioral differences in this task in comparison to their control littermates (**Fig. 9B**).

During exploration of an environment the predominant oscillatory patterns in the mouse and rat hippocampus are theta- and gamma-waves (Vanderwolf, 1969; Buzsaki et al., 2003). In Cx36$^{-/-}$ mice the power of CA1 gamma-oscillations is reduced *in vitro* as well as *in vivo* (Hormuzdi et al., 2001; Buhl et al., 2003). To investigate if there is a direct relationship between alterations in the power of the predominant oscillatory network activity during exploration and the associated behavior, we analyzed mice of both genders in an open field arena (**Fig. 9C + D**). Surprisingly, horizontal activity was strongly enhanced in Cx36$^{-/-}$ females compared to wt females, while there was no difference between wt and Cx36$^{-/-}$ males. This result together with the data from electrophysiological recordings in male Cx36$^{-/-}$ mice led us to the conclusion that the decrease in power of CA1 gamma-oscillations is not directly linked to the observed alterations in behavior. Along these lines, GluR-D$^{-/-}$ and GluR-A$^{PvCre-/-}$ mice, two mouse models in which power of *in vitro* gamma oscillations in the hippocampus is reduced, displayed even reduced or unaltered exploratory activity respectively in the open field test (Fuchs et al., 2007). This further supported the notion that gamma oscillatory power does not correlate with exploratory activity in the open field test.

To delineate the hippocampal alterations underlying the novelty induced hyperactivity in Cx36$^{-/-}$ females, we used expression analysis of the immediate-early gene cFos, a general marker for neuronal activity (Sagar et al., 1988), as a means to assess network functionality. Since expression of cFos has been shown to be induced by exploration of novel environments in the hippocampus of rats (Hess et al., 1995), we subjected male and female mice to an exploratory test (**Fig. 10**) and subsequently analyzed cFos expression (**Fig. 11 + Fig. 12**). The focus of the analysis was on the DG because it is the first processing step for most incoming information into the hippocampus and is thought to function as a filter for this input (Gilbert et al., 2001). Furthermore, the existence of place fields has been shown for DG granule cells (Jung and McNaughton, 1993) and since exploration is a task dependent on processing of spatial information, alterations in network function should be detectable in the DG.

In accordance with previous literature, the number of cFos positive, and thus of activated cells was low in cage control males of either genotype and in wt females (Hess et al., 1995; Chawla et al., 2005). Comparison of the number of activated cells in female wt and $Cx36^{-/-}$ cage control mice, however, revealed an increased baseline activation of the $Cx36^{-/-}$ DG under control conditions. Interestingly, the number of activated cells could not be further augmented in $Cx36^{-/-}$ females to reach the activation levels of wt females or those of males of either genotype. In line with previous reports, mice in the latter three groups showed a robust increase in cFos expressing cells subsequent to the exploratory test (Hess et al., 1995; Pace et al., 2005; Chawla et al., 2005).

Studies analyzing mechanisms of neural cFos induction in mice and rats showed that the expression of cFos in several brain regions, including the hippocampus, is positively regulated by estradiol. These studies, however, did not reach a conclusion on the influence of estradiol on cFos expression in the GCL of the DG (Rudick and Woolley, 2000; Dominguez-Salazar et al., 2006). Our data show that cFos induction in the DG is not positively correlated with estradiol concentration, since in $Cx36^{-/-}$ females estradiol concentrations were reduced (**Fig. 21**).

In addition to being regulated by estradiol, induction of cFos expression in neurons has been shown to precede apoptosis (Smeyne et al., 1993). In the course of this study we also quantified apoptotic cells and found a slight, albeit not significant, increase in cells undergoing programmed cell death in $Cx36^{-/-}$ females (**Fig. 17**). However, since we only found an increase in cFos positive cells in cage control but not in test $Cx36^{-/-}$ female mice, the probability that the difference in cFos expression was indicating increased apoptosis is very low.

Strikingly, besides the described behavioral and functional alterations, also the increase in immature granule cells was restricted to female $Cx36^{-/-}$ mice and may serve as an explanation for the observed functional impairments in DG network activation: Young dentate gyrus granule cells have been shown to display reduced thresholds for action potential firing and LTP induction (Wang et al., 2000; Schmidt-Hieber et al., 2004). Thus, weak excitatory input into the DG under cage control conditions should be more likely to activate young than fully mature granule cells. In this context the delayed maturation of newly generated granule neurons, and therefore increased proportion of immature cells, in the hippocampus of $Cx36^{-/-}$ females

explains the hyper-activation of the DG seen in the cFos expression study under control conditions.

However, this explanation does not answer the question why the DG of $Cx36^{-/-}$ females is not further activated by exploration. In one of the studies analyzing excitability of immature granule cells the authors mimicked *in vitro* the input onto DG granule cells that is expected in the center, at the border or outside of the cells' place field. Their findings show that young granule cells respond with LTP to firing patterns corresponding to the input a cell receives in the center of the place field, but also to the input the cell would receive at the border, while LTP is evoked in mature neurons only at firing patterns corresponding to the place field center (Schmidt-Hieber et al., 2004). Combination of this data with our result that $Cx36^{-/-}$ females are more active during exploration without showing a concomitant rise in activated cells suggests that the formation of defined place fields is strongly impaired in these mice due to the shift in the ratio of immature to mature granule neurons.

IV.2 Anatomical Analysis of the DG and Analysis of Adult Neurogenesis

As a first step to understand why the DG of control Cx36$^{-/-}$ females displayed many more activated granule cells than the DG of control wt females, we investigated the main cell populations of the DG by immunohistochemistry. These cell types are PV-positive basket cells of the DG that are coupled by Cx36 in wt mice (Meyer et al., 2002), CR positive hilar interneurons (Liu et al., 1996) and CR positive immature granule cells (Brandt et al., 2003), as well as CB positive interneurons and mature granule cells (Baimbridge and Miller, 1982; Sloviter, 1989).

Besides the analysis of the general anatomy of the DG by Nissl stainings, also the analysis of PV-positive interneurons (**Tab. 5**) did not reveal any difference between wt and Cx36$^{-/-}$ in males or females. PV cells were neither altered in number nor obviously mislocated within the DG. Thus, lack of Cx36 does not seem to influence the development of this cell population. This was especially important because parvalbumin-deficiency has been shown to be involved in facilitation of gamma oscillations (Vreugdenhil et al., 2003). However, with the methods we used we could not exclude possible gender specific changes in the functionality of uncoupled PV-positive cells that might contribute to the phenotype of Cx36$^{-/-}$ females.

In contrast, we found a drastic increase in the number of CR expressing young granule cells in the SGZ and GCL (**Fig. 15, Tab. 6**) along with reduced expression of CB in patches of the GCL (**Fig. 14**) of female Cx36$^{-/-}$ mice but not in Cx36$^{-/-}$ males. This expression pattern in Cx36$^{-/-}$ females was reminiscent of the spatial distribution and timecourse of expression of the two markers during development of adult generated granule neurons (Kempermann et al., 2004). Subsequent analysis of adult SGZ neurogenesis in females using BrdU as a DNA synthesis marker (Gratzner, 1982) revealed that proliferation of precursor cells was unaltered, whereas survival was increased during a period of 28 d in female Cx36$^{-/-}$ mice (**Fig. 16**). Analysis of apoptosis by using active-caspase-3 as a marker (Porter and Janicke, 1999), revealed that, in accordance with previously reported data (Sun et al., 2004), there was overall only very little apoptosis detectable (**Fig. 17**). In males of both genotypes the number of apoptotic cells was virtually identical, while there was a statistically not significant trend towards increased programmed cell death in Cx36$^{-/-}$ females as compared to wt.

According to the model for granule cell development proposed by Kemperman et al. (2004), CR is expressed by postmitotic yet immature granule cells. Expansion of this cell

population in the Cx36$^{-/-}$ DG without alterations in neuronal birth or death, but accompanied by increased numbers of BrdU positive cells surviving 28 d, implies that functional maturation and thus switch to CB expression is delayed. In favor of this notion, CB expression was downregulated in patches distributed over the GCL of Cx36$^{-/-}$ females (**Fig. 14**).

However, we cannot definitely exclude that the maturation of CR negative cell populations is affected as well. Moreover, with these experiments we cannot pinpoint to the exact time course of CR expression or the point of developmental arrest during granule cell maturation in Cx36$^{-/-}$ females, because we analyzed BrdU incorporation only at two different time points (24 h and 28 d after the last administration), and did not perform double-labeling experiments for BrdU and markers other than NeuN. Co-labeling experiments for these two markers revealed that eventually the same proportion of adult generated cells develops a neuronal phenotype in wt and Cx36$^{-/-}$ mice (**Fig. 16**).

Physical activity is an important modulator of hippocampal neurogenesis and increases both proliferation and survival of newborn cells (van Praag et al., 1999b). Cx36$^{-/-}$ females which showed increased horizontal activity in the open field test, concomitantly displayed increased survival of new granule cells but no increase in proliferation. These observations argue against enhanced activity as cause for extended survival of newborn cells in Cx36$^{-/-}$ mice. Furthermore, in studies investigating the impact of enhanced activity on neurogenesis the mice are usually housed in larger cages with access to a running wheel (van Praag et al., 1999b; Brown et al., 2003). Cx36$^{-/-}$ females, however, displayed higher survival rates of newborn cells under normal housing conditions in standard mouse cages.

Therefore, increased physical and consequently increased hippocampal activity can be ruled out as the reason for the delayed maturation and extended survival of granule cells in females lacking Cx36.

Investigating the cause for the gender specificity of our results, we found that in Cx36$^{-/-}$ females the gonadal hormone estradiol was reduced (**Fig. 21**). Initial evidence for estrogen as a regulator of adult neurogenesis came from a study conducted in rats that found a 45 % increase in the number of neuroblasts 2 d after BrdU injection in females as compared to males. Comparison of cell proliferation across the different estrous cycle stages showed that proliferation is highest during proestrus, a cycle stage with high circulating estradiol levels, while

there is no difference in proliferation across the remaining stages of the estrous cycle (Tanapat et al., 1999). These findings were confirmed by several other studies conducted in rats and meadow voles (Ormerod and Galea, 2001; Ormerod et al., 2003; Tanapat et al., 2005).

In contrast to these reports, the only systematic study carried out in C57BL/6 mice did not detect any changes in proliferation during the course of the estrous cycle or between males and females, suggesting that proliferation of granule cell precursors is independent of estradiol in mice (Lagace et al., 2007). Commensurate with this finding the rate of granule cell precursor proliferation in female $Cx36^{-/-}$ mice did not differ from the proliferation rate in wt mice in spite of the reduced estradiol levels in $Cx36^{-/-}$ females (**Fig. 16A + C**). The overall higher numbers of BrdU positive cells in the study of Lagace et al. (2007) compared to our results are mainly due to the younger age of their mice at the time of experiment and the reported age dependent decline of progenitor cell proliferation (Kuhn et al., 1996).

Hence, in mice proliferation of precursor cells is not decreased by decreased estradiol.

The influence of estradiol on survival of newborn cells is not as extensively studied as the influence on proliferation. However, analysis of granule cell survival in female meadow voles during the non-breeding season, when estradiol levels are constantly low, demonstrated that low estradiol levels lead to increased survival of newborn cells as assessed 5 weeks after labeling with [^{3}H]-thymidine (Ormerod and Galea, 2001).

Along these lines our results demonstrated that cell survival was enhanced in $Cx36^{-/-}$ female mice with reduced estradiol levels in comparison to wt mice. Enhanced survival correlated with a general increase in CR expressing cells in the granule cell layer and subgranular zone while proliferation was unchanged.

These results suggest that a decrease in estradiol over a long period in time delays the functional maturation of adult generated granule cells. However, since we did not investigate the percentage of BrdU/CR double-positive cells in wt and $Cx36^{-/-}$ females 28 d after the last BrdU labeling pulse, we cannot definitely prove this delay but have to rely on correlative evidence.

IV.3 Gender Specificity

IV.3.1 Cx36 Expression Analysis

Reasons for gender specificity of a phenotype in knock-out mouse models can be expression of the gene of interest in different subsets of cells or different expression levels in males or females. To analyze potential expression differences of Cx36 between males and females, radioactive *in situ* hybridization studies and quantitative real-time PCR experiments were performed since antibodies directed against Cx36 are not specific in our hands in immunohistochemical stainings. To detect spatial and temporal expression differences at different postnatal ages, we employed *in situ* hybridization experiments on sagittal sections from male and female wt mice (**Fig. 18**). According to published data, the overall Cx36 expression level declined with time (Belluardo et al., 2000; Hormuzdi et al., 2001) so that in the adult expression was only easily detectable in the olfactory bulb, while at P12 expression was high and widespread in both males and females. At P12 the signal seemed to be higher on sections from the male brain but we cannot exclude that this is due to technical reasons. This difference was not detected at any other stage that was analyzed and we never found a spatial expression difference between males and females in the brain.

We were especially interested in potential expression differences in hippocampus and hypothalamus because of their role in brain and body function. Differences in hippocampal expression of Cx36 between males and females may directly account for the alterations in adult neurogenesis by altering network properties. In the hypothalamus, GnRH neurons are responsible for controlling the pulsatile release of LH and FSH from the anterior pituitary (Belchetz et al., 1978). Analysis of cell-coupling in a study using transgenic mice that express GFP under the control of the GnRH promoter revealed that coupling incidence was very low (Suter et al., 2000). However, Cx36 was shown to be expressed in the hypothalamus (Belluardo et al., 2000), and so far the connexin subtype coupling GnRH neurons *in vivo* has not been identified.

Because the expression level in the hippocampus and hypothalamus of adult mice was below detection threshold of the *in situ* hybridization experiments, we dissected hippocampi and hypothalami of wt mice and isolated total RNA to analyze Cx36 expression by quantitative real-time PCR (**Fig. 19**). Since also in these experiments we could not detect a significant difference between the normalized expression in males and females in hippocampus or

hypothalamus, we were confident that the observed phenotype in Cx36$^{-/-}$ females was not due to differential expression of Cx36 in the brain of male and female mice.

VI.3.2 Analysis of Hormonal and Metabolic Parameters

We analyzed estradiol concentration in Cx36$^{-/-}$ females for two reasons: First, all effects on behavior and neurogenesis were restricted to females but were not caused by gender specific expression of Cx36 in any analyzed region (**Fig. 18 + Fig. 19**). This suggested the involvement of female gonadal hormones. Second, lack of Cx36 alters *in vitro* insulin release from pancreatic β-cells (Ravier et al., 2005; Speier et al., 2007) and it had been shown in a couple of prior studies that activation of neuronal insulin receptors modulates secretion of GnRH, the key regulatory hormone in the hypothalamic-pituitary-gonadal axis (Bruning et al., 2000; Burcelin et al., 2003). Therefore we hypothesized that alterations of *in vivo* insulin concentrations may, via changes of gonadal hormone concentrations, result in the observed phenotype.

To test if insulin levels are altered in Cx36$^{-/-}$ mice *in vivo,* blood from overnight food deprived mice and from mice with free access to food was analyzed. It needs to be mentioned in this respect that all glucose concentrations obtained, also those from wt, were higher than to be expected from non-diabetic animals (Bruning et al., 2000). This increase could have been caused by environmental stress (personal communication, Dr. Deborah Burks). In the food deprived group, glucose concentration was significantly reduced in Cx36$^{-/-}$ mice of both genders, while insulin concentration was unaffected (**Fig. 20C + D**). According to published data, islets of Cx36$^{-/-}$ are more sensitive to glucose and thus secrete more insulin in response (Ravier et al., 2005), so that under fasting conditions blood glucose is expected to be lower in Cx36$^{-/-}$ than in wt mice. Due to large errors in the fasting insulin values, especially in males (**Fig. 20D**), we could not detect a concomitant increase in insulin in Cx36$^{-/-}$ mice. In the group of mice with *ad libitum* food access, there was no difference in the blood glucose concentration between genotypes. Fed insulin concentration, however, was approximately twice as high in female Cx36$^{-/-}$ mice in comparison to wt female mice. Why a corresponding difference could not be detected in male

mice remains to be determined (**Fig. 20A + B**). However, the result clearly demonstrated that Cx36$^{-/-}$ females were exposed to much higher insulin concentrations than wt females.

To test if the increase in insulin was paralleled by alterations in estradiol levels, the estrous cycle and subsequently hormone concentrations were analyzed. In fact the estrous cycle was perturbed in Cx36$^{-/-}$ females and determination of estradiol concentration during the stage of estrus revealed decreased serum estradiol levels in these mice (**Fig. 21**). We did not measure estradiol in other cycle phases, so that we cannot definitely rule out normal estradiol concentrations during the remainder of the estrous cycle. However, morphological analysis of Cx36$^{-/-}$ ovaries revealed a decrease in the number of antral follicles and reduced size and number of corpora lutea (**Fig. 22**). Since antral follicles are the main estradiol source in the female (Boland et al., 1993), reduction of serum estradiol is a logical consequence of reduced numbers of this type of follicle. Given the fact that the Cx36$^{-/-}$ ovaries were dysfunctional to various degrees according to the morphological analyses, we were confident to assume an overall reduction in serum estradiol. Nevertheless, all types of follicles, albeit reduced in number and size, could be detected in the ovaries of Cx36$^{-/-}$ mice and all estrous cycle phases were detectable by vaginal smears. Therefore, we concluded that cyclic fluctuations of estradiol were very likely. Summarizing, we assumed decreased but still cyclic fluctuating estradiol levels in Cx36$^{-/-}$ females.

IV.4 Conclusions and Outlook

In this study we demonstrate the connection between Cx36 and adult neurogenesis in the hippocampus and discuss the possible mechanism by which the previously unnoticed phenotype of Cx36$^{-/-}$ mice remains restricted to the female gender.

In Cx36$^{-/-}$ females the maturation of adult generated granule cells is delayed so that the composition of the granule cell network is shifted towards more, highly excitable immature cells. This shift is most likely eliciting the alterations observed in DG activation during exploratory activity. Correlative evidence indicates that increased insulin levels, observed exclusively in female Cx36$^{-/-}$ mice, cause decreased estradiol serum concentrations. Furthermore, we suggest that low estradiol concentrations extend survival of newborn granule cells in the DG by delaying the functional maturation.

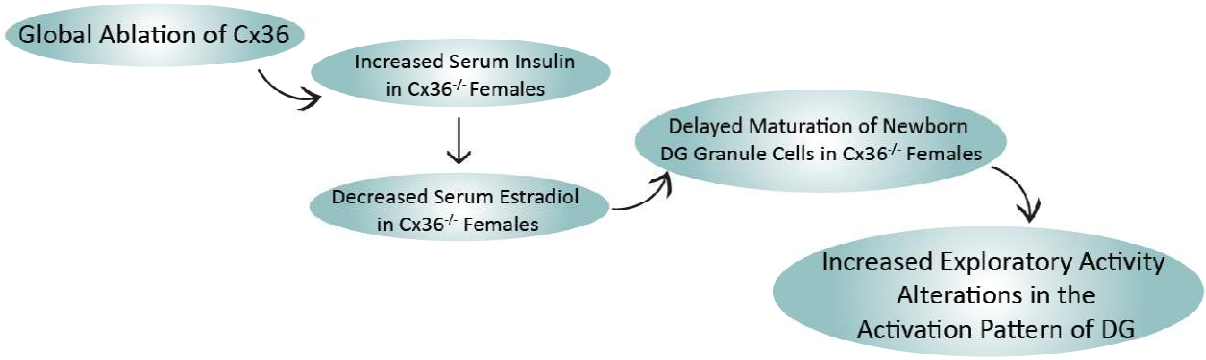

Figure 24: Suggested mechanism underlying the gender-specificity of the Cx36$^{-/-}$ phenotype.
Global ablation of Cx36 leads to an increase in serum insulin in Cx36$^{-/-}$ females and correlative evidence suggests this to be the cause for decreased serum estradiol. We suggest that decreased serum estradiol in Cx36$^{-/-}$ females delays the maturation of newborn DG granule cells and thus increases the ratio of young neurons with a low excitation threshold in the DG of Cx36$^{-/-}$ females. This shift in the cellular composition of the DG is most likely the cause for the observed differences in behavior and in the activation pattern of the DG.

To dissect the metabolic from the neuronal phenotype we are currently breeding mice in which exon 1 is flanked by two loxP sites (unpublished, generated in our group by Dr. Sheriar Hormuzdi) with mice expressing CRE-recombinase under the control of the nestin promoter as a transgene (Tronche et al., 1999). Using this strategy we will be able to ablate Cx36 only in

neurons, leaving pancreatic β-cells intact. Thus, if the increase in serum insulin was the cause for the phenotype in $Cx36^{-/-}$ female mice, estradiol concentration, neurogenesis and DG activation are expected to be unaltered in female conditional knock-out mice.

Moreover, we want to delineate the exact timecourse of the development of young granule cells in the hippocampus of $Cx36^{-/-}$ females to be able to explain how estradiol influences the maturational process.

V. Abbreviations

A	alpha
B	beta
Bp	basepairs
BrdU	5-bromo-2-deoxyuridine
BSA	bovine serum albumine
CA 1-3	cornu ammonis fields 1-3
CB	calbindin
CR	calretinin
Cx	connexin
$Cx36^{-/-}$	Cx36 knock-out
Cxs	connexins
D	day
DAB	3,3'diaminobenzidine
DCX	doublecortin
DG	dentate gyrus
DTT	dithiothreitol
E	embryonic day
ERα	estrogen receptor alpha
ERβ	estrogen receptor beta
Fig.	figure
FSH	follicle stimulating hormone
GCL	granule cell layer
GFAP	glial fibrillary acidic protein
GnRH	gonadotropin releasing hormone
h	hour
HCl	hydrochloride
HPG	hypothalamic-pituitary-gonadal
kb	kilo bases
kDa	kilo Dalton
LH	luteinizing hormone
loxP	locus of crossing over (for) phage P
µ	micro
m	meter
min	minute
NaCl	sodium chloride
NeuN	neuronal nuclear antigen

nmol	nano moles
P	postnatal day
PBS	phosphate buffered saline
PFA	paraformaldehyde
pS	pico Siemens
PSA-NCAM	polysialated neuronal cell adhesion molecule
PV	parvalbumin
RT	room temperature
S	seconds
SCN	suprachiasmatic nucleus
SGZ	subgranular zone
SVZ	subventricular zone
Tab.	table
Tris	tris(hydroxymethyl)aminomethane
VIP	vasoactive intestinal polypeptide
wt	wildtype

VI. List of References

Al-Ubaidi MR, White TW, Ripps H, Poras I, Avner P, Gomes D, Bruzzone R (2000) Functional properties, developmental regulation, and chromosomal localization of murine connexin36, a gap-junctional protein expressed preferentially in retina and brain. J Neurosci Res 59:813-826.

Altman J (1969) Autoradiographic and histological studies of postnatal neurogenesis. IV. Cell proliferation and migration in the anterior forebrain, with special reference to persisting neurogenesis in the olfactory bulb. J Comp Neurol 137:433-457.

Altman J, Das GD (1966) Autoradiographic and histological studies of postnatal neurogenesis. I. A longitudinal investigation of the kinetics, migration and transformation of cells incorporating tritiated thymidine in neonate rats, with special reference to postnatal neurogenesis in some brain regions. J Comp Neurol 126:337-389.

Altman J, Das GD (1965) Autoradiographic and histological evidence of postnatal hippocampal neurogenesis in rats. J Comp Neurol 124:319-335.

Andersen P, Bliss TV, Lomo T, Olsen LI, Skrede KK (1969) Lamellar organization of hippocampal excitatory pathways. Acta Physiol Scand 76:4A-5A.

Andersen P, Eccles JC, yoning Y (1963) Recurrent inhibition in the hippocampus with identification of the inhibitory cell and its synapses. Nature 198:540-542.

Babu H, Cheung G, Kettenmann H, Palmer TD, Kempermann G (2007) Enriched monolayer precursor cell cultures from micro-dissected adult mouse dentate gyrus yield functional granule cell-like neurons. PLoS ONE 2:e388.

Baimbridge KG, Miller JJ (1982) Immunohistochemical localization of calcium-binding protein in the cerebellum, hippocampal formation and olfactory bulb of the rat. Brain Res 245:223-229.

Belchetz PE, Plant TM, Nakai Y, Keogh EJ, Knobil E (1978) Hypophysial responses to continuous and intermittent delivery of hypopthalamic gonadotropin-releasing hormone. Science 202:631-633.

Belluardo N, Mudo G, Trovato-Salinaro A, Le GS, Charollais A, Serre-Beinier V, Amato G, Haefliger JA, Meda P, Condorelli DF (2000) Expression of connexin36 in the adult and developing rat brain. Brain Res 865:121-138.

Belluzzi O, Benedusi M, Ackman J, LoTurco JJ (2003) Electrophysiological differentiation of new neurons in the olfactory bulb. J Neurosci 23:10411-10418.

Bennett MV, Barrio LC, Bargiello TA, Spray DC, Hertzberg E, Saez JC (1991) Gap junctions: new tools, new answers, new questions. Neuron 6:305-320.

Biebl M, Cooper CM, Winkler J, Kuhn HG (2000) Analysis of neurogenesis and programmed cell death reveals a self-renewing capacity in the adult rat brain. Neurosci Lett 291:17-20.

Blurton-Jones M, Tuszynski MH (2002) Estrogen receptor-beta colocalizes extensively with parvalbumin-labeled inhibitory neurons in the cortex, amygdala, basal forebrain, and hippocampal formation of intact and ovariectomized adult rats. J Comp Neurol 452:276-287.

Boland NI, Humpherson PG, Leese HJ, Gosden RG (1993) Pattern of lactate production and steroidogenesis during growth and maturation of mouse ovarian follicles in vitro. Biol Reprod 48:798-806.

Brandt MD, Jessberger S, Steiner B, Kronenberg G, Reuter K, Bick-Sander A, von der BW, Kempermann G (2003) Transient calretinin expression defines early postmitotic step of neuronal differentiation in adult hippocampal neurogenesis of mice. Mol Cell Neurosci 24:603-613.

Brannvall K, Korhonen L, Lindholm D (2002) Estrogen-receptor-dependent regulation of neural stem cell proliferation and differentiation. Mol Cell Neurosci 21:512-520.

Brightman MW, Reese TS (1969) Junctions between intimately apposed cell membranes in the vertebrate brain. J Cell Biol 40:648-677.

Brown J, Cooper-Kuhn CM, Kempermann G, van PH, Winkler J, Gage FH, Kuhn HG (2003) Enriched environment and physical activity stimulate hippocampal but not olfactory bulb neurogenesis. Eur J Neurosci 17:2042-2046.

Bruning JC, Gautam D, Burks DJ, Gillette J, Schubert M, Orban PC, Klein R, Krone W, Muller-Wieland D, Kahn CR (2000) Role of brain insulin receptor in control of body weight and reproduction. Science 289:2122-2125.

Bruzzone R, Hormuzdi SG, Barbe MT, Herb A, Monyer H (2003) Pannexins, a family of gap junction proteins expressed in brain. Proc Natl Acad Sci U S A 100:13644-13649.

Bruzzone R, White TW, Paul DL (1996) Connections with connexins: the molecular basis of direct intercellular signaling. Eur J Biochem 238:1-27.

Buhl DL, Harris KD, Hormuzdi SG, Monyer H, Buzsaki G (2003) Selective impairment of hippocampal gamma oscillations in connexin-36 knock-out mouse in vivo. J Neurosci 23:1013-1018.

Burcelin R, Thorens B, Glauser M, Gaillard RC, Pralong FP (2003) Gonadotropin-releasing hormone secretion from hypothalamic neurons: stimulation by insulin and potentiation by leptin. Endocrinology 144:4484-4491.

Buzsaki G, Buhl DL, Harris KD, Csicsvari J, Czeh B, Morozov A (2003) Hippocampal network patterns of activity in the mouse. Neuroscience 116:201-211.

Buzsaki G, Eidelberg E (1981) Commissural projection to the dentate gyrus of the rat: evidence for feed-forward inhibition. Brain Res 230:346-350.

Buzsaki G, Horvath Z, Urioste R, Hetke J, Wise K (1992) High-frequency network oscillation in the hippocampus. Science 256:1025-1027.

Buzsaki G, Leung LW, Vanderwolf CH (1983) Cellular bases of hippocampal EEG in the behaving rat. Brain Res 287:139-171.

Chawla MK, Guzowski JF, Ramirez-Amaya V, Lipa P, Hoffman KL, Marriott LK, Worley PF, McNaughton BL, Barnes CA (2005) Sparse, environmentally selective expression of Arc RNA in the upper blade of the rodent fascia dentata by brief spatial experience. Hippocampus 15:579-586.

Cina C, Bechberger JF, Ozog MA, Naus CC (2007) Expression of connexins in embryonic mouse neocortical development. J Comp Neurol 504:298-313.

Cohen PE, Zhu L, Nishimura K, Pollard JW (2002) Colony-stimulating factor 1 regulation of neuroendocrine pathways that control gonadal function in mice. Endocrinology 143:1413-1422.

Condorelli DF, Parenti R, Spinella F, Trovato SA, Belluardo N, Cardile V, Cicirata F (1998) Cloning of a new gap junction gene (Cx36) highly expressed in mammalian brain neurons. Eur J Neurosci 10:1202-1208.

Corkin S (2002) What's new with the amnesic patient H.M.? Nat Rev Neurosci 3:153-160.

Deans MR, Gibson JR, Sellitto C, Connors BW, Paul DL (2001) Synchronous activity of inhibitory networks in neocortex requires electrical synapses containing connexin36. Neuron 31:477-485.

Degen J, Meier C, Van Der Giessen RS, Sohl G, Petrasch-Parwez E, Urschel S, Dermietzel R, Schilling K, De Zeeuw CI, Willecke K (2004) Expression pattern of lacZ reporter gene representing connexin36 in transgenic mice. J Comp Neurol 473:511-525.

des Portes V, Pinard JM, Billuart P, Vinet MC, Koulakoff A, Carrie A, Gelot A, Dupuis E, Motte J, Berwald-Netter Y, Catala M, Kahn A, Beldjord C, Chelly J (1998) A novel CNS gene required for neuronal migration and involved in X-linked subcortical laminar heterotopia and lissencephaly syndrome. Cell 92:51-61.

Desouza LA, Ladiwala U, Daniel SM, Agashe S, Vaidya RA, Vaidya VA (2005) Thyroid hormone regulates hippocampal neurogenesis in the adult rat brain. Mol Cell Neurosci 29:414-426.

Dominguez-Salazar E, Shetty S, Rissman EF (2006) Rapid neural Fos responses to oestradiol in oestrogen receptor alphabeta double knockout mice. J Neuroendocrinol 18:195-202.

Draguhn A, Traub RD, Schmitz D, Jefferys JG (1998) Electrical coupling underlies high-frequency oscillations in the hippocampus in vitro. Nature 394:189-192.

Elfgang C, Eckert R, Lichtenberg-Frate H, Butterweck A, Traub O, Klein RA, Hulser DF, Willecke K (1995) Specific permeability and selective formation of gap junction channels in connexin-transfected HeLa cells. J Cell Biol 129:805-817.

Filippov V, Kronenberg G, Pivneva T, Reuter K, Steiner B, Wang LP, Yamaguchi M, Kettenmann H, Kempermann G (2003) Subpopulation of nestin-expressing progenitor cells in the adult murine hippocampus shows electrophysiological and morphological characteristics of astrocytes. Mol Cell Neurosci 23:373-382.

Freund TF, Buzsaki G (1996) Interneurons of the hippocampus. Hippocampus 6:347-470.

Frisch C, De Souza-Silva MA, Sohl G, Guldenagel M, Willecke K, Huston JP, Dere E (2005) Stimulus complexity dependent memory impairment and changes in motor performance after deletion of the neuronal gap junction protein connexin36 in mice. Behav Brain Res 157:177-185.

Fuchs EC, Zivkovic AR, Cunningham MO, Middleton S, LeBeau FE, Bannerman DM, Rozov A, Whittington MA, Traub RD, Rawlins JN, Monyer H (2007) Recruitment of parvalbumin-positive interneurons determines hippocampal function and associated behavior. Neuron 53:591-604.

Fukuda S, Kato F, Tozuka Y, Yamaguchi M, Miyamoto Y, Hisatsune T (2003) Two distinct subpopulations of nestin-positive cells in adult mouse dentate gyrus. J Neurosci 23:9357-9366.

Fukuda T, Kosaka T, Singer W, Galuske RA (2006) Gap junctions among dendrites of cortical GABAergic neurons establish a dense and widespread intercolumnar network. J Neurosci 26:3434-3443.

Galea LA (2008) Gonadal hormone modulation of neurogenesis in the dentate gyrus of adult male and female rodents. Brain Res Rev 57:332-341.

Ge S, Goh EL, Sailor KA, Kitabatake Y, Ming GL, Song H (2006) GABA regulates synaptic integration of newly generated neurons in the adult brain. Nature 439:589-593.

Gilbert PE, Kesner RP, Lee I (2001) Dissociating hippocampal subregions: double dissociation between dentate gyrus and CA1. Hippocampus 11:626-636.

Gleeson JG, Allen KM, Fox JW, Lamperti ED, Berkovic S, Scheffer I, Cooper EC, Dobyns WB, Minnerath SR, Ross ME, Walsh CA (1998) Doublecortin, a brain-specific gene mutated in human X-linked lissencephaly and double cortex syndrome, encodes a putative signaling protein. Cell 92:63-72.

Goodenough DA (1976) The structure and permeability of isolated hepatocyte gap junctions. Cold Spring Harb Symp Quant Biol 40:37-43.

Gougeon A (1996) Regulation of ovarian follicular development in primates: facts and hypotheses. Endocr Rev 17:121-155.

Gratzner HG (1982) Monoclonal antibody to 5-bromo- and 5-iododeoxyuridine: A new reagent for detection of DNA replication. Science 218:474-475.

Gray GD, Soderstein P, Tallentire D, Davidson JM (1978) Effects of lesions in various structures of the suprachiasmatic-preoptic region on LH regulation and sexual behavior in female rats. Neuroendocrinology 25:174-191.

Green S, Walter P, Kumar V, Krust A, Bornert JM, Argos P, Chambon P (1986) Human oestrogen receptor cDNA: sequence, expression and homology to v-erb-A. Nature 320:134-139.

Gulisano M, Parenti R, Spinella F, Cicirata F (2000) Cx36 is dynamically expressed during early development of mouse brain and nervous system. Neuroreport 11:3823-3828.

Hansen KA, Torborg CL, Elstrott J, Feller MB (2005) Expression and function of the neuronal gap junction protein connexin 36 in developing mammalian retina. J Comp Neurol 493:309-320.

Harris AL (2007) Connexin channel permeability to cytoplasmic molecules. Prog Biophys Mol Biol 94:120-143.

Hastings NB, Gould E (1999) Rapid extension of axons into the CA3 region by adult-generated granule cells. J Comp Neurol 413:146-154.

Herbison AE (1998) Multimodal influence of estrogen upon gonadotropin-releasing hormone neurons. Endocr Rev 19:302-330.

Herrick SP, Waters EM, Drake CT, McEwen BS, Milner TA (2006) Extranuclear estrogen receptor beta immunoreactivity is on doublecortin-containing cells in the adult and neonatal rat dentate gyrus. Brain Res 1121:46-58.

Hess US, Lynch G, Gall CM (1995) Regional patterns of c-fos mRNA expression in rat hippocampus following exploration of a novel environment versus performance of a well-learned discrimination. J Neurosci 15:7796-7809.

Hillarp (1949) The functional organization of the peripheral autonomic innervation. Acta Physiol Scand 17:120-129.

Hormuzdi SG, Pais I, LeBeau FE, Towers SK, Rozov A, Buhl EH, Whittington MA, Monyer H (2001) Impaired electrical signaling disrupts gamma frequency oscillations in connexin 36-deficient mice. Neuron 31:487-495.

Iijima T, Matsumoto G, Kidokoro Y (1992) Synaptic activation of rat adrenal medulla examined with a large photodiode array in combination with a voltage-sensitive dye. Neuroscience 51:211-219.

Isgor C, Watson SJ (2005) Estrogen receptor alpha and beta mRNA expressions by proliferating and differentiating cells in the adult rat dentate gyrus and subventricular zone. Neuroscience 134:847-856.

Jensen E, Jacobson H (1962) Basic guides to the mechanism of estrogen action. Recent Progress in Hormone Research 18:387-408.

Jung KH, Chu K, Kim M, Jeong SW, Song YM, Lee ST, Kim JY, Lee SK, Roh JK (2004) Continuous cytosine-b-D-arabinofuranoside infusion reduces ectopic granule cells in adult rat hippocampus with attenuation of spontaneous recurrent seizures following pilocarpine-induced status epilepticus. Eur J Neurosci 19:3219-3226.

Jung MW, McNaughton BL (1993) Spatial selectivity of unit activity in the hippocampal granular layer. Hippocampus 3:165-182.

Kaplan MS (2001) Environment complexity stimulates visual cortex neurogenesis: death of a dogma and a research career. Trends Neurosci 24:617-620.

Kaplan MS, Hinds JW (1977) Neurogenesis in the adult rat: electron microscopic analysis of light radioautographs. Science 197:1092-1094.

Kee N, Teixeira CM, Wang AH, Frankland PW (2007) Preferential incorporation of adult-generated granule cells into spatial memory networks in the dentate gyrus. Nat Neurosci 10:355-362.

Kempermann G, Jessberger S, Steiner B, Kronenberg G (2004) Milestones of neuronal development in the adult hippocampus. Trends Neurosci 27:447-452.

Kempermann G, Kuhn HG, Gage FH (1997) More hippocampal neurons in adult mice living in an enriched environment. Nature 386:493-495.

Kistler WM, De Jeu MT, Elgersma Y, Van Der Giessen RS, Hensbroek R, Luo C, Koekkoek SK, Hoogenraad CC, Hamers FP, Gueldenagel M, Sohl G, Willecke K, De Zeeuw CI (2002) Analysis of Cx36 knockout does

not support tenet that olivary gap junctions are required for complex spike synchronization and normal motor performance. Ann N Y Acad Sci 978:391-404.

Kosaka T (1983a) Gap junctions between non-pyramidal cell dendrites in the rat hippocampus (CA1 and CA3 regions). Brain Res 271:157-161.

Kosaka T (1983b) Neuronal gap junctions in the polymorph layer of the rat dentate gyrus. Brain Res 277:347-351.

Koval M (2006) Pathways and control of connexin oligomerization. Trends Cell Biol 16:159-166.

Kreuzberg MM, Sohl G, Kim JS, Verselis VK, Willecke K, Bukauskas FF (2005) Functional properties of mouse connexin30.2 expressed in the conduction system of the heart. Circ Res 96:1169-1177.

Kronenberg G, Reuter K, Steiner B, Brandt MD, Jessberger S, Yamaguchi M, Kempermann G (2003) Subpopulations of proliferating cells of the adult hippocampus respond differently to physiologic neurogenic stimuli. J Comp Neurol 467:455-463.

Kuhn HG, Biebl M, Wilhelm D, Li M, Friedlander RM, Winkler J (2005) Increased generation of granule cells in adult Bcl-2-overexpressing mice: a role for cell death during continued hippocampal neurogenesis. Eur J Neurosci 22:1907-1915.

Kuhn HG, ckinson-Anson H, Gage FH (1996) Neurogenesis in the dentate gyrus of the adult rat: age-related decrease of neuronal progenitor proliferation. J Neurosci 16:2027-2033.

Kuiper GG, Enmark E, Pelto-Huikko M, Nilsson S, Gustafsson JA (1996) Cloning of a novel receptor expressed in rat prostate and ovary. Proc Natl Acad Sci U S A 93:5925-5930.

Lagace DC, Fischer SJ, Eisch AJ (2007) Gender and endogenous levels of estradiol do not influence adult hippocampal neurogenesis in mice. Hippocampus 17:175-180.

Landisman CE, Long MA, Beierlein M, Deans MR, Paul DL, Connors BW (2002) Electrical synapses in the thalamic reticular nucleus. J Neurosci 22:1002-1009.

Lee I, Hunsaker MR, Kesner RP (2005) The role of hippocampal subregions in detecting spatial novelty. Behav Neurosci 119:145-153.

Lee JE, Hollenberg SM, Snider L, Turner DL, Lipnick N, Weintraub H (1995) Conversion of Xenopus ectoderm into neurons by NeuroD, a basic helix-loop-helix protein. Science 268:836-844.

Leuner B, Gould E, Shors TJ (2006) Is there a link between adult neurogenesis and learning? Hippocampus 16:216-224.

Levine JE (1997) New concepts of the neuroendocrine regulation of gonadotropin surges in rats. Biol Reprod 56:293-302.

Levine JE, Ramirez VD (1982) Luteinizing hormone-releasing hormone release during the rat estrous cycle and after ovariectomy, as estimated with push-pull cannulae. Endocrinology 111:1439-1448.

Li X, Olson C, Lu S, Nagy JI (2004) Association of connexin36 with zonula occludens-1 in HeLa cells, betaTC-3 cells, pancreas, and adrenal gland. Histochem Cell Biol 122:485-498.

Liu M, Pleasure SJ, Collins AE, Noebels JL, Naya FJ, Tsai MJ, Lowenstein DH (2000) Loss of BETA2/NeuroD leads to malformation of the dentate gyrus and epilepsy. Proc Natl Acad Sci U S A 97:865-870.

Liu Y, Fujise N, Kosaka T (1996) Distribution of calretinin immunoreactivity in the mouse dentate gyrus. I. General description. Exp Brain Res 108:389-403.

Lledo PM, Alonso M, Grubb MS (2006) Adult neurogenesis and functional plasticity in neuronal circuits. Nat Rev Neurosci 7:179-193.

Llinas R, Welsh JP (1993) On the cerebellum and motor learning. Curr Opin Neurobiol 3:958-965.

Lomo T (1971) Patterns of activation in a monosynaptic cortical pathway: the perforant path input to the dentate area of the hippocampal formation. Exp Brain Res 12:18-45.

Long MA, Deans MR, Paul DL, Connors BW (2002) Rhythmicity without synchrony in the electrically uncoupled inferior olive. J Neurosci 22:10898-10905.

Lorente de Nó R. (1934) Studies on the structure of the cerebral cortex-II. Continuation of the study of the ammonic system. Journal of Physiological Neurology 46:113-177.

Magavi SS, Mitchell BD, Szentirmai O, Carter BS, Macklis JD (2005) Adult-born and preexisting olfactory granule neurons undergo distinct experience-dependent modifications of their olfactory responses in vivo. J Neurosci 25:10729-10739.

Maier N, Guldenagel M, Sohl G, Siegmund H, Willecke K, Draguhn A (2002) Reduction of high-frequency network oscillations (ripples) and pathological network discharges in hippocampal slices from connexin 36-deficient mice. J Physiol 541:521-528.

Makowski L, Caspar DL, Phillips WC, Goodenough DA (1977) Gap junction structures. II. Analysis of the x-ray diffraction data. J Cell Biol 74:629-645.

Mann EO, Paulsen O (2007) Role of GABAergic inhibition in hippocampal network oscillations. Trends Neurosci 30:343-349.

Marr D (1971) Simple memory: a theory for archicortex. Philos Trans R Soc Lond B Biol Sci 262:23-81.

Martin AO, Mathieu MN, Chevillard C, Guerineau NC (2001) Gap junctions mediate electrical signaling and ensuing cytosolic Ca2+ increases between chromaffin cells in adrenal slices: A role in catecholamine release. J Neurosci 21:5397-5405.

Mechawar N, Saghatelyan A, Grailhe R, Scoriels L, Gheusi G, Gabellec MM, Lledo PM, Changeux JP (2004) Nicotinic receptors regulate the survival of newborn neurons in the adult olfactory bulb. Proc Natl Acad Sci U S A 101:9822-9826.

Meyer AH, Katona I, Blatow M, Rozov A, Monyer H (2002) In vivo labeling of parvalbumin-positive interneurons and analysis of electrical coupling in identified neurons. J Neurosci 22:7055-7064.

Milks LC, Kumar NM, Houghten R, Unwin N, Gilula NB (1988) Topology of the 32-kd liver gap junction protein determined by site-directed antibody localizations. EMBO J 7:2967-2975.

Milner TA, Ayoola K, Drake CT, Herrick SP, Tabori NE, McEwen BS, Warrier S, Alves SE (2005) Ultrastructural localization of estrogen receptor beta immunoreactivity in the rat hippocampal formation. J Comp Neurol 491:81-95.

Milner TA, McEwen BS, Hayashi S, Li CJ, Reagan LP, Alves SE (2001) Ultrastructural evidence that hippocampal alpha estrogen receptors are located at extranuclear sites. J Comp Neurol 429:355-371.

Mirescu C, Gould E (2006) Stress and adult neurogenesis. Hippocampus 16:233-238.

Moreno AP, Lau AF (2007) Gap junction channel gating modulated through protein phosphorylation. Prog Biophys Mol Biol 94:107-119.

Morgan JI, Cohen DR, Hempstead JL, Curran T (1987) Mapping patterns of c-fos expression in the central nervous system after seizure. Science 237:192-197.

Mueller AL, Chesnut RM, Schwartzkroin PA (1983) Actions of GABA in developing rabbit hippocampus: an in vitro study. Neurosci Lett 39:193-198.

Mullen RJ, Buck CR, Smith AM (1992) NeuN, a neuronal specific nuclear protein in vertebrates. Development 116:201-211.

Nlend RN, Michon L, Bavamian S, Boucard N, Caille D, Cancela J, Charollais A, Charpantier E, Klee P, Peyrou M, Populaire C, Zulianello L, Meda P (2006) Connexin36 and pancreatic beta-cell functions. Arch Physiol Biochem 112:74-81.

O'Keefe J (1976) Place units in the hippocampus of the freely moving rat. Exp Neurol 51:78-109.

O'Keefe J, Dostrovsky J (1971) The hippocampus as a spatial map. Preliminary evidence from unit activity in the freely-moving rat. Brain Res 34:171-175.

Ormerod BK, Galea LA (2001) Reproductive status influences cell proliferation and cell survival in the dentate gyrus of adult female meadow voles: a possible regulatory role for estradiol. Neuroscience 102:369-379.

Ormerod BK, Lee TT, Galea LA (2004) Estradiol enhances neurogenesis in the dentate gyri of adult male meadow voles by increasing the survival of young granule neurons. Neuroscience 128:645-654.

Ormerod BK, Lee TT, Galea LA (2003) Estradiol initially enhances but subsequently suppresses (via adrenal steroids) granule cell proliferation in the dentate gyrus of adult female rats. J Neurobiol 55:247-260.

Pace TW, Gaylord R, Topczewski F, Girotti M, Rubin B, Spencer RL (2005) Immediate-early gene induction in hippocampus and cortex as a result of novel experience is not directly related to the stressfulness of that experience. Eur J Neurosci 22:1679-1690.

Papanicolaou GN (1942) A NEW PROCEDURE FOR STAINING VAGINAL SMEARS. Science 95:438-439.

Paul DL (1986) Molecular cloning of cDNA for rat liver gap junction protein. J Cell Biol 103:123-134.

Pelegrin P, Surprenant A (2006) Pannexin-1 mediates large pore formation and interleukin-1beta release by the ATP-gated P2X7 receptor. EMBO J 25:5071-5082.

Phelan P (2005) Innexins: members of an evolutionarily conserved family of gap-junction proteins. Biochim Biophys Acta 1711:225-245.

Porter AG, Janicke RU (1999) Emerging roles of caspase-3 in apoptosis. Cell Death Differ 6:99-104.

Rakic P (1985) DNA synthesis and cell division in the adult primate brain. Ann N Y Acad Sci 457:193-211.

Rakic P (2002) Adult neurogenesis in mammals: an identity crisis. J Neurosci 22:614-618.

Ramón y Cajal S. (1893) Estructura del asta de Ammon y fascia dentate. Ann Soc Esp Hist Nat 22.

Ramón y Cajal S. (1911) Histologie du Systeme Nerveux de l'Homme et des Vertebres tomme II. Paris: Maloine.

Rash JE, Yasumura T, Dudek FE, Nagy JI (2001) Cell-specific expression of connexins and evidence of restricted gap junctional coupling between glial cells and between neurons. J Neurosci 21:1983-2000.

Ravier MA, Guldenagel M, Charollais A, Gjinovci A, Caille D, Sohl G, Wollheim CB, Willecke K, Henquin JC, Meda P (2005) Loss of connexin36 channels alters beta-cell coupling, islet synchronization of glucose-induced Ca2+ and insulin oscillations, and basal insulin release. Diabetes 54:1798-1807.

Revel JP, Karnovsky MJ (1967) Hexagonal array of subunits in intercellular junctions of the mouse heart and liver. J Cell Biol 33:C7-C12.

Robertson (1963) The occurrence of a subunit pattern in the unit membranes of club endingsin Mauthner cell synapse in goldfish brains. J Cell Biol 19:201-221.

Rochefort C, Gheusi G, Vincent JD, Lledo PM (2002) Enriched odor exposure increases the number of newborn neurons in the adult olfactory bulb and improves odor memory. J Neurosci 22:2679-2689.

Rolls E (1989) Function of neuronal networks in the hippocampus and neocortex in memory. In: Neural models of plasticity: theoretical and empirical approaches. (Byrne JH, Berry WO, eds), pp 240-265.

Rudick CN, Woolley CS (2000) Estradiol induces a phasic Fos response in the hippocampal CA1 and CA3 regions of adult female rats. Hippocampus 10:274-283.

Sagar SM, Sharp FR, Curran T (1988) Expression of c-fos protein in brain: metabolic mapping at the cellular level. Science 240:1328-1331.

Saxe MD, Malleret G, Vronskaya S, Mendez I, Garcia AD, Sofroniew MV, Kandel ER, Hen R (2007) Paradoxical influence of hippocampal neurogenesis on working memory. Proc Natl Acad Sci U S A 104:4642-4646.

Schaffer K (1892) Beitrag zur Histologie der Ammonshornformation. Arch Mikrosk Anat 39:611-632.

Schmidt-Hieber C, Jonas P, Bischofberger J (2004) Enhanced synaptic plasticity in newly generated granule cells of the adult hippocampus. Nature 429:184-187.

Scoville WB, Milner B (1957) Loss of recent memory after bilateral hippocampal lesions. J Neurol Neurosurg Psychiatry 20:11-21.

Seki T, Arai Y (1993) Highly polysialylated neural cell adhesion molecule (NCAM-H) is expressed by newly generated granule cells in the dentate gyrus of the adult rat. J Neurosci 13:2351-2358.

Seri B, Garcia-Verdugo JM, McEwen BS, varez-Buylla A (2001) Astrocytes give rise to new neurons in the adult mammalian hippocampus. J Neurosci 21:7153-7160.

Serre-Beinier V, Le GS, Belluardo N, Trovato-Salinaro A, Charollais A, Haefliger JA, Condorelli DF, Meda P (2000) Cx36 preferentially connects beta-cells within pancreatic islets. Diabetes 49:727-734.

Shors TJ, Miesegaes G, Beylin A, Zhao M, Rydel T, Gould E (2001) Neurogenesis in the adult is involved in the formation of trace memories. Nature 410:372-376.

Shors TJ, Townsend DA, Zhao M, Kozorovitskiy Y, Gould E (2002) Neurogenesis may relate to some but not all types of hippocampal-dependent learning. Hippocampus 12:578-584.

Sloviter RS (1989) Calcium-binding protein (calbindin-D28k) and parvalbumin immunocytochemistry: localization in the rat hippocampus with specific reference to the selective vulnerability of hippocampal neurons to seizure activity. J Comp Neurol 280:183-196.

Smart I (1961) The subependymal layer of the mouse brain and its cell production as shown by autoradiography after [H3]-thymidine injection. J Comp Neurol 116:325-347.

Smeyne RJ, Vendrell M, Hayward M, Baker SJ, Miao GG, Schilling K, Robertson LM, Curran T, Morgan JI (1993) Continuous c-fos expression precedes programmed cell death in vivo. Nature 363:166-169.

Smith PD, McLean KJ, Murphy MA, Turnley AM, Cook MJ (2005) Seizures, not hippocampal neuronal death, provoke neurogenesis in a mouse rapid electrical amygdala kindling model of seizures. Neuroscience 136:405-415.

Sohl G, Degen J, Teubner B, Willecke K (1998) The murine gap junction gene connexin36 is highly expressed in mouse retina and regulated during brain development. FEBS Lett 428:27-31.

Sohl G, Maxeiner S, Willecke K (2005) Expression and functions of neuronal gap junctions. Nat Rev Neurosci 6:191-200.

Sohl G, Odermatt B, Maxeiner S, Degen J, Willecke K (2004) New insights into the expression and function of neural connexins with transgenic mouse mutants. Brain Res Brain Res Rev 47:245-259.

Speier S, Gjinovci A, Charollais A, Meda P, Rupnik M (2007) Cx36-mediated coupling reduces beta-cell heterogeneity, confines the stimulating glucose concentration range, and affects insulin release kinetics. Diabetes 56:1078-1086.

Srinivas M, Rozental R, Kojima T, Dermietzel R, Mehler M, Condorelli DF, Kessler JA, Spray DC (1999) Functional properties of channels formed by the neuronal gap junction protein connexin36. J Neurosci 19:9848-9855.

Staley K, Scharfmann H (2005) A Woman' s Prerogative. Nat Neurosci 8:697-699.

Starling EH (1905) The Croonian Lecture on The Chemical Correlation of the Functions of the Body. The Lancet 166:339-341.

Steiner B, Zurborg S, Horster H, Fabel K, Kempermann G (2008) Differential 24 h responsiveness of Prox1-expressing precursor cells in adult hippocampal neurogenesis to physical activity, environmental enrichment, and kainic acid-induced seizures. Neuroscience.

Sun W, Winseck A, Vinsant S, Park OH, Kim H, Oppenheim RW (2004) Programmed cell death of adult-generated hippocampal neurons is mediated by the proapoptotic gene Bax. J Neurosci 24:11205-11213.

Suter KJ, Wuarin JP, Smith BN, Dudek FE, Moenter SM (2000) Whole-cell recordings from preoptic/hypothalamic slices reveal burst firing in gonadotropin-releasing hormone neurons identified with green fluorescent protein in transgenic mice. Endocrinology 141:3731-3736.

Tanapat P, Hastings NB, Gould E (2005) Ovarian steroids influence cell proliferation in the dentate gyrus of the adult female rat in a dose- and time-dependent manner. J Comp Neurol 481:252-265.

Tanapat P, Hastings NB, Reeves AJ, Gould E (1999) Estrogen stimulates a transient increase in the number of new neurons in the dentate gyrus of the adult female rat. J Neurosci 19:5792-5801.

Teubner B, Degen J, Sohl G, Guldenagel M, Bukauskas FF, Trexler EB, Verselis VK, De Zeeuw CI, Lee CG, Kozak CA, Petrasch-Parwez E, Dermietzel R, Willecke K (2000) Functional expression of the murine connexin 36 gene coding for a neuron-specific gap junctional protein. J Membr Biol 176:249-262.

Theis M, Mas C, Doring B, Degen J, Brink C, Caille D, Charollais A, Kruger O, Plum A, Nepote V, Herrera P, Meda P, Willecke K (2004) Replacement by a lacZ reporter gene assigns mouse connexin36, 45 and 43 to distinct cell types in pancreatic islets. Exp Cell Res 294:18-29.

Thompson RJ, Zhou N, MacVicar BA (2006) Ischemia opens neuronal gap junction hemichannels. Science 312:924-927.

Tozuka Y, Fukuda S, Namba T, Seki T, Hisatsune T (2005) GABAergic excitation promotes neuronal differentiation in adult hippocampal progenitor cells. Neuron 47:803-815.

Tronche F, Kellendonk C, Kretz O, Gass P, Anlag K, Orban PC, Bock R, Klein R, Schutz G (1999) Disruption of the glucocorticoid receptor gene in the nervous system results in reduced anxiety. Nat Genet 23:99-103.

Unwin PN, Zampighi G (1980) Structure of the junction between communicating cells. Nature 283:545-549.

van der Beek EM, Wiegant VM, van der Donk HA, van den HR, Buijs RM (1993) Lesions of the suprachiasmatic nucleus indicate the presence of a direct vasoactive intestinal polypeptide-containing projection to gonadotrophin-releasing hormone neurons in the female rat. J Neuroendocrinol 5:137-144.

van der Beek EM, Wiegant VM, van Oudheusden HJ, van der Donk HA, van den HR, Buijs RM (1997) Synaptic contacts between gonadotropin-releasing hormone-containing fibers and neurons in the suprachiasmatic nucleus and perichiasmatic area: an anatomical substrate for feedback regulation? Brain Res 755:101-111.

van Praag H, Christie BR, Sejnowski TJ, Gage FH (1999a) Running enhances neurogenesis, learning, and long-term potentiation in mice. Proc Natl Acad Sci U S A 96:13427-13431.

van Praag H, Kempermann G, Gage FH (1999b) Running increases cell proliferation and neurogenesis in the adult mouse dentate gyrus. Nat Neurosci 2:266-270.

van Praag H, Schinder AF, Christie BR, Toni N, Palmer TD, Gage FH (2002) Functional neurogenesis in the adult hippocampus. Nature 415:1030-1034.

Vanderwolf CH (1969) Hippocampal electrical activity and voluntary movement in the rat. Electroencephalogr Clin Neurophysiol 26:407-418.

Veenstra RD, Wang HZ, Beyer EC, Ramanan SV, Brink PR (1994) Connexin37 forms high conductance gap junction channels with subconductance state activity and selective dye and ionic permeabilities. Biophys J 66:1915-1928.

Venance L, Rozov A, Blatow M, Burnashev N, Feldmeyer D, Monyer H (2000) Connexin expression in electrically coupled postnatal rat brain neurons. Proc Natl Acad Sci U S A 97:10260-10265.

Vreugdenhil M, Jefferys JG, Celio MR, Schwaller B (2003) Parvalbumin-deficiency facilitates repetitive IPSCs and gamma oscillations in the hippocampus. J Neurophysiol 89:1414-1422.

Wang S, Scott BW, Wojtowicz JM (2000) Heterogenous properties of dentate granule neurons in the adult rat. J Neurobiol 42:248-257.

Weiland NG (1992) Estradiol selectively regulates agonist binding sites on the N-methyl-D-aspartate receptor complex in the CA1 region of the hippocampus. Endocrinology 131:662-668.

Weiland NG, Orikasa C, Hayashi S, McEwen BS (1997) Distribution and hormone regulation of estrogen receptor immunoreactive cells in the hippocampus of male and female rats. J Comp Neurol 388:603-612.

Wisden W, Morris BJ (2002) In Situ Hybridization Protocols for the Brain. London: Academic Press.

Woolley CS, McEwen BS (1992) Estradiol mediates fluctuation in hippocampal synapse density during the estrous cycle in the adult rat. J Neurosci 12:2549-2554.

Wray S, Hoffman G (1986) A developmental study of the quantitative distribution of LHRH neurons within the central nervous system of postnatal male and female rats. J Comp Neurol 252:522-531.

Zhang CL, Zou Y, He W, Gage FH, Evans RM (2008) A role for adult TLX-positive neural stem cells in learning and behaviour. Nature 451:1004-1007.

Zhao C, Deng W, Gage FH (2008) Mechanisms and functional implications of adult neurogenesis. Cell 132:645-660.

Zhao C, Teng EM, Summers RG, Jr., Ming GL, Gage FH (2006) Distinct morphological stages of dentate granule neuron maturation in the adult mouse hippocampus. J Neurosci 26:3-11.